TISSUE PROTECTIVE HYDROPHILIC POLYMER SOLUTIONS AND SURFACE MODIFICATIONS

By

KHALID MENTAK

A DISSERTATION PRESENTED TO THE GRADUATE SCHOOL
OF THE UNIVERSITY OF FLORIDA IN PARTIAL FULFILLMENT
OF THE REQUIREMENTS FOR THE DEGREE OF
DOCTOR OF PHILOSOPHY

UNIVERSITY OF FLORIDA

1993

To the memory of my grandmother Hajja Melike whose love and devotion are still a source of guidance

ACKNOWLEDGEMENTS

I would like to express my deepest gratitude to my adviser and doctoral committee chairman Dr Eugene F Goldberg for his teaching guidance and relentless encouragement that allowed for the completion of this work My sincere thanks also go to the members of my supervisory committee: Dr Hatch Dr Brennan Dr Gates and Dr Shah for their advice and teaching

Thanks are extended to Dr Ali Yehiaoui for his help and encouragement Many thanks must go to Paul Martin Dr H Hattori Dr L Peck Dr J Quigg and Steve Farnworth for their collaboration Also thanks to Dr Moshe Levy for his wise and lively discussions I would also like to thank my fellow students and friends for their advice and support

My sincere thanks also go to my friend Zakaryae Fathi for his friendship and to Hamid Baidi for his help in the preparation of this manuscript I wish also to thank Hassan Oukacha and Mustapha Oukacha for their advice and encouragement Most of all I am grateful to my wonderful family for their love support and encouragement

TABLE OF CONTENTS

LIST OF FIGURES

LIST OF TABLES

Abstract of Dissertation Presented to the Graduate School
of the University of Florida in Partial Fulfillment of the
Requirements for the Degree of Doctor of Philosophy

TISSUE PROTECTIVE HYDROPHILIC POLYMER SOLUTIONS AND SURFACE MODIFICATIONS

By

KHALID MENTAK
May 1993

Chairman: Dr. Eugene P. Goldberg
Major Department: Materials Science and Engineering

The occurrence of tissue damage is the source of serious postoperative complications in a wide range of surgical procedures. This damage is a result of tissue handling and adverse interfacial implant tissue interactions. This research deals with different aspects of tissue damage and the use of hydrophilic polymers to minimize tissue trauma.

In cataract surgery, the use of intraocular lens (IOL) polymeric prosthesis to restore vision have gained widespread acceptance. More than 2,000,000 IOLs will be implanted in 1993. However, adverse hydrophobic interactions between IOLs and ocular tissues result into substantial tissue damage. The first part of this research involved the synthesis and characterization of hydrophilic surface grafts onto two primary IOL polymers: Polymethylmethacrylate (PMMA) and Polydimethylsiloxane (PDMS) by radiation induced polymerization. A novel approach to surface grafting using mixtures of

N vinylpyrrolidone (NVP) and polyvinylpyrrolidone (PVP) grafted thi
and highly stable hydrophilic grafts Surface graft polymerization o
some anionic vinyl sulfonic acid monomers onto PMMA and PEME was also
achieved The preparation of composite hydrophilic grafts containing
carboxymethylcellulose (CMC) and hyaluronic acid (HA) was described
Surfaces were characterized using gravimetric analysis goniometry
Fourier transform infrared by attenuated total reflectance (FTIR/ATR)
X ray photoelectron spectroscopy (XPS) staining/light microscopy and
scanning electron microscopy (SEM) In vitro evaluation of hydrophilic
surfaces revealed significantly reduced adhesion induced tissue damage

Another approach to minimizing tissue damage is the use of tissue
protective hydrophilic polymer solutions In this context the
properties of carboxymethylcellulose (CMC) solutions were investigated
and empirical equations relating concentration to rheological behavior
were developed Solution purification by filtration and autoclaving was
described and subsequent changes in rheology characterized The results
suggested that rheological properties of CMC are may be due to the
formation of stable intermolecular associations (junction zones)

Tissue damage can also cause postsurgical adhesions The
preparation and characterization of insolubilized CMC membranes as
adhesion prevention devices was investigated Insolubilization by ionic
complexation and thermal treatment has produced CMC membranes with a
wide range of properties
In vivo evaluation in a rat cecal model revealed that CMC membranes
significantly reduce the incidence and severity of peritoneal adhesions

CHAPTER 1
GENERAL INTRODUCTIO

The occurrence of tissue damage is recognized to be one of the most serious postoperative complications in a wide range of surgical procedures. This damage is a result of tissue handling, inadvertent contact with surgical instruments, and chronic tissue abrasion caused by prosthetic implants. This research deals with different aspects of tissue damage and the use of hydrophilic polymers to alleviate some of the complications associated with tissue trauma.

The problem of tissue damage is a major concern in cataract surgery. Cataract is an opacification of the natural lens which may significantly reduce vision. It is the most prevalent visually disabling eye disease which accounts for 45% of blindness in the world (1). No medical treatment has been proven effective to delay, prevent or reverse the development of cataract in adults. It is usually remedied by surgical extraction of the opaque natural lens and replacement by a prosthetic lens or intraocular lens (IOL). Implantation of modern IOLs is recognized to be a safe and effective procedure. The incidence of complications has decreased because of IOL improvement, increased experience by ophthalmic surgeons, and improved surgical procedures. However, some adverse reactions are still seen (2,3). Early studies in our laboratories demonstrated that extensive damage may be caused to ocular tissues even upon brief contact with prosthetic lens surfaces (4).

[illegible] polymeric lens materials not only significantly reduces ocular tissue damage but also results in low cell adhesion to IOL surfaces and reduced postsurgical inflammation (5 6 7)

Gamma radiation graft copolymerization of hydrophilic monomers onto a variety of polymeric IOL substrates has been shown to produce homogeneous lubricious chemically bonded hydrophilic grafts (8) These surface modified lenses have been tested clinically patented and trademarked (Hydrograft®) by the University of Florida

Chapter 2 deals with the synthesis and characterization of a variety of hydrophilic polymer grafts onto two primary ocular implant materials (polymethylmethacrylate (PMMA) and polydimethylsiloxane(PDMS)) with special attention to graft stability and to some problems inherent to PDMS A novel approach to surface grafting using mixtures of N vinylpyrrolidone (NVP) and polyvinylpyrrolidone (PVP) produced thin permanent and highly stable grafts Surface graft polymerization of some anionic vinyl sulfonic acid monomers and their copolymers with NVP was also investigated

A more sophisticated approach to surface modification of hydrophobic polymers is the immobilization of bioactive molecules within the hydrophilic grafts This novel concept combines the tissue protection afforded by the lubricious hydrated hydrogel graft with the bioactivity of the immobilized molecules In this context the immobilization of two polysaccharides hyalaronic acid (HA) and carboxymethylcellulose (CMC) within PVP grafts was studied In contrast to conventional methods, where the bioactive molecules are

directly coupled to the substrate during organic reaction [illegible] cross method may provide biomolive grafts with enhanced stability and no residual toxic chemical by products

This study was also designed to shed some light on cell behavior on hydrophilic surfaces with different tonicity in general which may help tailor surfaces with certain desired properties such as antithrombogenic linings of endothelial cells on small diameter vascular grafts

Chapter 3 deals with the preparation and properties of Hydrophilic Polymer Solutions for tissue protection in ophthalmic surgery and the prevention of postsurgical adhesion formation

During the last decade viscous solutions of HA have become an important device in surgical procedures such as IOL implantation and retinal detachment surgery (10) In cataract surgery these viscoelastic solutions are used to maintain the anterior chamber of the eye thereby protecting fragile ocular tissues from traumatic contact with surgical instruments and the implant itself (11) However HA is extremely expensive requires extensive purification is only moderately stable and cannot be readily sterilized by autoclaving In addition the use of HA in the anterior chamber of the eye requires subsequent removal by irrigation and even then is usually accompanied by a rise in the intraocular pressure (IOP) which may cause postsurgical glaucoma (12) The desirable properties of a viscoelastic substance are intimately tied to its chemical and rheological properties An understanding of the structure property relationships of these polymers

can help [illegible] the desired properties

The preparation and characterization of [illegible]rified viscosurgical CMC solutions with a wide range of properties were investigated in this research A unique processing technique was developed to help achieve higher solution viscosities at lower CMC concentration

Postoperative adhesion (POA) formation is a major complication in a variety of surgical procedures Adhesions which are undesired collagenous connective tissue are responsible for mortality in cardiac surgery infertility in pelvic surgery and intestinal obstruction in abdominal surgery (13 14) Formation is believed to involve an inflammatory response following trauma to tissues caused by handling and contact with surgical instruments In this research hydrophilic polymer solutions were investigated as tissue protective coatings to reduce the incidence and severity of such adhesions

Another approach to the prevention of adhesion formation is the use of resorbable membranes as mechanical barriers to separate traumatized tissue and thereby allow normal healing without adhesion formation (15) In this context the preparation and properties of CMC membranes were studied These membranes were modified to alter their solubility in physiological media using ionic complexation and a novel heat treatment method The CMC membranes obtained by these methods behave as "degradable hydrogels" having a wide range of water contents (20 4990%) and residence times in water varying from hours to weeks In

additior to heir use as adhesio prever on devi es host membras

may have potential use as drug delivery carriers and as wound dressings

CHAPTER 2
HYDROPHILIC SURFACE MODIFICATION OF OCULAR IMPLANT POLYMERIC MATERIALS

2.1 Introduction

Cataract is an opacification of the natural lens of the eye which interferes with normal vision and may cause blindness (Figure 2.1). It is usually remedied by the surgical removal of the cataractous lens. The three most common methods of optical correction used to restore vision after removal of the clouded natural lens include spectacle glasses, contact lenses and intraocular lenses (IOLs). The most widely used technique for visual rehabilitation, inducing the least magnification with no alteration of peripheral vision has become IOL implantation (15).

Since the introduction of the first IOL by Harold Ridley in 1949 a considerable amount of research has been directed toward improving the performance of these widely used prostheses (17). Recent improvements in design, manufacturing, and surgical techniques have made the implantation of modern IOLs among the safest and most effective surgical procedures. However, postoperative complications due to interfacial interactions between IOL material and fragile ocular tissue are still seen (18).

Although modern IOLs are available in a wide variety of designs, they usually consists of an optic and fixation devices called haptics (Figure 2.2). The most commonly used optic material is polymethylmethacrylate (PMMA), the haptics are usually made of

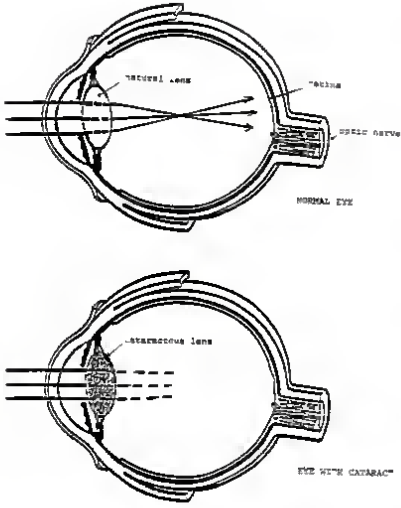

Figure 2.1 Schematic representation of a normal eye and an eye with cataract

polypropylene or PMMA [illegible] such as polydimethylsiloxane (PDMS) have been extensively studied as potential implant materials because of their flexibility which might allow insertion of folded lenses through a very small incision (2) However postoperative complications are still present even with the best designed IOLs primarily because of the hydrophobic nature of these polymers (21)

Hydrophilic surface modification of biopolymers has been proposed to enhance the long term biocompatibility of IOL materials by minimizing tissue damage and reducing cell and protein deposits (22 23 24) and is the basis for this phase of the research reported here

2.2 Background

2.2.1 Intraocular lens materials and related problems

PMMA was among the first polymers to be developed in the second and third decade of the twentieth century In 1949 Ridley discovered that fragments of splintered airfighter canopies made of high purity PMMA (Perspex PMMA) found in the eyes of pilots were tolerated fairly well by ocular tissues (25) This discovery initiated the development of modern IOLs and PMMA is still the polymer of choice for IOLs This thermoplastic amorphous polymer is also widely used in dental restoration fixation of joint replacements and repair of cranial defects (26) At room temperature PMMA is an optically clear (ca 92% transmission of light) rigid and stable material However its use as an IOL material is also complicated by some drawbacks due mainly to undesirable interfacial interactions with ocular tissues Because of its relatively low glass transition temperature (T_g 105°C) and its

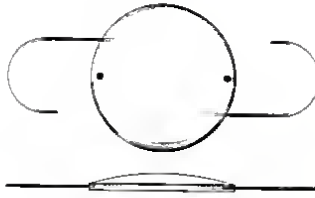

The ... cap poster.or .hamber .ens

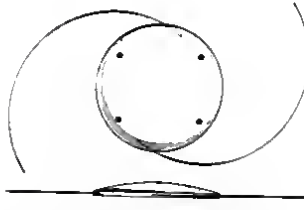

The C.loss poste ic ... om er .ens

... re 7 ... Popu...

chemical structure [illegible] steam sterilization (27) [illegible] hydrophobicity and rigidity have been implicated in ocular tissue trauma, mechanical abrasion of fragile ocular tissues, and adhesion of residual natural lens material which may cause postoperative inflammation (28 29). In addition, cataract removal can now be performed through small incisions (ca. 3mm) using phacoemulsification techniques which may minimize postoperative astigmatism and allow early rehabilitation. With PMMA, an advantage of the phacoemulsification procedure is lost since the small initial incision needs to be enlarged to allow the insertion of the rigid PMMA IOL. Along with PMMA, other polymers have also been investigated for use as optic materials. PDMS and PHEMA have long been investigated because of their flexibility and autoclavability (30 31). Flexible PDMS or PHEMA IOLs can be folded and inserted trough a small incision which may represent an advantage over PMMA.

PDMS has been extensively used in biomedical applications especially when flexibility and softness are required (32). It is a crosslinked polysiloxane elastomer with the chemical structure shown in Figure 2.3. Because of its molecular structure PDMS has a low glass transition temperature ($T_g \sim$ -123°C), and is a highly mobile macromolecule at room temperature. This accounts for its unusual oxygen permeability and active molecular rearrangements at the surface. However, animal studies have showed PDMS IOLs to cause significant adhesion induced damage to ocular tissues, postoperative inflammation due to residual lens material, and loss of IOL optical properties

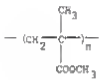

PMMA

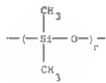

PDMS

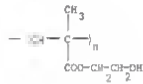

PHEMA

Figure 2 3 Chemical structures of IOL materials

[illegible] silicone also reduced refractive [illegible] lipid absorption and impurities (33 34 35)

Hydrogels are another class of biopolymers [illegible] investigated for IOL applications These crosslinked polymer networks swell in water but do not dissolve Their similarity to natural tissues makes them the material of choice in a variety of biomedical applications such as contact lenses drug delivery devices and soft tissue prostheses (36) Several studies report hydrogel IOLs to be better tolerated by ocular tissues in general and to cause less damage to the endothelial cells (37 38) However these materials usually display poor mechanical properties and may be damaged during surgical insertion (39 40) Attempts to enhance the mechanical properties of these systems by fiber reinforcement crosslinking or copolymerization with hydrophobic monomers have not yet been successful in developing acceptable hydrogel IOLs

It appears then that hydrophobic polymers such as PMMA and PDMS may exhibit suitable mechanical and physical properties to be used as implant materials but their biocompatibility is less desirable mainly because of unfavorable interfacial interactions with living tissues On the other hand hydrogels possess excellent biocompatibility but suffer from poor mechanical properties Hydrophilic surface modification techniques may therefore be used to coat the hydrophobic polymers with a chemically bound thin hydrogel layer without affecting their bulk properties Surface modified polymeric implants can combine the mechanical properties of the substrate with the superior biocompatibility afforded by the grafted hydrogel (41)

2.2.2 Corneal Endothelial Cell Damage

The corneal endothelium is a single layer of [illegible] hexagonal cells covering the inner surface of the cornea [illegible] Figure 2.4. Its major function consists of preserving water balance to keep the cornea relatively dry to ensure optical clarity (42). Normally the cornea has a constant thickness (ca. 0.5 mm) and has a water content of ca. 80% (43). If the endothelium is damaged, excessive water enters the stroma causing it to swell. This is clinically known as corneal edema. The excess water also disturbs the crystalline morphology of the collagen responsible for the optical clarity of the cornea which results in corneal cloudiness.

Kaufmann et al. pointed out that even a brief contact of a PMMA lens with the cornea causes extensive damage to the endothelium (4). PMMA lenses adhere to the endothelium on contact and subsequent movement or attempt to separate the two surfaces results in stripping away of the endothelium cell layer. Adhesion induced damage is recognized to be a complication in IOL implantation since adult endothelium does not regenerate.

Improvements in surgical techniques, increased awareness of the surgeons, and the use of hydrophilic viscoelastic solutions to prevent contact between the IOL and the endothelium have helped minimize these problems. However, some complications associated with the use of viscoelastic substances are still seen (44, 45). A part of this research was dedicated to investigate these materials, and their drawbacks are discussed in section 3.2.

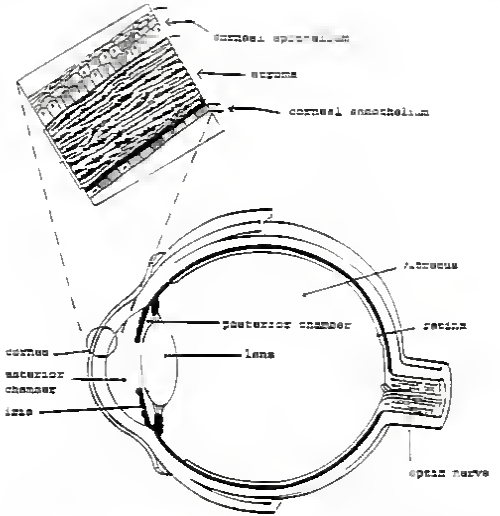

Figure 2.4 A schematic representation of the anatomy of the human cornea showing the corneal layers and eye

Hydrophilic surface modification is used to produce soft and lubricious hydrogel like coatings onto hydrophobic materials to provide protection for the endothelium during [illegible] reduce chronic abrasion throughout the lifetime of the implant

2.2.3 Cell behavior on polymer surfaces

Cell behavior on material surfaces in general is a highly complex phenomenon governed by numerous factors which include the nature of the cells, the physicochemical properties of the substrate surface and initial protein adsorption. When an implant is exposed to the natural physiological medium, adsorption of proteins occurs almost instantaneously (46). The extent of this adsorption is of paramount importance to the subsequent response of cells to an implant surface (47). Also important is the mechanical rigidity of the protein layer which provides support to cell attachment (48). Proteins such as fibronectins, laminin, and collagen which strongly promote cell adhesion and spreading (49) have specific active sites for cell membranes. Protein adsorption involves electrostatic interactions, hydrophilic/hydrophobic forces, and hydrogen bonding (47).

The molecular mobility of the surface is believed to play an important role in cell adhesion. Hard surfaces provide the rigidity necessary to allow protein scaffolding and the molecular stiffness to retain the cells (48). Hydrated hydrogels can have high surface mobility and are generally poor substrates for cell adhesion (49, 50).

Surface energy or wettability of the substrate surface can also affect cell attachment and proliferation. Schrader has studied cell adhesion on surfaces with a wide range of surface energies. He reported

[illegible] adhesion to be minimal at surface energy [illegible] dyn/cm (51) Subsequent studies by Baier have also suggested that platelet adhesion is minimum at values between 20 and 30 dyn/cm then increases with increasing surface tension to reach a maximum at around 45 dyn/cm However further increase in the critical surface tension caused a marked decrease in platelet adhesion and spreading for values higher than 60 dyn/cm (52)

The ionicity of the surface along with its charge density are also among the parameters to be taken into consideration Proteins have an amphoteric character (i.e., possess both cationic and anionic groups) and can adsorb on charged surfaces regardless of the nature of the charge Sulfonated polystyrene surfaces have been shown to exhibit increasing cell adhesion with increasing negative charge density (53) Cell behavior on charged surfaces was also shown to be strongly dependent on the nature of the chemical group holding the charge Using the zeta potential to measure charge density Kishida has studied the behavior of HeLa S3 cells onto polyethylene surfaces modified with neutral, cationic, and anionic sulfonic monomers (54) He showed that cell adhesion does not occur until the zeta potential exceeds a value of +12 mV for cationic polymers and -45 mV for anionic polymers He also concluded that the strong cell attachment and spreading observed for styrenesulfonic acid (SSA) grafted surfaces compared to those modified with acrylamido methylpropane sulfonic acid (AMPSA) another sulfonic monomer is due to an unusually high protein adsorption (e.g. albumin) exhibited by SSA modified surfaces. The aromatic structure of SSA was regarded as responsible for such behavior (54)

The ability of IOL materials as well as other medical devices to support cell adhesion and spreading is of prime importance in the performance of implants. After cataract removal, epithelial cells, cortex material, and inflammatory cells are discarded into the anterior chamber. If the IOL polymers supports cell proliferation, these cellular precipitates will deposit on the IOL surface and cause excessive light scattering and posterior membranes opacification which may require explantation (55, 56). These cellular precipitates were also implicated in severe acute and chronic postoperative inflammations (57).

2.2.4 Gamma induced surface modification of polymers

Modification of the surface properties of polymers is an important and emerging area in the biomedical field. The growing interest in surface modification techniques is the result of the increased research dedicated to elucidate interfacial phenomena between implants and living tissues. A variety of techniques for chemical and biochemical modification of polymer surfaces have been investigated over the past years. The polymer surface can be activated chemically and the monomers reacted with the specific functional groups that are introduced. High energy radiation such as gamma radiation has also been used to prepare surface graft copolymers (58).

Surface graft copolymerization using gamma radiation offers several advantages. First, this method can generate free radicals in monomers and solid polymers which makes it especially attractive for graft copolymerization.

Second it minimizes the presence of toxic residual [illegible] chemical initiators and catalysts are not needed

In this study polymeric substrates were irradiated in the presence of the monomer Two simultaneous reactions occur by this method surface graft polymerization and homopolymerization in the surrounding monomer solution The grafting occurs via radicals created on the substrate surface which react with the monomer Homopolymerization is the result of solution polymerization of the vinyl monomer Excessive homopolymerization can reduces the diffusion of the monomer to the reactive sites on the substrate surface thereby decreases the grafting efficiency (58 59)

The two major factors affecting gamma induced grafting are the rate of generation of radicals on the substrate and their accessibility to the monomer (58) Repulsive forces between the hydrophobic substrate surface and the hydrophilic monomer solution create a monomer depleted interface and can make the grafting difficult A process method developed in our laboratory by Ali Yahiaoui has been found to enhance grafting by creating a monomer rich interface and allow enhanced monomer diffusion into the substrate surface The details of this method were reported elsewhere (8)

2.2.4.1 Radiation chemistry of various polymers

2.2.4.1.1 Radical formation in PMMA and PBMB

The radiolysis of PMMA has been extensively studied (58 60) The G value or number of radicals produced by 100 eV reported for PMMA is relatively high (G (R·) ~12) The radicals formed during gamma irradiation of PMMA have been identified by several authors (61 62 63)

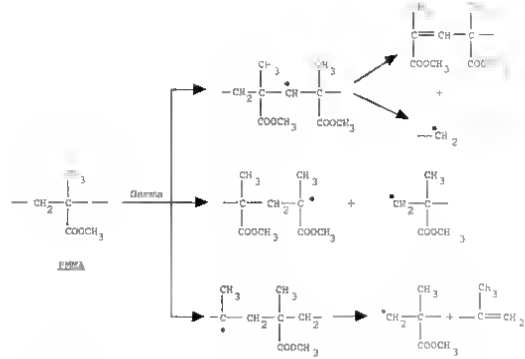

Figure 2 5 Free radical formation in PMMA by gamma radiation

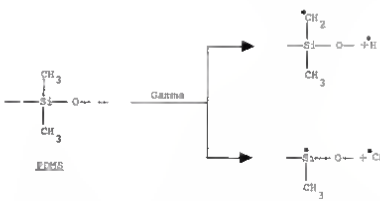

Figure 2 6 Free radical formation in PDMS by gamma radiation

The creation of [redacted] in PMMA by gamma [redacted] shown in Figure 2 [redacted]

In contrast to PMMA PDMS is much more resistant to gamma [redacted] and its G value is reported to be 2 6 Irradiation of PDMS causes [redacted] cission of both C-H and Si C bonds, leading to the formation of radicals as shown in Figure 2 6 (64)

2.2.4.1.2 Radical formation in HA and CMC

The mechanism of radical formation in HA and CMC has not been specifically reported in the literature However some insight into the effect of gamma radiation on these biopolymers can be gained by reviewing the extensive literature available on the radiation chemistry of polysaccharides The chemical structure and properties of these two biopolymers are discussed in section 3 2.2 3 The production of radicals in polysaccharides can be initiated by different agents such as radiation oxidants and metal ions (65 66) Gamma radiation produced by a Co^{60} source was shown to cause radical depolymerization of cellulosic materials (67) A reduction in the extent of depolymerization and hence in the number of radicals produced has been observed for polysaccharides modified with axemetic groups Arthur has shown that methyl glucosides are protected during irradiation by phenyl and benzoyl groups (68) The presence of small groups such as carboxymethyl in CMC and N acetyl glucosamine in HA are not expected to have a large effect on radical production in the monosaccharide units (69) Some initial pulse radiolytic studies in aqueous solutions of CMC have demonstrated the possible presence of peroxy radicals (69) The radicals shown in Figure 2 7 are commonly observed during gamma

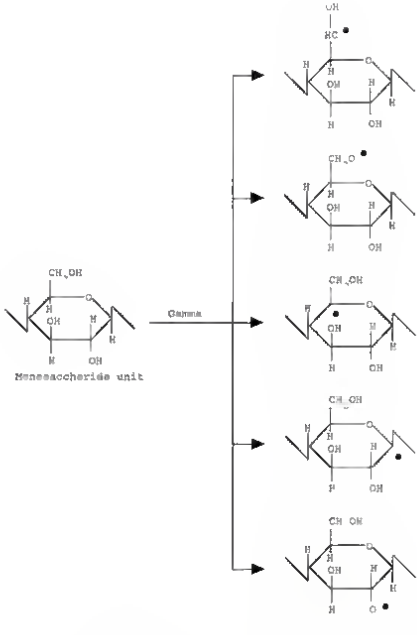

Figure 2.7 Free radical formation in polysaccharides during gamma irradiation

irradiation of polysaccharides and are most likely to be present in gamma irradiated HA and CMC (78)

2.2.4.1.2 Effect of oxygen

The presence of oxygen has a large effect on the effect of radiation on polymers. During irradiation oxygen is believed to act as radical scavenger which tend to accelerate the degradation of polymers and retards homopolymerization of vinyl monomers. This may be due to the formation of weak peroxidic bonds in the main polymeric chain (71). These bonds decompose and cause oxidative degradation as shown in Figure 2.8. Infrared studies have shown the formation of carbonyl and hydroxyl groups during irradiation of various polymers in air (72)

The effect of oxygen during irradiation is also dependent on the nature of the polymer. Polymers which crosslink when irradiated such as polyethylene, polypropylene, polystyrene, or polyvinylpyrrolidone (PVP) can degrade if irradiated in oxygen (73). At low dose rates, oxygen can diffuse into the bulk of the polymer fast enough to provide sufficient oxygen for peroxide formation. At high dose rates, the effect of oxygen is less pronounced since it is rapidly consumed(74). In thick polymer samples the effect of oxygen is confined to the surface (75, 76).

It is still not clear whether oxygen acts by accelerating scission or by retarding crosslinking. In polymers such as polystyrene and polyethylene the acceleration of scission during irradiation is the main effect of oxygen while the crosslinking rate is virtually unaffected (77). In PMMA and polyisobutylene the rate of scission has been shown to be unaffected by the presence of oxygen.

Formation of weak peroxidic bonds

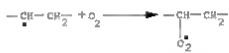

Subsequent decomposition causing oxidative degradation

Figure 2.8 Formation of peroxidic bonds during gamma irradiation in the presence of oxygen

In this study [illegible] samples were systematically [illegible] then backfilled with argon to remove any dissolved oxygen

2.2.4.2 Copolymerization of vinyl monomers with HA and CMC

In this study HA and CMC were incorporated into the hydrophilic grafts by simultaneous irradiation of the substrate in the presence of HA/NVP or CMC/NVP solutions The copolymerization of these polysaccharides with NVP may provide hydrophilic HA and CMC grafts with improved stability This section is a review of the different aspects of this novel copolymerization of vinyl monomers with polysaccharides which are relevant to this research

Studies have been directed toward the modifications of natural polysaccharides by copolymerization with a variety of vinyl monomers Copolymerization techniques their mechanisms and the properties of the resulting products have been comprehensively summarized (79) Graft copolymerization of cellulose and its derivatives with vinyl monomers has yielded a range of products with interesting properties Homogeneous grafting of styrene hydroxyethylmethacrylate (HEMA) and methylmethacrylate has been accomplished in several solvent systems (78 80)

The simultaneous irradiation method of polysaccharides and vinyl monomers has the advantage of initiating polymerization of the monomer directly on the polysaccharide macroradical thereby taking advantage of both long and short lived radicals shown to be present in such reactions (81 82)

[illegible] Copolymerization of NVP and vinyl sulfonic [illegible]

The radiation induced polymerization of vinyl monomers in aqueous solutions usually proceeds via a free radical mechanism (58) Normal kinetics are observed at relatively low radiation dose rates such as those used in this study (≤ 1000 rad/min) (58)

NVP copolymerizes with various simple ionic and zwitterionic monomers in solution (63) Copolymers of NVP with carboxylate monomers (e g acrylic acid sodium acrylate) have been well studied (64) However only few studies dealing with the copolymerization of NVP with vinyl sulfonic monomers have been reported The availability of new vinyl sulfonic monomers such as styrene sulfonic acid (SSA) acrylamide methyl propanesulfonic acid (AMPSA) sulfopropylacrylate (SPA) and sulfopropylmethacrylate (SPMA) has prompted new interest in their copolymerization with N vinylpyrrolidone (NVP) to produce synthetic water soluble polyelectrolyte solutions (65) Schulz reviewed the synthesis kinetics and solution properties of these copolymers (65) The rate of copolymerization of AMPSA with NVP was shown to be several orders of magnitude faster than the other sulfonate monomers and reached a maximum at a 1 1 We attributed this behavior to the donor acceptor character of this monomer pair His results also indicate that NVP and AMPSA have a tendency to alternate as shown by their respective reactivity ratios (r_{NVP} = 0 13 r_{AMPSA} = 0 66) On the other hand SSA copolymerizes with NVP with preferential incorporation of SSA Copolymerization of NVP with KSPA and SPMA has not been reported in the literature

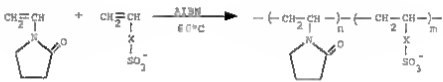

—X— : Linking Chemistry

Figure 2.9 Copolymerization of NVP with sulfonate monomers

A significant property of these copolymers is their pol[illegible] behavior which is evidenced by a drastic decrease of [illegible]r water with increasing salt concentrations (35) This supports the fact that the sulfonate group (SO_3^-) is preserved throughout the copolymerization reaction NVP copolymerizes with sulfonate monomers according to the equation in Figure 2 3 (83)

In view of the foregoing discussion the research reported here involved the preparation of anionic hydrophilic grafts using vinylsulfonic monomers and their copolymers with NVP onto PMMA and PDMS in order to study cell behavior on neutral and anionic surfaces The substrates were irradiated in the presence of aqueous sulfonic monomer solutions or comonomer solutions of NVP and various vinylsulfonic monomers Characterization was carried out using gravimetric analysis goniometry FTIR/ATR and XPS In vitro cell adhesion and spreading was conducted using rabbit lens capsule epithelial cells

2.3 Materials and Methods

2.3.1 Materials

2.3.1.1 PMMA and PDMS substrates

PMMA and PDMS are the major IOL optic materials used currently The substrates used in this research were donated by Pharmacia Ophthalmics Inc Pennsdens CA These include PMMA (UVEX® from Pharmacia) PDMS (KE 1935 from Shin Etsu Silicones of America) PMMA samples were cut into rectangular strips of approximately 1x6cm PDMS samples were cut into rectangular strips of approximately 1x6cm

2.3.1.2 Monomers and reagents for surface grafting

The monomers used in this study were: 2 N vinyl pyrrolidone (NVP from Kodak) purified by distillation under reduced pressure (1 2 mm Hg at 55 60°C) and stored at 4°C until use Sodium styrene sulfonate as sodium salt (SSA) and sodium 2 acrylamide 2 methyl 1 propanesulfonate (AMPSA) potassium sulfopropylacrylate (KSPA) and potassium sulfopropylmethacrylate obtained from Aldrich and used as received and Polyvinylpyrrolidone (K90 PVP, pharmaceutical grade) with a MW of 0 6x10^6 obtained from GAF and used as received

Pharmaceutical grade carboxymethylcellulose (CMC) with MW varying from 90x10^3 to 1 0x10^6 and degree of substitution (DS) varying from 0 7 to 1 2 was obtained from Aqualon Hyaluronic Acid (HA) as powdersrum form (1 2x10^6 MW) was kindly provided by Genzyme Corporation Inc Figure 2 10 shows the chemical structures of monomers and polymers used in this research

2.3.1.3 Gamma polymerized polyvinylpyrrolidone (γ PVP)

Gamma polymerized polyvinylpyrrolidone (γ PVP) was prepared as follows: An aqueous solution containing 10% by weight of NVP in distilled water was first prepared 30 ml of this solution was transfered to 40 ml glass tubes with screw caps vacuum degassed for 10 minutes then backfilled with argon To allow homogeneous gamma irradiation the tubes were mounted on a rotary device rotating at 10 rpm and irradiated to a total dose of 0 15 Mrad at 701 rad/min

Gamma induced polymerization of aqueous solutions of NVP was studied by Satoshi Sakurai from our group He reported that the polymerization of a solution of 10% NVP proceeds to completion when

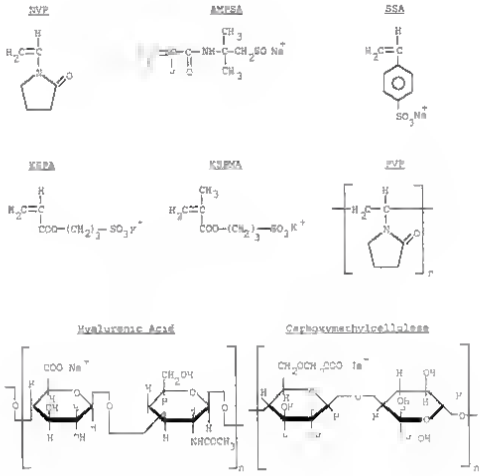

Figure 2 1b Chemical structure of monomers and polymers used for grafting

irradiated to 0.5 Mrad at 0°C in radiation gamma polymerised PVP has a viscosity of 22700 Cps (Brookfield RV DVII CP 52 1 s^{-1}) and water soluble. The weight average molecular weight (Mw) obtained from intrinsic viscosity measurement using Mark Houwink Sakurada equation a values of K = 39.3 x 10^{-3} and a = 0.59 obtained from polymer handbook was ca. 1.0x10^{5}. However the molecular weight measured using gel permeation chromatography (GPC) gave a value of 2.1x10^{5}.

This discrepancy has been reported by other investigators and attributed to the branched structure of PVP prepared by this method (85). Charlesby has studied the effect of branching on the intrinsic viscosity by using gamma radiation to produce controlled degrees of branching in vinyl polymers (87). Katsura has also studied the structure of polymers prepared by gamma induced polymerization of vinyl monomers and concluded that such polymers may exhibit highly branched structures (88). Charlesby has also described the formation of long chain branching during radiation induced polymerization of vinyl monomers (89). This process involves abstraction of a hydrogen atom from a previously formed polymer molecule by a growing free radical which is thereby terminated. The polymer chain from which a hydrogen has been abstracted is converted into a free radical capable of adding to monomer and initiating a branch chain. Branching may be regarded as an intermediate stage for crosslinking.

2.3.2 Methods

2.3.2.1 Substrate cleaning

PMMA samples (1cm x 4cm x 2.4mm) were first individually sonicated in a 0.1% Triton X 100 (Fisher) aqueous soap solution in borosilicate

glass tubes (16mm x 125mm) for 30 minutes then sonicated (15 minutes each) in distilled water at ambient temperature.

PDMS samples (1cm x 4mm x 1.9mm) were individually sonicated in borosilicate glass tubes three times for 20 minutes each in followed by a similar procedure as in PMMA cleaning. The drying procedure was the same for all samples and consisted of drying under vacuum for 12 hours and storing in a desiccator until further use.

2.3.2.2 Gamma induced graft polymerization

2.3.2.2.1 Presoaking

Cleaned and dried samples were immersed in 6 ml of a 40% NVP aqueous solution in individual sealed borosilicate test tubes (16mm x 125 mm) and kept in a water bath at 60°C for four hours unless otherwise described. Samples were then removed from the grafting solution, gently shaken to remove excess monomer solution and finally transferred to the grafting solution.

2.3.2.2.2 Degassing

As described in section 2.2.4.1.2, dissolved oxygen may act as radical scavenger and effect gamma induced polymerization. To exclude oxygen prior to gamma irradiation, monomer solutions were degassed as follows: borosilicate glass test tubes containing the samples and the grafting monomer solutions were vacuum degassed for 15 minutes, then back filled with argon. Test tubes were then sealed with polypropylene caps then irradiated.

2.3.2.2.3 Gamma Irradiation

After degassing, test tubes containing substrates in monomer solutions were exposed to a 600 Curie ^{60}Co gamma source. A schematic diagram of the gamma source is shown in Figure 2.11.

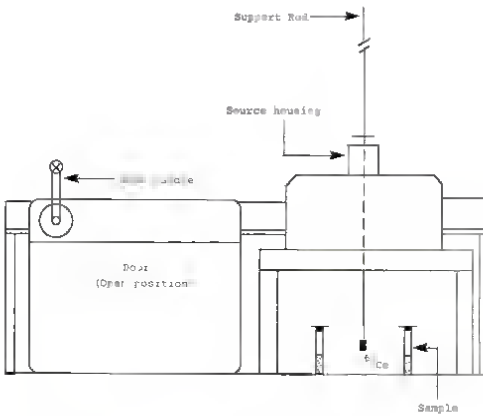

Figure 2.11 Schematic Drawing of the ^{60}Co Gamma radiation Source

The test tubes were mounted on polypropylene supports and placed a certain distance from the source. The dose rate is determined by the distance from the source as suggested from Fricke dosimetry. The dose is determined by the dose rate and the exposure time. At the completion of the irradiation samples were removed from the gamma source and washed as described in the next section.

2.3.2.2.4 Washing

After irradiation the substrates were removed from the graft ng solution and thoroughly rinsed with warm distilled water (50°C) to remove any physically adsorbed ungrafted homopolymer. The substrates were then soaked in 18 ml distilled water at 50°C in individual borosilicate glass test tubes (16mm x125mm) for 3 days with frequent changes of water. Finally samples were soaked in 10 ml of distilled water at room temperature for 4 days with frequent water changes to remove any water soluble materials. Samples were removed from distilled water and dried in vacuo at (55°C) for 24 hours.

2.3.2.2.5 Two step gamma induced grafting

A two step irradiation technique was designed to protect radiation sensitive materials such as HA and CMC from excessive irradiation. The grafting was performed as follows:

Step I

1 presoak in 8 ml of 40% NVP at 50°C for 4 hrs as described in section 2 3 2 2 1

2 immediately transfer to individual borosilicate glass tube (16mm x 125mm) containing 8ml of 15% NVP then vacuum degas as described in section 2 3 2 2 2

3 gamma irradiate to [illegible] Mrad at [illegible] rate

4 remove substrate from the solution thoroughly rinse with distilled water then dry at 60°C under vacuum for 12 hours

Step II

1 transfer dried pregrafted substrates to individual borosilicate glass test tubes containing 9 ml of the appropriate grafting solutions (aqueous solutions of NVP/CMC or NVP/HA of various ratios and concentrations)

2 vacuum degas for 10 15 minutes depending upon the viscosity of the grafting solution Viscous solutions require relatively longer degassing time Open in argon atmosphere and seal with polypropylene caps prior to gamma irradiations

3 gamma irradiate to 0 05 Mrad at dose rate of 781 rad/min

4 remove samples from the solution wash and dry to constant weight as described in section 2 3 2 2 4

2.3.2.3 Characterization

Some of the most significant advances in the biomaterial field over the past years have been related to the use of new or improved analytical techniques to characterize biomaterials A thorough and reliable characterization is particularly important in the field of surface modifications of biopolymers

2.3.2.3.1 Gravimetric analysis

Gravimetric analysis is a simple analytical technique used to investigated the extent of grafting Samples were weighed dry before and after grafting using a Sartorius Research electronic balance (model R 200 D) having a precision of ± 0 02 mg

[illegible] were determined as follows

$$\% \text{ weight gain} = (W_g - W_o/W_o)\times 10 \quad (\text{illegible})$$

where W_o and W_g are the dry weights before and after [illegible] respectively

Typical weights for PMMA samples used in this [illegible] (1 cm x 2 4 mm) were approximately 1 0 g Weight gain of 0 1% corresponds to a weight change of approximately 1 mg and can be measured with an accuracy of ± 2% since the sensitivity of the balance used in this research is 0 02 mg Typical weights for PDMS samples (1cm x 4cm x 1 8mm) were approximately 0 8 g Weight gain of 0 1% for PDMS samples corresponds to a weigth change of 0 8mg and is measurable with an accuracy of 3% For both PMMA and PDMS, weight gains less than 0 1% were considered not significant

2.1.2.1.2 Contact angle

Contact angle techniques are routinely used in the characterization of biomaterial surfaces to describe wettability or to estimate surface energy Contact angle can be measured by exposing the sample surface to either a drop of liquid or an air bubble (Figure 2 12) The angle θ which the drop or the bubble forms with the sample surface depends on the nature of the surface and is described by Young's equation

$$\cos\theta = (\gamma_{sv} - \gamma_{sl})/\gamma_{lv} \quad (2\ 2)$$

where

γ_{sv} is the solid vapor interfacial free energy

γ_{sl} is the solid liquid interfacial free energy

γ_{lv} is the liquid vapor interfacial free energy

Contact angles were measured using the captive air bubble technique. A Rame Hart contact angle goniometer (Mountain Lakes New Jersey) was used. An acrylic immersion chamber filled with distilled water at room temperature. The substrate was attached to a microscope glass slide with rubber bands and the slide positioned across the immersion chamber as shown in Figure 2.13. Air bubbles were deposited onto the substrate surface using a microsyringe. The contact angle is usually obtained by averaging the contact angles measured on both sides of five air bubbles across the surface.

2.1.2.1.3 FT IR/ATR

Fourier transform infrared (FT IR) in its classical form is limited to materials through which infrared radiation can be transmitted and thus provide information from the bulk of the material. However this powerful technique can be used to characterize polymer surfaces by allowing the IR beam to probe the surface of the sample only. The most popular IR technique used for surface analysis is attenuated total reflection (ATR) which consists of using crystals with high refractive indices (2.3 to 4.0). The IR beam is reflected when it passes from a medium of high refractive index (i.e. crystal) to a medium of lower refractive index (i.e. sample). The depth at which the incident IR beam decays to 1/e of its initial value is defined as the depth of penetration (d_p) and is described by the relation

$$d_p = \frac{\lambda}{2\pi n_1 [\sin^2\theta - (n_2/n_1)^{1/2}]} \qquad (2.3)$$

where λ - wavelength of the IR radiation

n_1 refractive index of the IRE crystal

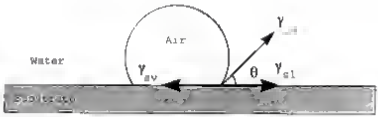

Figure 2.12 Interfacial energies involved at the solid water interface

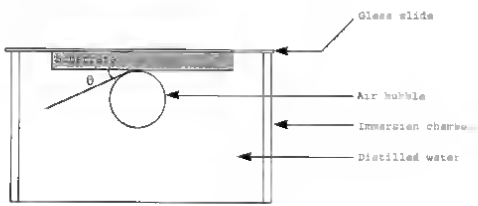

Figure 2.13 Schematic representation of contact angle measurement using captive air bubble

[illegible] refractive index of [illegible]

θ = angle of incidence and exit of IR beam

Figure 2.14 shows the sampling configuration used in this research. FTIR-ATR spectroscopy was proven to be a very useful technique in surface chemistry characterization of polymers. In the biomaterial field, it has been used extensively to investigate surface chemistry and chemical bonding.

The depth of penetration for this technique ranges from 1.0 to 3.3 μm depending on n_{21}, λ, and θ and can be calculated from equation 3.3 for various IRE crystal materials and configurations. The FT IR/ATR spectra were obtained with a Nicolet 50SX spectrometer using a parallelogram ZnSe crystal (50mmx10mmx2mm from Spectra Tech). The ZnSe crystal is placed between two samples (1x4 cm) and the spectra collected using 100 scans with a resolution of 4cm^{-1}. The depth of penetration obtained with this crystal was 0.65μ as calculated from equation (2.3).

2.2.5.4 X-ray photoelectron spectroscopy

X-ray photoelectron spectroscopy (XPS), also known as electron spectroscopy for chemical analysis (ESCA), is another powerful analytical technique for studying the chemical composition of polymer surfaces. Its exceptional sensitivity and quantification abilities have made XPS a very useful analytical tool in the characterization of biopolymer surfaces.

XPS is based on the photoelectric effect during the interaction of the material surface with a photon beam (e.g., X-rays). The X-ray beam causes electrons of certain energies to be emitted (Figure 2.15). The

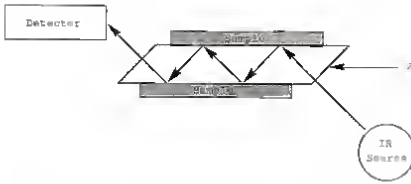

Figure 2 14 A typical Optical Program for Attenuated Total Reflecta
(ATR) Spectroscopy

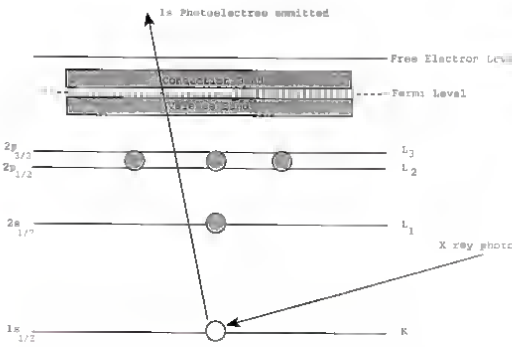

Figure 2 15 Schematic view of the interaction of an X ray photon
with an atomic orbital

kinetic energy of such electrons is measured and can be related to the binding energy by the following equation

$$E_b = h\nu \quad E_k \quad F \qquad (2\ 4)$$

where E_b is the electron binding energy characteristic of the element from which it was ejected E_k is the electron kinetic energy measured by the instrument $h\nu$ is the photon energy (h is the Plank s constant and ν is the X ray frequency) and F is the work function The binding energy recorded can hence provide information about the elemental composition and the chemical bonding states of each element except hydrogen The sampling depth of this technique is related to the distance that photoelectrons can travel before undergoing inelastic scattering defined as the mean free path λ The sampling depth of XPS for perfectly flat samples, d is given by the following equation

$$d = \lambda \sin \theta \qquad (2\ 5)$$

where is the photoelectron take off angle measured relative to the plane of the sample surface The depth of penetration varies typically from ca 10Å for a take off angle of 10° to 50Å for a take off angle of 90°

The XPS spectra were recorded using a Kratos model XSAM 800 spectrometer with an Mg K_α X ray source The X ray gun was operated at 20 kV and 23 mA and the pressure in the analyzer chamber was 10^{-7} to 10^{-8} torr Quantification was performed using a Kratos software (DS800) The binding energy scale was fixed by assigning E_b = 285 0 eV to the C1s peak

2.3.2.5.5 Graft thickness measurements

Graft thickness were measured by light microscopy using cross sections of stained samples Eosin staining was used for PMMA samples and consisted of immersing PMMA samples in 2% aqueous eosin solution

tom 12 hours Samples were removed from the [illegible]
throughly rinsed with distilled water and sectioned using a [illegible]
blade asw

PDMS samples were stained with 2% aqueous solution of crystal violet Light microscopy was performed using a Nikon optical microscope and graft thickness obtained using an eye piece with a measuring grid

2.3.2.5.6 SEM

Studies in our group have shown that high energy electron beam (5 10 Kev) used in SEM can cause damage to polymer surfaces and hence erroneous morphological observations In this research low voltage SEM was used to prevent damage to sample surfaces Scanning electron micrographs were obtained on uncoated polymer samples using a scanning electron microscope (JEOL 6990) with a low voltage scanning beam (0 5 1 5 Kev) Scanning electron micrographs of other samples (i e cornea from endothelial damage test) were obtained using a (JEOL JSM 35CF) SEM The surfaces were coated with gold palladium using a Hummer V sputter coater (Technics Alexandria Virginia) Low voltage and corneal endothelium SEM was performed by Paul Martin

2.3.2.5.7. Lens epithelial cell adhesion and spreading

Cell adhesion and spreading in vitro experiments were performed using epithelial cells from the anterior lens capsule of New Zealand white rabbits according to the method of Hofmeister (90) A slight modification was introduced in the staining technique as crystal violet was used instead of hematoxylin and eosin stains Light microscopy was performed using an inverted Nikon microscope This experiment was performed with the assistance of Paul Martin

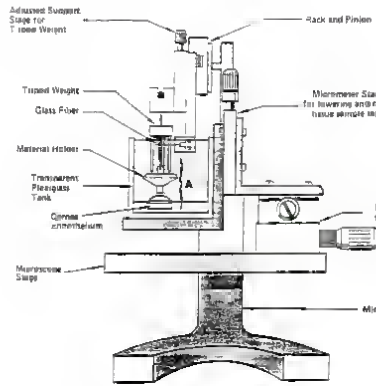

Figure 2 16 Drawing of the corneal endothelium damage test instrument

2.3.2.5.6 Corneal endothelial cell damage

The corneal endothelial damage was quantitatively evaluated using an instrument developed in our laboratory (Figure 2.16). This instrument was originally designed to measure adhesive forces between polymer surfaces and corneal endothelium (91). This method consists of allowing a PMMA stub to come in contact with a fresh corneal endothelium button. A controlled pressure was applied on the PMMA stub to allow more reproducible results. Following endothelial touch, the cornea were removed, critical point dried, gold palladium coated, and the damage observed by SEM. This experiment was performed by Paul Martin and Dr. Kirmyukl Hetteri.

2.4 Results and Discussion

During the past ten years, studies on hydrophilic surface modification of hydrophobic IOL polymers have suggested that this technique can help improve the overall biocompatibility of ocular implant materials. Several studies conducted in our laboratories showed that hydrophilic graft copolymer surface modification of hydrophobic polymers can reduce tissue trauma and post operative inflammation associated with IOL implantation (23).

This research was devoted to the synthesis and characterization of a variety of new hydrophilic grafts onto two primary ocular implant polymers: PMMA and PDMS.

2.4.1 Surface Graft Polymerization of PVP/NVP Systems onto PMMA and PDMS

Radiation induced graft polymerization of NVP onto PMMA and PDMS has been previously studied in this group(S 91).

The results indicate that grafts can be developed by [illegible] surface modification techniques but can be inhibited using aqueous monomer solutions by repulsive forces between the hydrophobic polymer and the hydrophilic monomers used in the grafting solutions. The grafting efficiency can be significantly enhanced by using a "pressoak method" (8) which consists of presoaking the substrate in concentrated aqueous solutions of NVP prior to gamma irradiation. The NVP diffuses into the substrate and creates a monomer rich interface between the substrate and the monomer solution which helps reduce the hydrophobic/hydrophilic repulsions at the interface.

However, in the case of PDMS, changes in optical resolution has been observed upon folding of PVP surface modified PDMS IOLs. The possible reasons for such behavior are believed to be due to excessive diffusion of NVP into the bulk of the PDMS and subsequent polymerization during gamma irradiation.

PDMS has a low glass transition temperature (T_g ~ 123°C) and behaves as an ideal elastomer at room temperature. When it is unfolded, PDMS recovers its initial state without any residual changes. On the other hand, dry PVP has a much higher glass transition temperature (T_g=180°C) and is a relatively rigid glassy material at room temperature. Upon folding of PVP g PDMS, the PVP within the bulk of PDMS may undergo irreversible deformation and possible phase separation which may account for the changes in optical properties.

In an effort to reduce the diffusional effects and enhance the mechanical integrity of surface grafts, aqueous PVP solutions were used during the radiation grafting. The rationale of this approach is as follows: First, PVP is a relatively large molecule. Which would be

ess susceptible to diffusing into the substrate than NVP. Second, both PDMS and PMMA surfaces wet well which may provide the PVP radicals with better accessibility to the radicals generated on the substrate surface. The wetting properties of PVP are due to its strong amphiphilic character arising from the presence of polar am dic groups and apolar methylene and methine groups. This unusual property is also responsible for the fact that PVP is soluble in polar solvents such as water as well as in a wide range of other organic solvents and its ability to complex with small molecules (82). Third, aqueous solutions of PVP crosslink readily with gamma radiation and might afford crosslinked grafts with superior stability and enhanced mechanical integrity because of long chain crosslinks. In addition the presence of small amounts of NVP in the grafting solutions may help provide more reactive sites.

This research focused on the gamma radiation induced graft copolymerization of PVP/NVP systems onto PMMA and PDMS with special attention to graft thickness and stability on PDMS.

2.3.1 Gravimetric analysis and air bubble contact angle

In this experiment substrate samples were irradiated in PVP/NVP aqueous solutions. Polyvinylpyrrolidone (PVP) is a neutral water soluble polymer with high thermal and hydrolytic stability. It is used in the medical and pharmaceutical field in a variety of applications because of its biocompatibility and stability. PVP is also used as wetting agent for a wide range of materials because of its surface active properties. Two types of PVP were used throughout this research: K30 PVP and y PVP.

K30 PVP is a linear polymer with a MW of 3×10^4 obtained by

suspension polymerization of N vinylpyrrolidone (83) The total concentration of K90 PVP/NVP aqueous solutions was 10% and the rat o K90 PVP NVP ranged from 1 0 to 0 1 γ PVP was prepared in our laboratories by gamma induced polymerization of an aqueous solution o 10% NVP using a dose of 0 15 Mrad at a dose rate of 701 rad/min The preparation and properties of γ PVP are described in section 2 3 1 3 There have been several reports suggesting that PVP prepared by gamma may have a branched structure and crosslinks readily if higher doses are used (87)

In this study a dose of 0 15 Mrad was used for PMMA PDMS being more radiation resistant was irradiated to a dose of 0 2 Mrad The dose rate was 781 rad/min and remained the same for both PMMA and PDMS

The following abbreviations were used throughout this manuscript NVP g PMMA and NVP g PDMS designate PMMA and PDMS samples which were gamma irradiated in aqueous NVP solutions respectively (K90 PVP/NVP) g PMMA and (K90 PVP/NVP) g PDMS designate samples irradiated in mixtures of K90 PVP and NVP of various ratios (γ PVP/NVP) g PMMA and (γ PVP/NVP) g PDMS were those samples prepared by gamma irradiation of substrates in mixtures of γ PVP and NVP

As discussed in section 2 3 2 3 1 PMMA samples used in this research have a typical weight of approximately 1 5 g and a surface area of 18 3 cm^2 calculated from sample dimensions (1cmx4cmx2 4mm) In this case a weight gain of 0 1% which corresponds to a weight change of 1mg can be measured with an accuracy of 2%

The results of the gravimetric analysis and the contact angle for PMMA grafts are shown in Table 2 1 Hydrophilic surfaces were obtained

Table 2 1 Gravimetric analysis and contact angle data of grafted films of γ PVP/NVP and K90-PVP/NVP systems onto PMMA [C [illegible] 701 rad/min]

Sample	γ PVP %	K90 PVP %	NVP %	%Wg	C A (°)	Vi Cps
PMMA 1	10 0	0 0	0 0			gelled
PMMA 2	5 0	0 0	0 0	0 2	28	18000
PMMA 3	2 5	0 0	0 0	0 3	30	8100
PMMA 4	5 0	0 0	5 0	1 4	18	5200
PMMA 5	2 5	0 0	7 5	2 1	17	11300
PMMA 6	2 5	0 0	2 5	0 2	25	4600
PMMA 7	0 0	10	0 0	0 0	27	18000
PMMA 8	0 0	5 0	0 0	0 3	30	6200
PMMA 9	0 0	2 0	0 0	0 3	32	1200
PMMA 10	0 0	0 0	1 0	0 3	25	6400
PMMA 11	0 0	0 0	2 0	0 9	17	5000
PMMA 12	0 0	5 0	5 0	0 8	22	6200
PMMA 13	0 0	2 0	0 0	1 1	20	2200
PMMA 14	0 0	1 0	0 0	0 4	25	2100
PMMA 15	0 0	0 0	10 0	0 0	30	8600
PMMA 16[2]	0 0	0 0	10 0	3 0	18	9800

[1] Viscosity of grafting solutions after irradiation measured using a Brookfield viscometer RVII CP52 at a shear rate of 1 0 s^{-1}

[2] This sample was presoaked in 40% NVP at 80°C for 4 hours

for the majority of PMMA samples (γ PVP/NVP) g PMMA samples showed increased hydrophilicity in comparison with unmodified PMMA surfaces which has typical contact angle values of 70° Slightly lower contact angle values were obtained for samples with a total concentration of 10% and γ PVP:NVP ratios of 1:3 and 1 1 These samples also showed relatively higher weight gains Hydrophilic surfaces were also obtained for (K90 PVP/NVP) g PMMA samples (PMMA 7 PMMA 14) when compared to unmodified PMMA (70°) Lower contact angles and slightly higher weight gains were obtained for a total K90 PVP/NVP concentration of 10% and K90 PVP NVP ratios of 4 1 1 1 and 1:4 PMMA samples irradiated in aqueous 10% NVP (NVP g PMMA) without presoak (PMMA 15) showed no measurable weight gain and a contact angle of 30° Shown in Table 2 2 are the results obtained for PDMS As in the case of PMMA good hydrophilicity was achieved for virtually all of the PDMS samples in comparison with unmodified PDMS which has a contact angle of 100° For (γ PVP/NVP) g PDMS a higher weight gain was obtained for a total γ PVP/NVP concentration of 10% and a ratio γ PVP NVP of 1 3 For (K90 PVP/NVP) g PDMS contact angles observed varied from 43° to 19° and the weight gains from 0 88 to 1 9% PDMS sample irradiated in 10% NVP to a dose of 2 0 Mrad (NVP g PDMS) with no presoak gave a contact angle of 45° and no measurable weight gain Radiation induced graft polymerization using simultaneous irradiation of polymeric substrates in the presence of monomers involves heterogeneous polymer monomer reactions where the rate of polymerization is diffusion controlled (8) These reactions are mainly governed by the rate of production of free radicals on the substrate surfaces and their accessibility to the monomer

Table 2-2 Gravimetric analysis and contact angle data of graft[illegible] γ PVP/NVP and K90 PVP/NVP systems onto PDMS (0 2 Mrad 701 rad/min)

Sample	γ-PVP %	K90 PVP %	NVP %	%Wg	C A (°)	Vis Cps
PDMS 1	5 0	0 0	0 0			gelled
PDMS 2	2 5	0 0	0 0	0 1	25	22400
PDMS 3	5 0	0 0	5 0	0 1	25	5580
PDMS 4	2 5	0 0	7 5	2 0	17	15000
PDMS 5	2 5	0 0	2 5	0 2	20	8100
PDMS 6	0 0	10	0 0	0 0	43	22000
PDMS 7	0 0	5 0	0 0	0 5	27	7300
PDMS 8	0 0	2 0	0 0	0 5	35	5000
PDMS 9	0 0	9 0	1 0	0 6	25	8500
PDMS 10	0 0	8 0	2 0	0 4	22	7500
PDMS 11	0 0	5 0	5 0	0 9	30	6800
PDMS 12	0 0	2 0	0 0	1 9	19	3400
PDMS 13	0 0	1 0	9 0	0 5	25	2400
PDMS 14	0 0	0 0	10 0	0 0	45	18300
PDMS 15	0 0	0 0	10 0	2 0	18	16380

(1) Viscosity of grafting solutions after irradiation measured using a Brookfield viscometer MVII CP52 at a shear rate of 1 0 s^{-1}

(2) This sample was presoaked in 40% NVP at 80°C for 4 hours

The presence of repulsive forces between hydrophobic PMMA surfaces and hydrophilic NVP polymers may inhibit graft polymerization reactions.

Because of its good surface wetting properties, the use of PVP in the grafting solution may provide the free radicals produced in the monomer solution with better accessibility to free radicals produced on the substrate surface.

Many polymers in solutions undergo simultaneous intermolecular crosslinking and degradation when irradiated. The overall effect of radiation is believed to be a kinetic phenomenon where the rate of crosslinking or degradation predominates. Chapiro has pointed out that polymers with heat of polymerization higher than 16 kcal/mol have a tendency to crosslink(53). Kiran and Rodriguez have studied the effect of gamma radiation on aqueous K90 PVP solutions (54). At relatively higher K90 PVP concentrations, intermolecular crosslinking is favored and is believed to occur by formation of macroradicals on the polymer backbone. The macroradicals react so as to stabilize themselves and may cause crosslinking and/or chain scission. These macroradicals may also react directly with radicals produced on the substrate surface or with low molecular radicals produced during gamma irradiation of NVP. A mechanism proposed by Hoeglein suggests that macroradicals may react favorably with low molecular weight radicals because of increased mobility(95). This, in addition to chain transfer to monomer, may account for the fact that the viscosities of solutions after irradiation were lower in the presence of NVP which minimizes intermolecular crosslinking. This may also help enhance grafting reactions since chains induced graft

polymerization is diffusion controlled

It was also observed that γ PVP/NVP systems yielded slightly higher weight gains than K90 PVP/NVP for the same concentration And PVP/NVP ratios for both PMMA and PDMS This may be due to structural differences between γ PVP and K90 PVP A higher number of radicals may be produced in γ PVP because of the branched structure Weber et al have measured the G value of polymers with various degrees of branching and concluded that increased branching usually results in greater yield of radicals (96)

Gamma induced grafting of K90 PVP/NVP and γ PVP/NVP systems onto PMMA and PDMS may involve complex homogeneous and heterogeneous reactions between all of the three components of the system (i e substrate PVP and NVP) with concomitant crosslinking of PVP

For both PMMA and PDMS samples prepared by presoaking the substrates in 40% NVP at 60°C for 4 hours prior to gamma irradiation in 10% NVP (PMMA 16 and PDMS 15) gave relatively higher weight gains and contact angles lower than 20° The presoak method was developed in our laboratories by Ali Yahiaoui and is described in detail in his doctoral research dissertation (8) Presoaking substrates in nonirradiated aqueous solutions of NVP at wide range of temperatures and for various times was studied and presoaking conditions optimized for various substrates (e g PMMA PP PDMS) Presoaking in 40% NVP at 60°C for 4 hours was found to enhance grafting of NVP onto PMMA without affecting its optical properties The diffusion of significant amounts of the monomer into the substrate during presoaking creates a monomer rich interface and helps reduce hydrophobic repulsions between the substrate and aqueous monomer

solution One of the goal of this research was to compare grafts obtained by gamma irradiation of PMMA and PDMS in aqueous solutions of NVP in combination with presoaking in 4P% NVP at 60° for 4 hours to those obtained in a single step irradiation of PMMA and PDMS in KPO PVP/NVP or γ PVP/NVP aqueous solutions of various concentrations and PVP NVP ratios A comparative study on the structure (i e thickness and chemical structure) of grafts obtained by these two methods was conducted using surface analytical techniques with different probing depths and is described in the next sections

The significance of these observations resides in the fact that it may be possible to surface modify PMMA and PDMS implant surfaces in a single step process using aqueous PVP/NVP solutions (i e KPP PVP/NVP or γ PVP/NVP) The use of PVP may also help provide grafts with increased stability and less penetration in the bulk of the substrate since PVP is a large molecule which is less susceptible to diffusing into the substrate The structure and stability of the graft may prove to be important to the surface optical and mechanical properties as well as to the long term performance of implants

2.4.1.1 Light microscopy of stained grafts

This technique provides a convenient way to visualize and measure relatively thick polymer grafts (>3μ) Grafts with a thickness lower than ca 3μ are difficult to visualize because of the resolution of the optical microscope (ca 1μ) and other optical artifacts (e g , edge effects) Figure 2 17 shows a photomicrograph of a cross section of stained unmodified PMMA which indicates that crystal violet does not stain PMMA Figure 2 18 shows a cross section of crystal violet stained NVP g PMMA prepared with presoaking

in 40% NVP for at 60°C for 4 hours then irradiating in 10% NVP to 0.15 Mrad at 701 rad/min Figure 2 19 shows a dark layer of ca at the surface of the sample which corresponds to the PVP graft The color fading away toward the bulk of the substrate is characteristic of the diffuse layer structure of the PVP grafts obtained with the presoak method Both crystal violet stained (KSO PVP/NVP) g PMMA and (Y PVP/NVP) g PMMA samples showed very slight bluewish color but the grafts could not be viewed by light microscopy (samples not shown here)

A cross section of crystal violet stained unmodified PDMS is shown in Figure 2 19 Figure 2 20 shows a cross section of stained NVP g PDMS prepared by presoaking in 40% NVP at 60°C for 4 hours then irradiating in 10% NVP to 0 2 Mrad at 701 rad/min which gave a graft thickness of ca 50µm As in PMMA (KSO PVP/NVP) g PDMS and (Y PVP/NVP) g PDMS could not be visualized by light microscopy

The results of these graft thickness measurements are given in Table 2 3 For this experiment 5 samples were prepared for each set of conditions graft thicknesses were averaged and the standard deviations reported NVP g PMMA prepared by presoaking in 40% NVP at 60°C for 4 hours prior to irradiating in 10% NVP to 0 15 Mrad at 701 rad/min gave an average graft thickness of ca 100± 20 µm NVP g PDMS prepared with the same presoaking conditions followed with gamma irradiation in 10% NVP to 0 2 Mrad at 701 Mrad yielded an average graft thickness of 50 ±15 µ The difference in thickness observed for these two substrates arises from their inherently different structure and can be explained in terms of their respective sorption behavior

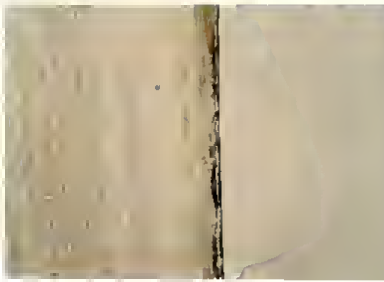

Figure 2.17 Light microscopy micrograph of crystal violet stained cross section of unmodified PMMA

Figure 2.18 Light microscopy micrograph of a stained cross section of NVP g PMMA (presoak in 40% NVP at 60°C for 4 hours 0.15 Mrad at 701 rad/min) showing a graft thickness of 100 μ

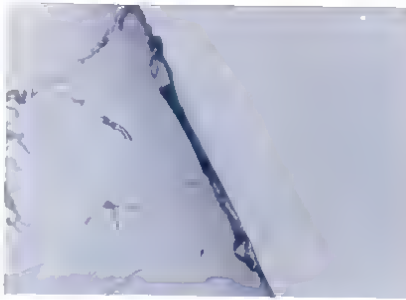

Figure 2 19 Light microscopy micrograph of a stained cross section of unmodified PDMS

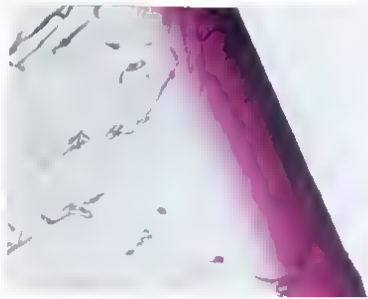

Figure 2 20 Light microscopy micrograph of a stained cross section of NVP g PDMS (presoak in 40% NVP at 60°C for 4 hours 0 2 Mrad at 701 rad/min) showing a graft thickness of 50 µ

Table 2.3 Graft thickness measured [illegible]

Sample	[illegible] thickness, μm
NVP-g-PMMA[1] no preoak	could not be visualized
NVP-g-PMMA[1] preoak[2]	180±20
(γ-PVP/NVP)-g-PMMA[1] (γ-PVP) NVP at 1.3	could not be visualized
(K90 PVP/NVP)-g-PMMA[1] (K90 PVP) NVP at 1.4	could not be visualized
NVP-g-PDMS[3] no preoak	could not be visualized
NVP-g-PDMS[3] preoak[2]	50±15
(γ-PVP/NVP)-g-PDMS[3] (γ-PVP) NVP at 1.3	could not be visualized
(K90 PVP/NVP)-g-PDMS[3] (K90-PVP) NVP at 1.4	could not be visualized

[1] Irradiated in 10% NVP to 0.15 Mrad at 701 rad/min

[2] Preoak was conducted in 40% NVP at 60°C for 4 hours

[3] Irradiated in 10% NVP to 0.2 Mrad at 701 rad/min

In these experiments presoaking was conducted in 40% NVP a[illegible] At this temperature the diffusion of NVP into PMMA was enhanced[illegible] Physical aging studies have shown that below the glass transition temperature of PMMA (T_g~105°C) some relaxation phenomena occur above the β relaxation temperature (45°C) and may account for this enhanced diffusion (37) At the completion of the presoak the PMMA samples were transferred to the grafting solution containing 10% NVP and gamma irradiation was performed at room temperature. Some NVP is expected to diffuse out from the substrate due the negative concentration gradient In the case of PMMA however only limited diffusion might take place since molecular motions are "frozen" at this temperature In contrast PDMS (T_g~ 123°C) has very high chain mobility at room temperature and the diffusion of NVP out of the bulk of PDMS during gamma radiation is probably more significant despite the crosslinked structure This may account for the lower graft thickness observed

The results of graft thickness measurements by light microscopy suggest that for both PMMA and PDMS grafts obtained with presoaking in 40% NVP at 80°C for 4 hours have high penetration into the bulk of the base substrate in contrast to those obtained using PVP/NVP solutions (i e Y PVP/NVP or K90 PVP/NVP solutions) with no NVP presoak This is particularly important to PDMS which has been shown to undergo changes in optical properties upon grafting of NVP with the NVP presoak method Gamma induced graft polymerization of Y PVP/NVP and K90 PVP/NVP to PMMA and PDMS without NVP presoak may afford PVP grafts with less penetration in the substrate

2.4.1.2 FTIR/ATR analysis

As discussed in section 3.1.2.1.1 the depth of penetration of the probing beam in this technique depends upon the type of crystal used (refractive index, angle of incidence). The crystal used here is a ZnSe 60° crystal which gives a depth of penetration of 0.66μm as calculated from equation 2.3. The FTIR/ATR spectrum of unmodified PMMA is shown in Figure 2.21. The assignments for the major absorption peaks are shown in Table 2.4. Shown in Figure 2.22 is the FTIR/ATR spectrum of NVP g PMMA prepared with preswelling in 40% NVP at 60°C for 4 hours. Inspection of the carbonyl region reveals the appearance of a new peak at 1665 cm^{-1} assigned to the PVP amide carbonyl. A typical spectrum of a (γ PVP/NVP) g PMMA sample is shown in Figure 2.23. A new peak from the PVP carbonyl is also visible at the same wavenumber (1665 cm^{-1}).

In order to compare the relative amounts of PVP present on these surfaces, the ratio of the absorbance of the amide carbonyl from PVP (1665 cm^{-1}) to the ester carbonyl of PMMA (1725 cm^{-1}) was evaluated for each spectrum. The results given in Table 2.6 suggest that within the depth of penetration of the method used here (0.66 μ) the concentration of PVP grafts for NVP g PMMA prepared using preswelling in 40% NVP at 60°C for 4 hours, then gamma irradiated in 10% NVP to a dose of 0.15 Mrad at dose rate of 701 rad/min, is only slightly higher than that of (γ PVP/NVP) g PMMA (10% total concentration, γ PVP:NVP ratio of 1:3) and (K90 PVP/NVP) g PMMA (10% total concentration, K90 PVP:NVP ratio of 1:4) prepared with the same dose and at the same dose rate.

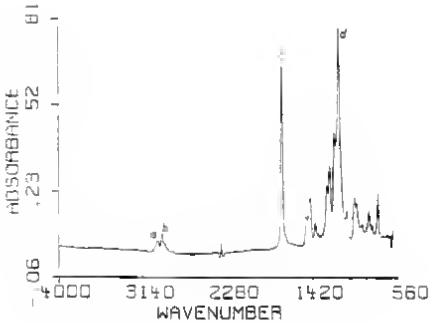

Figure 2 21 FTIR/ATR spectrum of unmodified PMMA

Table 2 4 Major IR absorption for PMMA

wavenumber (cm $^{-1}$)	peak	assignment
2950	a	CH_2 assymetric stretch
2844	b	CH_2 symmetric stretch
1725	c	ester carbonyl stretch
1118 1082	d	C O C stretch

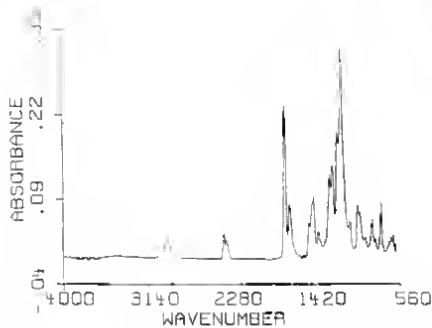

Figure 2 22 FTIR/ATR spectrum of NVP-g PMMA prepared with preswaking in 40% NVP at 80°C for 4 hours then 10% NVP/0 15 Mrad/701 rad/min

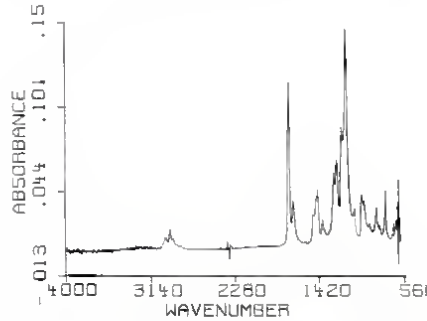

Figure 2 23 FTIR/ATR spectrum of (γ PVP/NVP) g PMMA with a γ PVP/NVP total concentration of 10% γ-PVP NVP ratio of 1 3 0 15Mrad/ 701rad/min

The FTIR/ATR spectrum of unmodified PDMS and its peak assignments are shown in Figure 2 24 and Table 2 5 respectively The FTIR/ATR spectrum of NVP g PDMS prepared with preSoaking in 40% NVP for 60°C for 4 hours then irradiating in 10% NVP to a dose of 0 2 Mrad at a dose rate of 761 rad/min is shown in Figure 2 25 As discussed for PMMA this spectrum shows a new absorption peak at 1665 cm^{-1} which was assigned to the amide carbonyl of PVP The spectrum of (γ PVP/NVP) g PDMS (10% total concentration γ PVP NVP ratio of 1:3) displayed in Figure 2-26 also shows a peak for the amide carbonyl of PVP The intensities of these carbonyl absorption were compared to the absorption of the Si CH_3 stretch at 1255 cm^{-1} The results are given in Table 2 6 These samples show similar relative intensities The results of FTIR analysis suggest that within the depth of penetration of the method used here (0 66μm) PVP concentrations in the grafts prepared by presoaking in 40% NVP at 60°C for 4 hours then irradiating in 10% NVP are comparable to those in PVP grafts obtained by using γ PVP/NVP or K90 PVP/NVP mixtures without presoaking It is important to note that for all of the samples analyzed here strong absorption bands from the base substrate can still be seen This has been previously observed for the PVP grafts prepared by the preSoak and attributed to the IPN structure of the graft which is embedded to some depth in the substrate (8) The diffusion of NVP into the substrate during presoaking and subsequent polymerization may account for this phenomenon However for samples prepared using γ PVP/NVP or K90-PVP/NVP solutions the penetration of the grafts to the base substrate is minimal

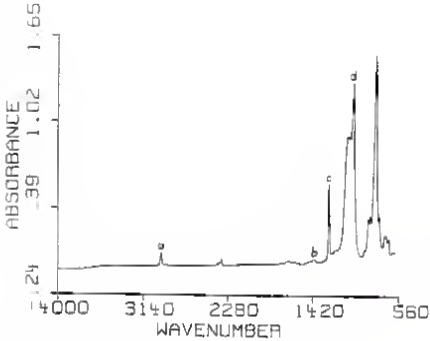

Figure 2 24 FTIR/ATR spectrum of unmodified PDMS

Table 2 5 Major IR absorption for PDMS

wavenumber (cm $^{-1}$)	peak	assignment
2961	a	CH_3 stretch
1412	b	CH_3 bend
1256	c	Si CH_3 stretch
1006	d	Si O Si stretch

Figure 2 25 FTIR/ATR spectrum of NVP g PDMS prepared with presoaking in 40% NVP at 60°C for 4 hours then irradiating in 10% NVP/0 2 Mrad/70l rad/min

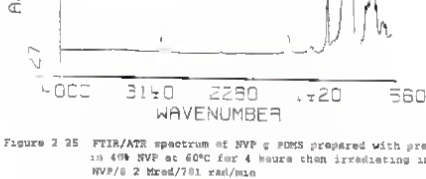

Figure 2 26 FTIR/ATR spectrum of (γ PVP/NVP) g PDMS with a γ PVP/NVP total concentration of 10% γ PVP/NVP ratio of 1 3 0 2Mrad/ 70lrad/min

Table 2 6 Relative absorbance of amide carbonyl in [illegible] various samples

Sample	R = A(1665)/A(1725)*
NVP @ PMMA pressak 40%NVP/60°C/4hrs 10%NVP/0 15Mrad/ 70lrad/min	0 35
(γ PVP/NVP) @ PMMA 10% γ PVP NVP af 1:3 0 15Mrad/ 70lrad/min	0 32
(K90 PVP/NVP) @ PMMA 10% K90 PVP NVP af 1 4 0 15Mrad/ 70lrad/min	0 26
	R = A(1665)/A(1256)*
NVP @ PBMS pressak 40%NVP/60°C/4hrs 10%NVP/0 2Mrad/ 70lrad/min	0 23
(γ PVP/NVP) @ PBMS 10% γ PVP NVP af 1 3 0 2Mrad/ 70lrad/min	0 22
(K90 PVP/NVP) @ PBMS 10% K90 PVP NVP af 1:4 0 2Mrad/ 70lrad/min	0 20

* A(1665) is the absorbance at 1665 cm^{-1}

A(1725) is the absorbance at 1725 cm^{-1}

A(1256) is the absorbance at 1412 cm^{-1}

2.4.1.3 XPS analysis

XPS analysis provides information about the elemental composition from the outermost region of the surface (ca 50 Å). Figure 2.27 shows an XPS survey scan of unmodified PMMA. As expected, the only elements present on the surface are carbon and oxygen. Figure 2.28 shows the XPS spectrum of NVP g PMMA prepared with presoaking in 40% NVP at 60°C for 4 hours then irradiating in 10% NVP to a dose of 0.15 Mrad at a dose rate of 7.81 rad/min. This spectrum shows the presence of a nitrogen peak (N1s) at a binding energy of 402 eV. Displayed in Figure 2.29 is an XPS spectrum of (y PVP/NVP) g PMMA prepared using a total concentration of 10% and a y PVP NVP ratio of 1:3 (@ 1.5 Mrad at 7.81 rad/min). This sample shows the presence of a more intense N1s peak. Typical XPS spectra for (KSP PVP/NVP) g PMMA (not shown here) also show the presence of a N1s peak.

The atomic concentrations for various samples measured by XPS are shown in Table 2.7. Experimental values obtained for unmodified PMMA and PDMS are close to theoretical values. The small discrepancy observed can be accounted for by the presence of hydrocarbon contamination from the air. The experimental values for PVP gave a O1s/N1s (O1s/N1s = 1.8) higher than that expected from theoretical calculations (O1s/N1s = 1.0). The presence of higher oxygen content is may be due to surface oxidation and perhaps to some contamination from the the analysis chamber.

The XPS data for NVP g PMMA prepared with presoaking (40%/60°C/4hours) then irradiating in 10% NVP to a dose of @ 1.5 Mrad reveal the presence of a significant amount of nitrogen (4.2%) from

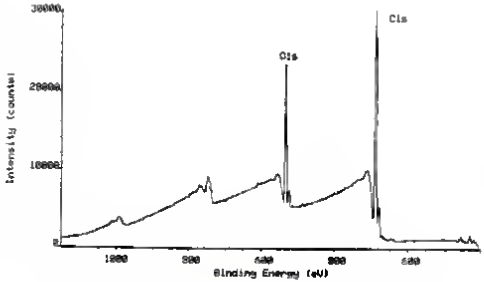

Figure 2 27 XPS spectrum of unmodified PMMA

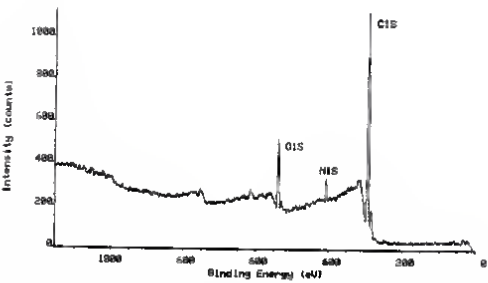

Figure 2 28 XPS spectrum of NVP g-PMMA prepared with preseaking in 40% NVP at 60°C for 4 hours then 10% NVP/0.15 Mrad/70% rad/min

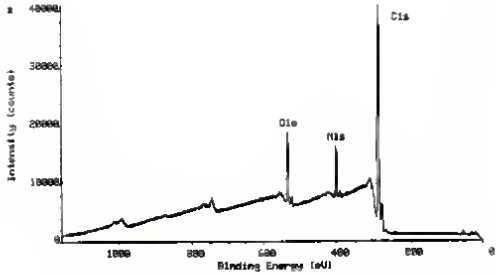

Figure 2.25 XPS spectrum of of (γ PVP/NVP) g PDMS with a γ PVP/NVP total concentration of 15% γ-PVP NVP ratio of 1 3 0.2Mrad/ 701rad/min

the PVP graft However this value is lower than that observed for a pure PVP surface also given in Table 2 7 (7 8%) This may be attributable to the fact that PVP grafts prepared with the pressak method penetrate into the substrate and may have an IPN structure (8) This discrepancy may also be due to the structural water contained within the PVP hydrogel in addition to surface oxidation and contamination

The XPS data for (γ PVP/NVP) g-PMMA prepared using a total concentration of 10% and a γ PVP:NVP ratio of 1 3 (@ 15 Mrad at 701 rad/min) shows a nitrogen content (6 8%) close to that observed for a pure PVP surface (7 7%) This suggests that PVP grafts obtained using γ PVP/NVP mixtures may be homogeneous and may have less penetration into the substrate However (K30 PVP/NVP) g PMMA (10% (K30 PVP) NVP of 1 4) irradiated to 0 15 Mrad showed a substantially lower nitrogen content (2 0%) The structural differences between γ PVP and K30 PVP discussed earlier may account for this observation

Figure 2 33 shows the XPS spectrum of unmodified PDMS The values obtained are in good agreement with those anticipated from theoretical calculations The XPS spectrum of NVP g PDMS prepared with pressak (40%/60°C/4hours) then gamma irradiation in 10% NVP (@ 15 Mrad, 701rad/min) shown in Figure 2 31 reveals the presence of a Nls peak Nitrogen is also present in the XPS spectrum of (γ PVP/NVP) g PMMA prepared using a total concentration of 10% and a γ PVP:NVP ratio of 1 3 (@ 15 Mrad at 701 rad/min) as shown in Figure 2 32

Quantitative elemental analysis of these samples given in Table 2 7, shows the presence of only 1 5% of nitrogen in NVP g PDMS

Table 2 7 XPS data for (γ PVP/NVP) and [illegible] PMMA and PDMS (701 rad/min)

sample	Atomic Concentration (%) C1s	O1s	N1s	Si2p	[illegible]
PMMA[1]	71 0	29 0			
PMMA-	76 3	24 7			
(γ PVP/NVP) g PMMA γ PVP NVP of 1 3 10%/0 15Mrad	76 8	16 4	6 8		[illegible]
(K90 PVP/NVP) g PMMA K90 PVP NVP of 1 4 10%/0 15Mrad	78 7	18 3	2 0		[illegible]
NVP g PMMA 10%/0 15Mrad	75 8	23 2	1 0		[illegible]
NVP g PMMA Presoak[3] 10%NVP/0 15Mrad	78 1	17 7	4 2		[illegible]
PDMS[1]	50 0	25 0		25 0	
PDMS[2]	51 1	27 7		21 2	
(γ PVP/NVP) g PDMS γ PVP NVP of 1 3 10%/0 15Mrad	50 3	28 1	3 5	17	[illegible]
(K90 PVP/NVP) g PDMS K90 PVP NVP of 1 4 10%/0 15Mrad	50 3	26 8	1 5	19 2	[illegible]
NVP g PDMS 10%NVP/0 15Mrad	50 4	28 5	0 6	20 5	[illegible]
NVP g PDMS Presoak[3] 10%NVP/0 15Mrad	49 0	30 5	1 5	19 0	[illegible]
PVP[1]	75 0	12 5	12_5		1 0
PVP-	78 1	14 0	7 9		1 8

[1] Theoretical [2] Experimental [3] presoak in 40% NVP/50°C/4heure

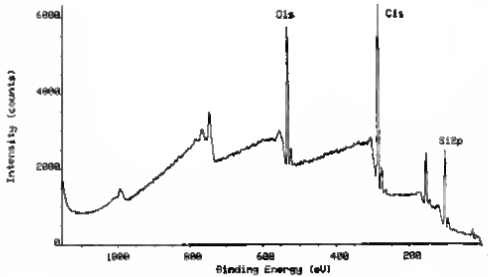

Figure 2 30 XPS spectrum of unmodified PDMS

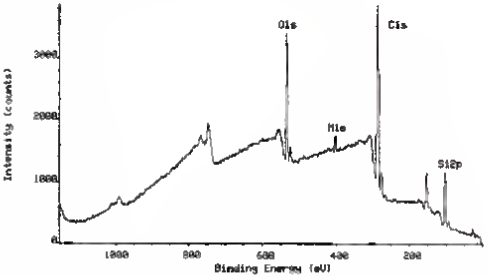

Figure 2 31 XPS spectrum of NVP g PDMS prepared with pressak (40% NVP/60°C/4hrs) then irradiation in 10% NVP (0 2 Mrad/701 rad/min)

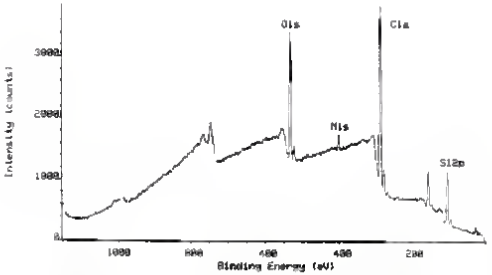

Figure 2 32 XPS spectrum of (γ PVP/NVP) g PDMS prepared using a total concentration of 10% and a γ PVP NVP ratio of 1 3 (0 2 Mrad/791 rad/min)

Figure 2 33 SEM micrograph of (γ PVP/NVP) g PMMA prepared using a total concentration of 10% and a γ PVP NVP ratio of 1 3 (0 15 Mrad/701 rad/min)

prepared using presoak PDMS has a dynamic molecular structure and is very susceptible to molecular rearrangements Hydrophilic PVP grafts may get buried in the bulk of substrate when PDMS tends to expose apolar methyl groups in the ultra high vacuum environment of the XPS analysis chamber (K90 PVP/NVP) g PDMS (10% (K90 PVP) NVP of 1:4) irradiated to a dose of 0 2 Mrad gave a similar nitrogen content (1 5%) (γ PVP/NVP) g PDMS prepared using a total concentration of 10% and a γ PVP:NVP ratio of 1 3 (0 2 Mrad at 701 rad/min) gave a higher nitrogen content (3 5%) and a substantially lower Cls/Nls ratio (0 3) Even though these values are not consistent with the elemental composition of pure PVP surface the use of (γ PVP/NVP) mixtures appears to improve grafting onto PDMS It is also possible that (γ PVP/NVP) g PDMS may be less susceptible to surface molecular reorganization due to reduced penetration of the graft in the host substrate and increased crosslinking afforded by the highly branched structure of γ PVP

The XPS results suggest that PVP grafts obtained using γ PVP/NVP solutions may be restricted to the outer surface of PDMA in contrast to those obtained using presoak (40%/60°C/4hours) which may have an IPN structure within the substrate This is evidenced by the elemental composition observed for (γ PVP/NVP) g PDMA prepared using a total concentration of 10% and a γ PVP NVP ratio of 1 3 (0 15 Mrad at 701 rad/min) which was close to that observed for pure PVP surface

The significance of the XPS data obtained for PDMS grafts resides in the fact that PVP grafts obtained using γ PVP/NVP may also have less penetration in the substrate as shown by a higher nitrogen

concen[illegible] such grafts may also be more stable to the molecular reorganization of PDMS surface and may perhaps reduce the change [illegible] optical properties of PVP modified PDMS IOLs The stability of PDMS grafts is discussed in detail in section 2 4 i 5

2.4.1.4 SEM

Previous studies in our laboratory have shown that high voltage electron beams (5 30 Kev) used during SEM can cause damage to polymer surfaces and hence give erroneous morphological observations Therefore SEM was conducted on uncoated samples using low voltage microscopy (0 5 1.0 Kev) Unmodified PMMA used in this study has a smooth surface (SEM not shown here) The purpose of SEM here is to provide some evidence that surface modification using γ PVP does not introduce any additional morphological artifacts An SEM micrograph of (γ PVP/NVP) g PMMA prepared using a total concentration of i0% and a γ PVP NVP ratio of i 3 (0 15 Mrad at 70i rad/min) in Figure 2 33 shows a smooth and homogeneous surface

2.4.1.5 Stability of PDMS grafts

because of mobile molecular structure (Tg- i23°C) the PDMS surface is very susceptible to molecular reorrengements To minimize free energy, PDMS tends to expose methyl groups when kept in a hydrophobic environment This raises the question of stability of hydrophilic grafts onto PDMS It is believed that thin covalently bonded and crosslinked grafts should be less susceptible to changes due to molecular motion and reorganization of the substrate material and hence be more stable Experiments were therefore carried out to investigate the stability of PVP grafts on PDMS

Samples grafted under different conditions were aged at [redacted] for 4 weeks Contact angles were measured once a week Samples were hydrated in distilled water for 10 minutes prior to contact angle measurements After aging samples were rinsed with distilled water dried and analyzed with XPS Contact angle and XPS data are shown in Table 2 S (γ PVP/NVP) g PDMS and (K90 PVP/NVP) g PDMS showed no significant change in contact angle after aging for 4 weeks at 80°C in air (an increase of 3° and 5° respectively) In contrast NVP g PDMS prepared with premask (40% NVP/60°C/4hours) then irradiation in 10% NVP (7 2 Mrad/70krad/min) showed a significant increase in contact angle (an increase of 12°) This is also confirmed by the XPS data which shows a more pronounced decrease in the nitrogen content after aging for NVP g PDMS (ca 50%) The decrease of nitrogen content after aging for (γ PVP/NVP) g PDMS and (K90 PVP/NVP) g PDMS was approximately 8% and 30% respectively

These results suggest that the PVP grafts obtained for PDMS using the γ PVP/NVP and K90 PVP/NVP solutions may be more stable to molecular motion of the bulk substrate than those obtained with premask (40% NVP/60°C/4hours) It is possible that the use of γ PVP/NVP and K90 PVP/NVP solutions reduces diffusion of the monomer in the bulk of the substrate and hence affords PVP grafts which are restricted to the surface of PDMS These solutions may also afford grafts with some degree of crosslinking which may enhance graft stability Thin and crosslinked PVP grafts which are restricted to the surface of PDMS may be less susceptible to molecular reorganization of the bulk substrate

Table 2 8 Contact angle and XPS data for PDMS grafted aged at 60°C in air

Sample	Contact Angle[1] (°)				XPS	
	week1	week2	week3	week4	week1	week4
(γ PVP/NVP) g PDMS γ PVP NVP of 1 3 10%/0 2Mrad	17	18	18	21	1 5	1 2
(K90 PVP/NVP) g PDMS K90 PVP NVP of 1 4 10%/0 2Mrad	19	20	25	25	1 5	1 0
NVP g PDMS 10%NVP/0 2Mrad	30	35	35	44	0 6	
NVP g PDMS Presoak[2] 10%NVP/0 2Mrad	18	20	25	30	1 5	0 7

[1] Samples were rehydrated in distilled water for 10 minutes prior to contact angle measurements

[2] Presoaking was conducted in 40% NVP at 60°C for 4 hours

2.4.1.5 Summary of grafting of PVP/NVP onto PMMA and PDMS

The use of γ-PVP/NVP and K90 PVP/NVP solutions for grafting has shown to produce thinner and less penetrating hydrophilic grafts with greater stability than those obtained by using only NVP monomer solutions in combination with NVP preseeking.

Grafts obtained using γ-PVP/NVP and K90 PVP/NVP solutions could not be visualized using optical microscopy and hence were estimated to be less than 3μm in thickness. Grafts prepared with NVP monomer solutions using NVP preseek (40% NVP/60°C/4hrs) were found to have a more penetration into the substrate. However FTIR/ATR analysis with a depth of penetration of 0.66μ showed the presence of comparable amounts of PVP for both methods. XPS analysis with a depth of penetration of 50Å revealed significantly more nitrogen for γ-PVP/NVP and K90 PVP/NVP solutions grafted samples. This suggests that the grafts obtained using γ-PVP/NVP and K90 PVP/NVP systems may be restricted to the outermost surface of the substrate.

Irradiation of PVP solutions (i.e. γ-PVP or K90 PVP) leads to the formation of macroradicals (i.e. radicals on the polymers chains) followed by intermolecular and intramolecular crosslinking. Since PVP is a good wetting agents for PDMS and PMMA, these radicals are readily accessible to free radicals produced on the substrate surface. Graft surface copolymerization can therefore occur by recombination of radicals with concomitant crosslinking of PVP as schematically shown in Figure 2.14. The presence of small amount of NVP may also create highly mobile low molecular weight radicals and enhance these reactions.

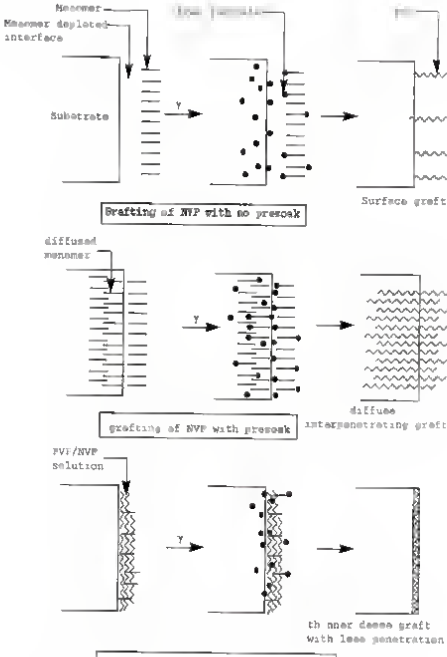

Figure 2.14 Schematic representation of gamma induced grafting of PVP/NVP and NVP

In fact simultaneous formation of macroradicals and low molecular weight radicals were shown to be the key factors in the crosslinking reactions (95)

The results also indicate that γ-PVP/NVP appears to graft more efficiently on both PMMA and PDMS γ PVP used in this research was prepared by irradiating an aqueous solution of 10% NVP to a dose of 0 15 Mrad at a dose rate of 781 rad/min As discussed in sections 2 3 1 3 this water soluble polymer may have a highly branched structure which can result in the generation of more free radicals during gamma irradiation and perhaps PVP grafts with some degree of crosslinking The G values of crosslinking for branched polymers have been found to be higher than those of linear polymers (96) PVP grafts on PDMS obtained using γ PVP/NVP or K90 PVP/NVP solutions were also found to be more stable than those prepared from NVP monomer alone using NVP prepolk

2.4.2 Surface Graft Polymerization of Vinyl Sulfonate Monomers onto PMMA and PDMS

Surface ionicity is one of the major factors which regulates polymer tissue interactions The anionic polyelectrolyte behavior of the majority of the bioactive molecules such as heparin and chondroitin sulfate is due to the presence of carboxyl and sulfonic acid groups The importance of heparin as a bioactive molecule with anticlotting properties has prompted the synthesis of heparin analogs derived from various polysaccharides in attempts to correlate their biological activities with structural features and perhaps produce

purely synthetic bioactive molecules with antithrombogenic properties. The synthesis of these analogs is usually achieved by introducing sulfonic acid groups onto polysaccharide substrates. It was therefore of interest to prepare surfaces modified by introducing sulfonic acid groups onto PMMA and PDMS and to examine their properties. Inagaki et al reported sulfonic acid group containing thin films prepared by plasma polymerization of hydrocarbon/SO_2 to be nonthrombogenic (99).

In this research, vinyl functional monomers containing sulfonic acid groups were radiation graft polymerized onto PMMA and PDMS. The monomers used were styrenesulfonic acid (SSA), acrylamide methyl propanesulfonic acid (AMPSA), potassium sulfopropylacrylate (KSPA), and potassium sulfopropylmethacrylate (KSPMA).

It is important to note that free radical polymerization of vinyl monomers containing carboxylic or sulfonic acid groups exhibits some departures from that of neutral polymers. The rate of polymerization is strongly dependent on the ionization state of the acid group. At low pH the acid group is not fully ionized and the rate of polymerization is high. A decrease in the polymerization rate is usually observed with increasing pH. This is believed to arise from electrostatic repulsions between the macroradical and the monomer due to increased acid dissociation. The rate of polymerization reaches a minimum when the macroradical and the monomer are fully ionized (e.g., pH of 6-7 for methacrylic acid) (99). With continued increase in the pH, the polymerization rate

increases perhaps because of ion pair formation which minimizes electrostatic repulsions The polymerization of vinyl monomers containing carboxylic and sulfonic acid groups is greatly affected by the pKa of the acid and the pH of the polymerization medium

Salts of sulfonic acid monomers were used in this research because of greater water solubility over their acid analogs and ionization over a wider range of pH

2.4.2.1 Surface graft polymerization of vinyl sulfonic acid monomers onto PMMA

Gamma radiation grafting of styrenesulfonic acid (SSA) and NVP on SSA onto PMMA was studied in detail PMMA samples (1cmx4cmx2 4mm) with a typical weight of 1 0 g were immersed in grafting solutions which consisted of aqueous SSA or NVP comonomer solutions with total concentrations varying from 10 to 40% and SSA NVP ratios of 1 0 1 1 and 2 1 Samples were vacuum degassed and backfilled with argon prior to gamma irradiation as described in section 2 3 2 2 2 Irradiation was conducted at room temperature to a dose of 0 15 Mrad at a dose rate of 701 rad/min

As shown in Table 2 5 grafting of pure SSA or comonomer solutions of SSA and NVP without NVP preoaking was not efficient This behavior has been previously observed and attributed to reduced diffusion of monomer into the substrate due to hydrophobic repulsion forces (8) This appears to be more prominent in the presence of SSA because of additional electrostatic forces introduced by the sulfonic acid group (SO_3^-) However it can be seen that significant weight gain (0 5%) and low contact angle was obtained for a total concentration

Table 2 9 Gravimetric analysis and contact angle data [illegible]
(SSA co NVP) g PMMA (0 15 Mrad 701 rad/min

SSA NVP ratio	Total Conc %	Precoak	W gain %	C A	[illegible] Time
1 0	10	na	0 0	60	5300
1 0	20	na	0 2	35	0400
1 1	20	na	0 4	31	1100
2 1	30	na	0 1	35	2300
1 1	40	na	0 5	22	1300
1 0	10	a	0 0	58	5300
1 0	20	a	0 3	35	0400
1 1	20	a	0 4	23	1100
2 1	30	a	0 4	25	2300
1 1	40	a	0 5	24	1300
1 0	10	b	0 4	25	5300
1 0	20	b	1 5	22	0400
1 1	20	b	3 2	10	1100
2 1	30	b	0 3	11	2300
1 1	40	b	6 1	13	1300

a Prasoaking in the same monomer solution at room temperature (ca 25°C) for 24 hours

b Prasoaking in 40% NVP at 60°C for 4 hours

* Viscosity was measured at 25°C using a Brookfield viscometer DV II (CP 52) at a shear rate of 1 0 s $^{-1}$

of 40% and a l[illegible] SSA:NVP this is may be due to the lower solution viscosity (the viscosity of monomer solution after gamma irradiation) obtained for this composition (1300 Cps). Since free radical polymerization is diffusion controlled, the diffusion of the monomer to the reactive site on the substrate surface is only slightly hindered. SSA may copolymerize with NVP with preferential incorporation of SSA according to their reactivity ratios (r_{NVP}=0.894, r_{SSA}=7.18) (43). The low viscosity observed may possibly arise from reduced propagation rate due to electrostatic repulsions between the sulfonate anion of the monomer and that of the growing macroradical, in analogy to those reported between carboxylate anions (COO^-) in free radical polymerization of acrylic and methacrylic acid in the 5-7 pH range where the carboxylic acid group is fully ionized (99).

To enhance grafting efficiency, different presoaking conditions were investigated. Method (a) consisted of presoaking samples in the grafting solution at room temperature for 24 hours prior to irradiation. Samples were immersed in grafting solutions, allowed to sit at room temperature for 24 hours, then degassed prior to gamma irradiation. Method (b) consisted of presoaking in 40% NVP at 55°C for 4 hours before transferring to the monomer solution.

Grafting results obtained for presoaking method(s) showed no significant improvement over grafting without presoak, except for a total concentration of 30% and a SSA:NVP ratio of 2:1, which gave a 10° decrease in contact angle. No further investigation was pursued with these presoaking conditions.

Presoaking in 40% NVP at 50°C for 4 hours (i e method (b)) prior to gamma irradiation gave significantly higher weight gains and lower contact angles Sample grafted with 10% SSA gave a relatively lower weight gain (0 4%) and a contact angle of 25° This may be explained in terms of homopolymerization kinetics of sulfonic acid group containing vinyl monomers which have been reported to polymerize to relatively lower molecular weights and conversion due to electrostatic repulsions (100) Increasing the concentration of SSA to 20% appears to increase grafting yield as evidenced by an increase in weight gain (to 1 5%) This may be due to reduction of repulsive forces due to ion pairs formation (101)

Copolymerization of SSA with NVP appears to enhance grafting yield as evidenced by significantly higher weight gains (3 2 6 1%) and slightly lower contact angles (18 13°) The most significant weight gain (6 1%) was obtained for a total concentration of 40% and SSA/NVP ratio of 1 1 Copolymerization of sulfonic acid group containing vinyl monomers (e g , SSA AMPSA) with neutral monomers has been used to obtain high molecular weight polyelectrolytes with higher stability and lower cost (100)

As shown in Figure 2 35 and Table 2 10 XPS elemental analysis reveals the presence of various amounts of sulfur on grafted PMMA SSA g PMMA prepared using a SSA concentration of 20% gave relatively lower sulfur content (1 0%) This is consistant with gravimetric analysis which gave a weight gain of only 1 4% A small amount of nitrogen (1 5%) can also be seen on this sample perhaps due to NVP from the precoat which polymerizes during gamma irradiation

Table 2.10 XPS elemental analysis data for SSA g PMMA and (SSA co NVP) g PMMA (0.15 Mrad 701 rad/min)

SSA:NVP ratio	Total Conc %	Pretreat	C1s (%)	O1s (%)	N1s (%)	S2p (%)	CA (°)
1:0	20	b	78.3	18.2	1.5	1.0	22
theoretical			80.7	25.8		3.3	
2:1	10	b	75.1	22.3	1.5	0.9	13
theoretical			80.8	21.9	3.1	0.2	
1:1	40	b	75.8	18.8	3.1	2.3	11
theoretical			70.0	20.0	5.0	5.0	
1:1	40	aa	78.1	29.8			22
theoretical			78.0	20.0	5.0	5.0	

a: Presoaking in the same monomer solution at RT for 24 hours

b: Presoaking in 40% NVP at 60°C for 4 hours.

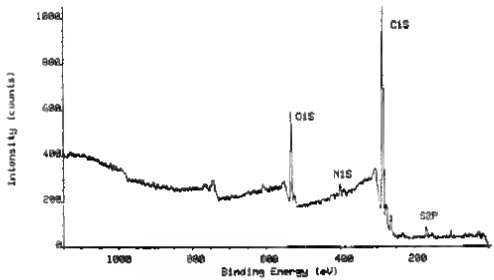

Figure 2.35 XPS spectrum of (SSA co NVP) g PMMA (40% SSA:NVP ratio of 1:1 0.15 Mrad 701 rad/min)

The highest sulfur content (2 3%) was obtained for (SSA co NVP) g PMMA with total concentration of 40% and 1 1 [illegible] SSA:NVP, and presoak method (h) (40%NVP/60°C/4hrs) This is also consistent with gravimetric analysis and contact angle measurements obtained for this sample (5 1% 13°C) However XPS data indicate that the elemental surface composition observed is not consistent with that anticipated from theoretical calculations (i e 5 0% nitrogen and 5 0% sulfur) This is possibly due to the fact that SSA co NVP grafts may form an IPN copolymer structure with the base substrate in contrast to a homogeneous layer of poly(SSA co NVP) Surface oxidation and contamination may also be responsible for this discrepancy The FTIR/ATR spectrum of (SSA co NVP) g PMMA (40%- 1 1 ratio of SSA NVP 0 15 Mrad, 70l rad/min) in Figure 2 36 showed little evidence of a thick graft

The graft data for other vinyl sulfonic acid monomers (i e sodium salt of acrylamide methyl propanesulfonic acid (AMPSA) potassium sulfopropylacrylate (KSPA)- and potassium sulfopropylmethacrylate (KSPMA)) onto PMMA is given in Table 2 11 Previous research conducted in our laboratories (8) and the results obtained here for SSA suggest that presoaking in 40% NVP for 4 hours at 60° enhances grafting significantly These NVP presoak conditions were therefore used with PMMA in further experiments Samples were presoaked in 40% NVP at 60°C for 4 hours then transferred to grafting solutions Total concentrations for AMPSA/NVP comonomer solutions were varied from 5 to 10% and AMPSA NVP ratios from 1 0 to 0 1 Total concentration for both SPMA/NVP and SPA/NVP comonomer solutions

Table 2.11 Gravimetric analysis and contact angle data for grafting of sulfonic acid monomers to PMMA Preemak in 40% NVP for 4 hours at 60° (701 rad/min)

AMPSA:NVP ratio	Total Conc %	Dose Mrad.	W gain %	CA (°)	Vis * (Cps)
1:0	5	0.05	0.3	50	2100
1:0	5	0.1	0.2	26	4200
1:0	10	0.05	1.3	22	8800
1:0	10	0.1			gel
1:4	10	0.05	2.2	14	6100
1:1	10	0.05	2.1	10	15000
4:1	10	0.05	2.5	10	17400
0:1	10	0.05	0.2	21	4200
SPMA:NVP ratio					
1:0	10	0.15	0.0	47	7600
1:0	20	0.15	0.1	41	8900
1:1	20	0.15	0.3	22	4500
2:1	30	0.15	0.4	34	3400
1:2	30	0.15	0.4	25	6500
KSPA:NVP ratio					
1:0	10	0.15	2.1	10	8800
1:0	20	0.15			gel
1:1	20	0.15	2.5	20	6500
2:1	30	0.15	3.1	21	5400
1:2	30	0.15	1.5	10	7500

* Viscosity was measured at 25°C using a Brookfield viscometer RV II (CP 52) at a shear rate of 1.0 s^{-1}

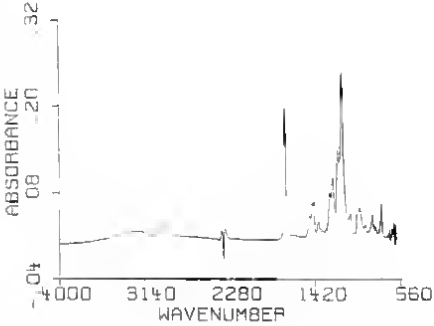

Figure 2 36. FTIR/ATR spectrum of (SSA co NVP) g PMMA (40% SSA NVP ratio of 1 1 0 15 Mrad 701 rad/min)

were varied from 10 to 30% with SPMA NVP and SPA NVP ratios of [illegible] 1 1 2 1, and 1 2 Samples were vacuum degassed then gamma irradiated to doses varying from 0 05 to 0 15 Mrad at a dose rate of 781 rad/min

AMPSA is very reactive and polymerizes at relatively low doses The gravimetric analysis and the contact angle data indicate that AMPSA can be graft copolymerized onto PMMA with radiation doses as low as 0 05 Mrad or less AMPSA g-PMMA prepared using 10% AMPSA with a dose of 0 05 Mrad gave a significant weight gain (1 3%) and a contact angle of 22°

Copolymerization of AMPSA with NVP was found to improve graft polymerization as evidenced by the increasing weight gain when NVP was added to the monomer solutions Weight gains were significantly higher for (AMPSA co NVP) g PMMA and varied from 2 1 to 2 5% Contact angles for (AMPSA co NVP) g PMMA were less than 20° AMPSA copolymerizes easily with NVP in solution at 60°C with AIBN as initiator (83) This copolymerization shows an enhancement near the 1 1 ratio of AMPSA NVP due to a donor acceptor character This is consistent with the results reported here This ratio gave a relatively higher viscosity (17400 Cps)

The XPS spectrum of AMPSA g PMMA (10% AMPSA 0 05 Mrad at 781 rad/min) in Figure 2-37 showed the presence of a S2p peak XPS analysis data is given in Table 2 12 Elemental analysis for AMPSA g PMMA shows the presence of 2 1% sulfur The small amount of nitrogen (0 3%) detected in this sample may be due to residual NVP from the premark

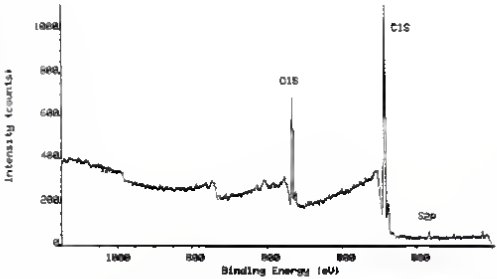

Figura [illegible]17 XPS spectrum o. AMPSA g PMMA (presoak 40% [illegible]VP/o0°C 4hrs [illegible]0% AMPSA 3 5 Mrad 701 rad/min)

Table 12 XPS elemental analysis of sulfonic acid monomers on NVP grafts on PMMA (pressed 40% NVP/60°C/4hrs 70% rel/min)

Sample	Total Conc %	Dose Mrad	C1s (%)	O1s (%)	N1s (%)	S2p (%)	CA (°)
AMPSA NVP 1:0	10	0.05	76.2	21.4	0.3	2.1	22
theoretical			54.0	30.0	8.0	8.0	
AMPSA NVP 4:1	10	0.05	74.8	21.1	2.4	1.7	18
theoretical			57.0	28.0	8.0	7.9	
SPMA:NVP 2:1	30	0.15	76.9	22.6	0.5		34
theoretical			62.1	26.5	4.7	4.7	
KSPA NVP 1:0	10	0.15	75.5	21.7	0.6	2.2	19
theoretical			54.9	36.3		8.9	
KSPA NVP 2:1	30	0.15	73.1	21.3	3.1	2.5	21
theoretical			59.0	32.0	3.0	6.0	
Control			76.3	25.7			

XPS analysis of (AMPSA co NVP) g PMMA prepared with a total concentration of 10% and a 4 1 ratio of AMPSA:NVP irradiated to a dose of 0 05 Mrad gave an elemental composition containing 1 7% sulfur and 2 4% nitrogen Since NVP and AMPSA have a tendency to alternate (r_{NVP} = 0 13 r_{AMPSA} = 0 55) and show little drift in the copolymer composition (94), the composition in the graft should be consistent with the stochiometry of the comonomer solution However the values observed were lower than those anticipated from theoretical elemental composition (8 0% nitrogen and 7 8% sulfur) This may be due to the fact that AMPSA co NVP grafts form an IPN copolymer structure with PMMA and are embedded to a certain depth (>50Å) in the base substrate

Even though SPMA polymerizes in solution by gamma radiation it appears from Table 2 11 that grafting to PMMA was minimal (i e no measurable weight gain contact angle of 47°) Results of XPS given in Table 2 12 indicate no detectable sulfur for SPMA g PMMA SPMA might have limited compatibility with PMMA and might not easily copolymerize with NVP for steric reasons as reported for some other sulfonic acid monomers (81)

Gamma induced grafting of KSPA to PMMA yields hydrophilic surfaces and significant weight gains KSPA g PMMA prepared using 10% KSPA irradiated to a dose of 0 15 Mrad gave a weight gain of 2 1% and a contact angle of 19° It can also be seen from Table 2 11 that grafting was enhanced by copolymerization of KSPA with NVP (KSPA co NVP) g PMMA prepared with total concentration of 30% and a ratio K3PA:NVP of 2 1 gave a contact angle of 21° and a weight gain

of 3 1% The appearance of a S2p peak in the XPS spectrum of KSPA g PMMA in Figure 2 37 provides further evidence of grafting Quantitative XPS analysis in Table 2 12 reveals the presence of 2 2% sulfur in KSPA g PMMA (10% KSPA 9 15 Mrad 701 rad/min) This is consistent with gravimetric analysis and contact angle measurement (KSPA co NVP) g PMMA gave a sulfur content (2 5%) lower than that anticipated from theory (5 9 %) However the nitrogen content(3 1%) was comparable to that of the theoretical elemental composition This is possibly due to the fact that KSPA may copolymerize with NVF with preferential incorporation of NVF The IPN structure of the graft should also not be ruled out

2.4.2.1 Surface graft copolymerization of vinyl sulfonic monomers to PDMS

In contrast to PMMA PDMS is well known for its radiation resistance therefore relatively higher radiation doses (1 e 20 15 Mrad) can be used to achieve good grafting This is particularly useful in the case of monomers which do not polymerize readily at low radiation doses

PDMS samples (1cmx4cmx1 9mm) with typical weight of 0 5g were presoaked in 40% NVF for 60°C for 4 hours, transferred to monomer solutions vacuum degassed then gamma irradiated

Total concentrations were varied from 5 to 40% with (NVF:vinyl sulfonic acid monomer) ratios ranging from 0 1 to 1 4 Radiation doses ranged from 0 05 to 0 5 Mrad at a fixed dose rate of 701 rad/min

As shown in Table 2 13, grafting of SSA onto PDMS yielded hydrophilic surfaces and significant weight gains Similar results

Table 2 13 Gravimetric analysis and contact angle data for (SSA co NVP) g PDMS and (AMPSA co NVP) g PDMS (pressak 40% NVP/50°C/4hours 701 rad/min)

SSA:NVP ratio	Total Conc. %	Dose Mrad	W gain %	C A (°)	Vis (Cps)
1 0	20	0 15	2 1	15	5300
1 0	20	0 25	2 2	17	6400
1 0	20	0 50	2 7	18	10300
1:1	40	0 05	2 1	19	940
1:1[2]	40	0 10			1050
2 1	30	0 05	3 0	15	960
2 1	30	0 10			1200
4:1	25	0 10	3 1	14	1000
4 1	25	0 15	2 5	15	1200
4 1[2]	25	0 20			1580
AMPSA NVP ratio					
1 0	5	0 15	0 0	50	2300
1:0	5	0 25	1 2	22	5600
1 0	10	0 05	0 0	35	8800
1:0	10	0 1			gel
1 4	10	0 05	0 2	45	6300
1:1	10	0 05	0 4	32	15600
4 1	10	0 05	1 3	21	17400

[1] Viscosity was measured at 25°C using a Brookfield viscometer DV II (CP 52) at a shear rate of 1 0 s [1]

[2] These samples became opaque and brittle

were achieved at much lower doses by copolymerization of SSA with NVP However when the dose was increased beyond 0 05 Mrad for a ratio of SSA NVP PDMS samples appeared opaque and brittle The deterioration of the mechanical and optical properties of PDMS was also observed for a 4 1 ratio of SSA NVP when the dose was increased beyond 0 15 Mrad It appears that high levels of grafting of SSA or NVP significantly affect the properties of PDMS The presence of large amounts of poly(SSA or NVP) within the PDMS may cause the formation of microdomains which effect optical and mechanical properties adversely This type of phase seperation has been previously observed for NVP g PDMS

It is interesting to note that SSA and SSA or NVP appear to graft copolymerize to PDMS more readily than to PMMA This may be due to the fact that PDMS may allow more diffusion of SSA molecules into the bulk due to high chain mobility In contrast diffusion of SSA in PMMA may be limited due to the large hydration sphere of sulfonate anion and low chain mobility of PMMA at room temperature (T_g(PMMA)~105°C) Chain mobility and free volume effects have been shown to play a major role in diffusional transport in polymers [102]

In the case of AMPSA weight gain and contact angle measurements indicate that grafting of AMPSA to PDMS is achieved when low monomer concentrations are used in combination with high doses AMPSA g PDMS (5% 0 25 Mrad) gave weight gain of 1 2% and a contact angle of 22° The copolymerization of AMPSA and NVP with a total concentration of 10% and a AMPSA:NVP ratio of 4 1 gave similar

results (1 3% Zr[*]) but at much lower dose (0 05 Mrad) In free radical polymerization of AMPSA solutions electrostatic repulsions between the monomer and the growing macroradical decrease the rate of polymerization and hinder the attainment of high molecular weights Copolymerization of AMPSA with NVP may reduce repulsion forces which may increase the rate of polymerization and allow higher MWs to be obtained The results of solution viscosity obtained here suggest that AMPSA is very reactive with NVP and that the onset of gelation occurs at very low radiation dose especially at AMPSA NVP ratio of 4 1 This may be due to some donor acceptor character for this monomer pair (103) Copolymerization between strong electron donor and strong electron acceptor monomers may involve complexation which leads to radical formation by electron transfer between monomers (104) In this study spontaneous initiation (i e copolymerization in the absence of gamma irradiation) of AMPSA with NVP was not observed However the copolymerization rate was greatly increased with gamma radiation

As shown by the contact angle values in Table 2 14 SPMA does not appear to readily graft copolymerize to PDMS under the conditions used Copolymerization of SPMA with NVP gave significantly higher weight gains and lower contact angles except for a SPMA NVP ratio of 1 1 which gave substantially higher contact angle of 58° This may be due to SPMA or NVP grafts not being homogeneously distributed on PDMS surface Due to the high permeability of PDMS SPMA or NVP grafts may also be located in the subsurface region

Surface graft copolymerization of KSPA to PDMS was conducted

using concentrations ranging from 10 to 20% and radiation doses varying from 0.15 to 0.2 Mrad. KSPA & PDMS (1M% 0.15 Mrad) gave significant weight gain (1.9%) and a low contact angle (21°). These results suggest that KSPA is more effectively grafted to PDMS. The grafting is further improved by copolymerization of KSPA with NVP as indicated by increased weight gains. The most significant weight gain was obtained for total concentration of 30% and a KSPA:NVP ratio of 2:1. As discussed earlier, high chain mobility of PDMS may allow better diffusion of KSPA into substrate and hence improved grafting.

2.4.7.1.1 FTIR/ATR and XPS analysis

The FTIR/ATR spectrum of SSA g PDMS (not shown) does not display any structural features attributable to a SSA graft. Major absorptions of poly(SSA) at 750-850 cm^{-1} from the 1,4 substituted benzene ring and 1150-1340 cm^{-1} from the sulfonate group are probably overshadowed by the strong absorption of the PDMS in this region. The FTIR/ATR spectrum of (SSA co NVP) g PDMS (greenoak 48% NVP/60°C/4hours, 25% total concentration, SSA:NVP ratio of 4:1, 0.10 Mrad, 701 rad/min) in Figure 2.38 shows the appearance of a new peak at ca. 1665 cm^{-1} assigned to the amide carbonyl of PVP.

The XPS elemental analysis in Table 2.15 revealed the presence of 1.5% sulfur in SSA g PDMS. This provides additional evidence that SSA is grafted to PDMS. In contrast to SSA, the FTIR/ATR spectrum of AMPSA g PDMS in Figure 2.39 showed a new peak at ca. 1665 cm^{-1} assigned to the amide carbonyl of poly(AMPSA). Further evidence of grafting is provided by XPS analysis which gave a AMPSA g PDMS elemental composition containing 1.8% sulfur. FTIR/ATR analysis

Table 2-14 Gravimetric analysis and contact angle data (SFMA co NVP) & FMMS and (KSFA co NVP) & PLMA (pressed 40% NVP/60°C/4hours 70l red/min)

SFMA:NVP ratio	Total Conc %	Dose Mrad	W gain %	C A (#)	Vis (Cps)
1 0	20	0 10	0 2	34	8900
1 0	20	0 15	0 3	32	6900
1 1	20	0 15	0 8	27	4500
2 1	30	0 15	0 2	50	3400
1:2	30	0 15	0 3	25	6500
KSFA NVP ratio					
1 0	10	0 15	1 9	21	8300
1 0	10	0 2			gel
1 0	20	0 15			gel
1 1	20	0 15	2 6	13	11500
2 1	30	0 15	3 4	17	15000
1:2	30	0 15	2 7	18	12000

[1] Viscosity was measured at 25°C using a Brookfield viscometer DV II (CP 52) at a shear rate of 1 0 s[-1]

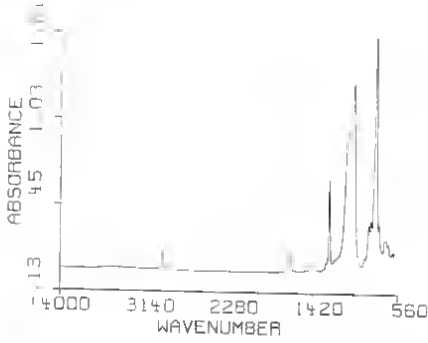

Figure 2.32 FTIR/ATR spectrum of (SSA co NVP) g PDMS (prepolk 40% NVP/50°C/4hours 25% total concentration SSA NVP ratio of 4 1.. 0.10 Mrad 701 rad/min)

showed no evidence of a thick graft for (SPMA co-NVP) g PDMS XPS analysis in Table 2 15 revealed no detectable sulfur in this sample

The FTIR/ATR spectrum of KSPA g PDMS is shown in Figure 2 4 For similar reasons discussed for SSA g PDMS the fact that major absorption bands of poly(KSPA) (i e , sulfonate at 1150 1340 cm and ester at 1730 cm^{-1}) overlap with those of PDMS makes poly(SSA) grafts difficult to detect by FTIR XPS analysis however, revealed the presence of a significant amount of sulfur (2 3%) in KSPA g PDMS

2.4.3 Hydrophilic Surface Modification of PMMA and PDMS using CMC and HA

2.4.3.1 Hydrophilic Surface modification of PMMA using HA and CMC

2.4.3.1.1 (HA-co-NVP) g PMMA

Hyaluronic acid (HA) is a natural polysaccharide containing alternating residues of N acetylglucosamine and glucuronic acid (Figure 2 10) At physiological pH and ionic strength the carboxyl groups are completely dissociated and HA has an anionic character HA is present in most human tissues at various concentrations The highest concentrations of HA are found in the umbilical cord (4100 mg/l) in synovial fluid (up to 3600 mg/l) and in the vitreous body of the eye (140 338 mg/l) (105) HA is present in cell membranes and has been found to form a coating around cells (e g fibroblasts) which is believed to have a protective effect(105) HA derives its bioactive properties from specific and non specific interactions with cell membranes Receptor mediated interactions of HA with cell surfaces have been established and HA receptors (i e proteins on cell surfaces which specifically bind HA) have been isolated and characterized(106)

Table 2.15 XPS elemental analysis of vinyl sul[illegible] monomers on NVP grafted to PDMS (Pre[illegible] NVP/80°C/4hrs 7.1 rad/min)

Sample	Total Conc. (%)	Dose Mrad	C1s (%)	O1s (%)	N1s (%)	S2p (%)	Si2p (%)	[illegible]
SSA:NVP 1:0	20	0.50	40.5	28.8	0.3	1.5	20.0	[illegible]
theoret			86.7	25.0		0.3		
AMPSA:NVP 1:0	5	0.25	48.0	28.2	1.2	1.0	20.6	[illegible]
theoret			54.0	30.0	8.0	8.0		
SPMA:NVP 1:2	30	0.15	48.5	28.2	8.2	0.0	21.1	[illegible]
theoret			52.1	28.5	4.7	4.7		
KSPA:NVP 1:0	10	0.15	48.5	27.7	0.6	2.3	20.8	[illegible]
theoret			54.0	38.0		8.0		
Unmodified PDMS			48.1	23.9			27.0	[illegible]

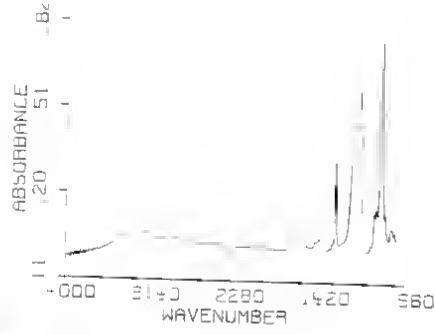

Figure 2.39 FTIR/ATR spectrum of AMPSA g PDMS (pressed 40% NVP/60°C/4 hours 5% AMPSA 0.25 Mrad 701rad/min)

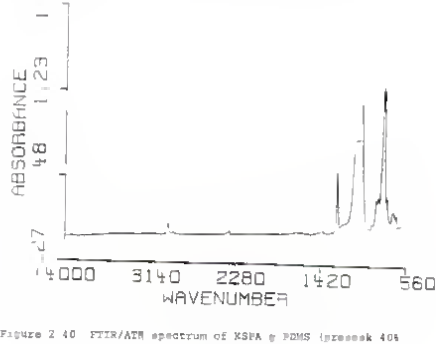

Figure 2.40 FTIR/ATR spectrum of KSPA g PDMS (pressed 40% NVP/60°C/4 hours 5% KSPA 0.25 Mrad 701 rad/min)

Larsson (107) has prepared and evaluated PMMA surfaces modified with HA. The method of preparation consisted of introducing primary amine groups on PMMA surfaces by physical adsorption of polyethyleneimine (PEI) with a MW of 50000. HA (1.4×10^6 MW) was activated by reaction with N ethyl N' (3 dimethylamino propyl) carbodiimide hydrochloride (EDC) then allowed to react with the aminated PMMA surfaces. HA modified PMMA surfaces showed 58% reduction in human fibroblast growth and a substantial reduction in granulocyte activation compared to unmodified PMMA surfaces. These surfaces have also been shown to have some anticlotting properties. Using similar surface modification technique, Fagerholm et al (108) have evaluated the corneal endothelial cell protection afforded by HA surface modified PMMA IOLs using SEM and staining techniques. HA modified PMMA IOLs have been found to cause significantly less corneal endothelium damage than unmodified PMMA IOLs.

The objective of this study was to prepare and evaluate HA modified PMMA and PDMS surfaces using gamma induced surface modification technique. This research provides a novel approach to immobilizing HA as polymer surfaces by incorporation into hydrophilic surface grafts. Such composite surface grafts which are covalently bound to polymer substrate may be more stable than those prepared by directly attaching the bioactive molecule to physically adsorbed (PEI). In addition, hydrophilic environments have been shown to enhance the stability of immobilized enzymes and bioactive molecules (109).

The use of HA in the biomedical field is largely due to the high viscosity of aqueous solutions at very low concentrations as discussed in section 3 2 In radiation induced grafting however high viscosity is a major drawback since the onset of gelation in viscous monomer solutions occurs earlier during polymerization thereby limiting the diffusion of monomer to the reactive sites on the substrate surface HA was therefore used at relatively low concentrations (0 1 P 4%)

The grafting method consisted of two step gamma irradiation process discussed in section 2 3 2 2 5 The first step involved the preparation of a PVP pregraft by presoaking in 40% NVP at 60°C for 4 hours then transferring to 15% NVP irradiating to a dose of 0 09 Mrad at a dose rate of 701 rad/min Samples were then washed and dried The second step consisted of transferring dry pregrafted PMMA samples to aqueous solutions of NVP or HA with 10% total concentration and HA NVP ratios varying from 1 9 to 4 6 Samples were degassed prior to gamma irradiation to a dose of 0 09 Mrad at a dose rate of 701 rad/min The two step grafting process was specially designed for molecules which are radiation sensitive (e g polysaccharides proteins enzymes) and has several advantages The exposure of labile molecules to high radiation doses is minimized Hydrophilic PVP pregrafts formed in the first step may have some affinity to NVP or HA solutions and may make free radicals produced in the PVP pregraft and the PMMA substrate more readily accessible to those produced in NVP and HA

It is important to note that HA does not have functional groups which may polymerize with gamma radiation However during the second step of the process irradiation of PVP pregrafted PMMA may involve complex heterogeneous and homogeneous free radical copolymerization reactions among all different system components NVP HA PVP pregraft and PMMA substrate First the irradiation of NVP or HA solutions may involve graft copolymerization of NVP to HA Homogeneous grafting of vinyl monomers (e g hydroxyethylmethacrylate (HEMA) styrene methylmethacrylate methylacrylate) to polysaccharides using high energy radiation has been well established (78) Gamma irradiation of polysaccharides produces a variety of radicals on the monosaccharide units The production of HA macroradicals was discussed in section 2 2 4 1 2 Macroradicals on HA backbones ($HA^{\bullet}$) may react with an NVP monomer unit or PVP chains and act as sites for grafting Radicals produced in NVP monomer or in PVP polymer chains may also abstract hydrogen atoms from HA to give additional sites for grafting Recombination of ($HA^{\bullet}$) with PVP macroradicals and NVP growing macroradicals should also not be ruled out Additional reactions may include heterogeneous graft copolymerization of NVP to PVP pregraft as well as to PMMA substrate The fact that these grafting reactions occur simultaneously may provide hydrophilic PVP grafts to which HA is covalently bound

The results of grafting experiments with HA on NVP are shown in Table 2 16 The control sample consisted of using a monomer solution of 10% NVP during the second step of the process Grafting of HA

Table 2 16 Gravimetric analysis and contact angle data for HA co NVP g PMMA using the two step process

HA %	NVP %	Total Conc %	Wt gain %	C A (°)	Vis (Cps)
0 0	10 0	10	2 2	18	4200
0 1	9 9	10	2 3	20	7300
0 2	9 8	10	3 0	18	12500
0 3	9 7	10	3 2	21	15700
0 4	9 6	10	3 8	17	22300
0 4	0 0	0 4	0 6	21	<100
NVP g PMMA (first step only)			0 6	24	5700

[1] First step Presoak 40% NVP/60°C/4hrs then transfer to 15% NVP degas and irradiate to 0 05 Mrad at 701 rad/min Wash and dry Second step Transfer to NVP/HA solution degas then irradiate to 0 06 Mrad at 701 rad/min

[2] Viscosity was measured at 25°C using a Brookfield viscometer DV II (CP 52) at a sheer rate of 1 0 s [1]

slone (15% NVP/0 09 Mrad followed by 0 4% HA/0 06 Mrad) yielded weight gain (8 6%) and contact angle (13°) comparable to that of NVP g PMMA obtained with the first step (15% NVP/0 09 Mrad) This suggests that grafting of HA in the absence of NVP is minimal HA solution has a random coil conformation with a very large hydrodynamic volume only small molecule can penetrate the domain occupied by HA molecules Large molecules (e g collagen fibrinogen) are excluded by steric exclusion (118) The minimal grafting observed for HA alone may be due to the fact that the PVP chains of the pregraft may not penetrate the domain occupied by HA molecules because of steric reasons This may make HA macroradicals less accessible to the PVP chains

Grafting of NVP on HA solutions gave significantly greater weight gains (2 2 3 8%) NVP may provide additional reactive sites for grafting reactions especially highly mobile low molecular weight macroradicals which may have higher collisional frequency In addition NVP is a small molecule which can penetrate the large hydrodynamic volume of HA and may have access to more HA macroradicals It can also be seen from Table 2 16 that there is a trend toward increasing grafting yield with increasing HA concentrations

The FTIR/ATR spectrum of a typical sample of (HA on NVP) g PMMA (15%NVP/0 09 Mrad followed by 0 4% HA/9 6% NVP 0 06 Mrad 701 rad/min) in Figure 2 42 exhibits a more intense peak at ca 1665 cm when compared to the spectrum of PVP g PMMA prepared under the same conditions (15%NVP/0 09 Mrad followed by 10% NVP/0 06 Mrad 701

rad/min in Figure 2 41 This increase in intensity is probably brought about by a contribution from the HA carboxylate group which absorbs at the same wavelength (1620 1670 cm^{-1}) as well as from the secondary amide carbonyl present in HA (ca 1665 cm^{-1}) An additional characteristic peak observed for (HA co NVP) g-PMMA appears as a broad band at 3400 3200 cm^{-1} This band is characteristic of polysaccharides and is assigned to the HA hydroxyl group stretching vibration It is important to note that at the completion of the second step grafted samples were washed in distilled water at 50°C for 3 days, then in distilled water at room temperature for 4 days as described in section 2 3 2 2 4 This will probably remove ungrafted homopolymer as well as any physically adsorbed or unbound HA FTIR/ATR analysis therefore provides strong evidence that HA was effectively incorporated into the graft

Due the presence of the same elements in the structure of both PVP and HA (i e C O and N) XPS elemental analysis does not conclusively show the presence of HA within the graft However as shown in Table 2 1f the elemental composition of the grafts where HA was used is significantly different from that of the PVP grafts prepared under the same conditions (15% NVP/5 49 Mrad then 10%NVP/0 06 Mrad) An increase in both the nitrogen and oxygen content was observed This further suggests that HA is present within the PVP graft However the elemental composition of (HA co NVP) g PMMA observed (28 3% oxygen and 6 5% nitrogen) is not consistent with that of (HA co NVP) anticipated from theoretical calculations This is may be due to the fact that the thickness of

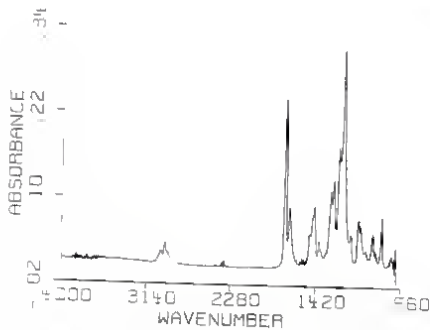

Figure 2.41 FTIR/ATR spectrum of PVF g PMMA using the two step process 15% NVP/0.05 Mrad followed by [illegible] Mrad)

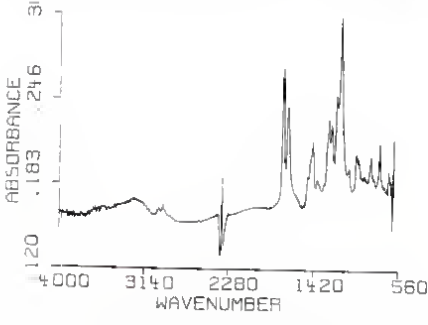

Figure 2.42 FTIR/ATR spectrum of (HA co NVP) g PMMA using the two step process (15%NVP/0.05 Mrad followed by 5.6% NVP/0.4%HA/0.05Mrad)

the (HA or NVP) prefix is less than the depth of penetration of XPS (5PÅ) and hence the underlying substrate can still be detected

2.4.3.1.2 (CMC co NVP) & PMMA

Carboxymethylcellulose (CMC) is another anionic natural polysaccharide similar to HA in molecular structure (Figure 2-10) but with greater thermal and chemical stability CMC is a cellulose ether produced by reacting alkali cellulose with sodium monochloroacetate The three possible positions for derivatization in cellulose are the hydroxyl groups at C2 C3 and C6 of the anhydroglucose unit The resulting product is a polymer with disaccharide repeating units containing carboxymethyl groups at C2 C3- and C6 positions linked with 1 4 glucosidic bonds The average number of hydroxyl groups substituted per anhydroglucose unit is known as the degree of substitution (DS) and vary from 0 4 to a theoretical maximum of 3-P- The physical properties of CMC are intimately related to the MW and DS Higher degrees of substitution give improved water solubility and compatibility with other soluble components such as salts and nonsolvent however, CMC grades with higher DS are very hygroscopic and tend to absorb up to 25% by weight moisture from the air

CMC is an anionic polyelectrolyte with a pK_a of approximately 4 and has poor solubility in water- Salts of CMC such as alkali metal salts (e g sodium salts) have greater solubility in water over a wide range of pH and ionic strength CMC, which is an anionic polyelectrolyte- is also compatible with monovalent (e.g potassium) and polyvalent cations (e g , calcium up to 50%) which are normally

present in physiological media. CMC is physiologically acceptable and is widely used as thickener or binder in a variety of food and cosmetics. Its pharmaceutical use may be therapeutic in which CMC is the primary ingredient such as laxatives and artificial eye drops or as excipient such as a suspending agent, tablet binding or thickener.

Molecules such as HA and heparin are believed to derive their bioactive properties in part from their polyanionic character. For example, heparin is suggested to induce conformational changes in antithrombin by specific interaction of carboxyl groups with the protein's lysine residues (111). Many of the biological activities are based on charge density effects, with higher negative charge density being associated with greater protein affinity. A lowering of heparin's anticlotting activity can be achieved by reducing the number of carboxylic groups.

As discussed earlier, CMC is also an anionic polyelectrolyte similar to HA in molecular structure and may therefore inhibit fibroblast growth and reduce lens epithelial cell adhesion and proliferation. In addition, CMC has excellent lubricating properties and may provide some protection against chronic abrasion of fragile ocular tissues by IOLs. The use of CMC in surface modification of biopolymers has not been reported in the literature. It was therefore of interest to prepare and evaluate PMMA and PDMS surfaces modified with CMC. As discussed for HA, gamma induced surface graft copolymerisation was used to incorporate CMC into a hydrograft for enhanced biostability.

CMC used in this experiment was a pharmaceutical grade low MW (90SH) product with a DS of 1.2 (12L2).

The results of the grafting experiments with CMC on NVP are given in Table 2.17. Here again grafting of CMC alone (15% NVP/0.59 Mrad followed by 4.0% CMC/0.05 Mrad) yielded weight gain (7.5%) and contact angle (19°) comparable to that of NVP & PMMA obtained with the first step (15% NVP/0.09 Mrad) which suggest that grafting of CMC in the absence of NVP is minimal. This may be due at least in part to the large hydrodynamic volume of CMC as discussed for HA.

Grafting of NVP on CMC solutions gave significantly greater weight gains (26.5 3%) and low contact angle values. It is important to note that the 1,4β glycosidic bonds which link the disaccharide units in CMC reduce the degrees of freedom significantly and make CMC a relatively rigid molecule. These conformational restrictions may reduce the flexibility of the polymeric chains and make CMC radicals less accessible to the reactive sites in the PVP grafted and to PMMA substrate. In addition to producing additional reactive sites, NVP may also have a plasticizing effect on CMC and hence increase chain flexibility.

As observed for HA, it can also be seen that graft yield increases with increasing CMC concentration. This is consistent with graft copolymerization of vinyl monomers to polysaccharides results observed previously and may be due to a large increase in the number of free radicals with increasing polysaccharide concentrations(78)

Table 2 17 Gravimetric analysis and contact angle data for (CMC co NVP) g PMMA using the two step process[1]

CMC %	NVP %	Total Conc %	W gain %	C A (°)	Vis[2] (Cps)
0 0	15 0	15 0	2 0	20	8400
1 0	14 0	15 0	2 6	17	9700
2 0	13 0	15 0	3 0	18	16900
3 0	12 0	15 0	4 2	14	24000
4 0	11 0	15 0	5 3	15	32400
4 0	0 0	4 0	0 6	21	<100
NVP g PMMA (first step only)			0 0	24	5700

[1] First step: Precoak 40% NVP/60°C/4hrs then transfer to 15% NVP degase and irradiate to 0 09 Mrad at 701 rad/min Wash and dry Second step: Transfer to NVP/CMC solution degase then irradiate to 0 06 Mrad at 701 rad/min

[2] Viscosity was measured at 25°C using a Brookfield viscometer DV II (CP 52) at a shear rate of 1 0 s^{-1}

The FTIR/ATR spectra for NVP g PMMA (15%NVP/0.05 Mrad followed by 15% NVP/0.05 Mrad 701 rad/min) and (CMC co NVP) g PMMA (15%NVP/5.09 Mrad followed by 4.0% CMC/11.0% NVP 0.05 Mrad 701 rad/min) are shown in Figures 2.44 and 2.45 respectively. As previously observed for (HA co NVP) g PMMA the absorption peak at ca 1665 cm^{-1} for (CMC co NVP) g PMMA is much more intense than that of PVP g PMMA.

This increase in intensity is attributed to the carboxylate group of CMC which absorbs in the same region. In addition the absorption peak at 1655 cm^{-1} for (CMC co-NVP) g PMMA is much more intense than that of the ester carbonyl at 1725 cm^{-1} form the PMMA base substrate. This suggests that substantial coverage of the substrate surface is achieved with these conditions. FTIR/ATR results are consistent with gravimetric analysis which gave significant weight gain for (CMC co NVP) g PMMA prepared with these conditions (5.3%). An additional absorption band is visible in the region of 3400-3200 cm^{-1} and is assigned to the stretching vibration of hydroxyl groups of CMC.

The XPS data in Table 2.19 show a significant increase in the oxygen content for (CMC co NVP) g PMMA (15.3%) relative to PVP g PMMA (17.5%). This may be due to the presence of CMC in the graft since CMC contains a high atomic concentration of oxygen but no nitrogen. The change in the surface composition, however, is not consistent with the stochiometry of CMC co NVP.

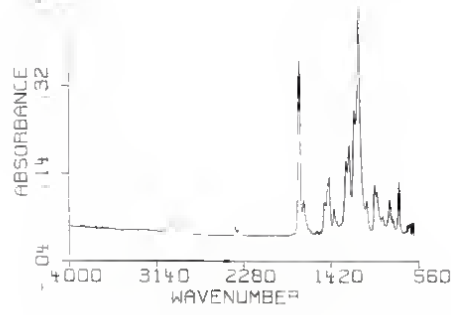

Figure 2 43 FTIR/ATR spectrum of NVF g PMMA using the two step process (15% NVF/0 05 Mrad 15% NVF/0 05 Mrad)

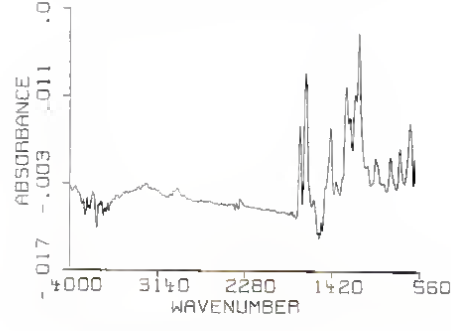

Figure 2 44 FTIR/ATR spectrum of (CMC co NVF) g PMMA using the two step process (15%NVF/0 05 Mrad 1% NVF/ 4%CMC/0 05Mrad)

Table 2 18 XPS elemental analysis of HA co NVP and CMC co[illegible] surface modified PMMA

Sample	C1s (%)	O1s (%)	N1s (%)	O1s/N1s
NVP-g PMMA[1]	78 1	17 3	5 6	3 9
(HA co NVP) g PMMA[2]	73 2	20 3	6 5	3 1
HA co NVP (theoretical)	66-0	22 0	12 0	1 8
NVP g PMMA[3]	78 4	17 5	5 1	3 9
(CMC co-NVP) g PMMA[4]	78 6	18 3	4 1	4 7
CMC co NVP (theoretical)	82-0	30 0	8 0	3 8

[1] NVP g PMMA 15% NVP/0 05Mrad then transfered to 10% NVP/0 05 Mrad

[2] 15% NVP/0 05Mrad then transfered to (9 6% NVP/0 4% HA)/0 05 Mrad

[3] NVP g PMMA 15% NVP/0 05Mrad then transferred to 15% NVP/0 05 Mrad

[4] 15% NVP/0 05Mrad then transfered to (11% NVP/ 4% CMC)/0 05 Mrad

2.4.3.1 Hydrophilic Surface Modification of PDMS using HA and CMC

The two step process used for PMMA was slightly modified for PDMS Since PDMS is relatively more radiation resistant higher doses can be used during the first step to form PVP pregrafts Grafting conditions for (HA co NVP) and (CMC co NVP) were as follows Step 1 precast in 40% NVP at 60°C for 4 hours immediately transfer to 10% NVP then irradiate to 0 15 Mrad at 701 rad/min wash and vacuum dry

Step 2 transfer to (HA co NVP) or (CMC co NVP) solutions vacuum degas and irradiate to 0 06 Mrad at 701 rad/min

The results for HA and NVP grafting experiments are given in Table 2-10 As observed for PMMA grafting of HA alone appears to be minimal Weight gains were significantly higher for (HA co NVP) g PDMS (3 1 to 4 2%) and increased with increased HA concentrations when HA was incorporated into the grafting solution The FTIR/ATR spectrum for (HA co-NVP) g PDMS in Figure 2 45 exhibits a more intense peak at 1660 cm^{-1} when compared to the spectrum of NVP g PDMS in Figure 2 46 This is attributed to contributions from HA carboxylate groups as previously discussed for PMMA

The results for CMC and NVP grafting to PDMS are given in Table 2 20 Here again grafting of CMC alone to PDMS was minimal as evidenced by the weight gain obtained for CMC g PDMS (10% NVP irradiated to 0 15 Mrad followed by 4 0% CMC irradiated to 0 06 Mrad at 701 rad/min) (2-3%) which was comparable to that of NVP g PDMS prepared with step 1 only (10% NVP irradiated to 0 15 Mrad at 701 rad/min) (2 2%) Greater weight gains were observed for

Table 2 19 Gravimetric analysis and contact angle data for (HA ca NVP) g PDMS using the two step process[1]

HA %	NVP %	Total Conc %	W gain %	C A (°)	Vis[2] (cps)
0 0	10 0	10 0	3 1	28	4200
0 1	9 9	10 0	3 0	20	7300
0 2	9 8	10 0	3 3	20	12500
0 3	9 7	10 0	4 0	28	15700
0 4	9 6	10 0	4 2	20	22300
0 4	0 0	0 4	2 2	21	<100
NVP g PDMS (first step only)			2 2	21	8700

[1] First step: Pressak 40% NVP/60°C/4hrs then transfer to 10% NVP degass and irradiate to 0 15 Mrad at 701 rad/min Wash and dry Second step Transfer to NVP/HA solution degass then irradiate to 0 06 Mrad at 701 rad/min

[2] Viscosity was measured at 25°C using a Brookfield viscometer DV II (CP 52) at a shear rate of 1 8 s^{-1}

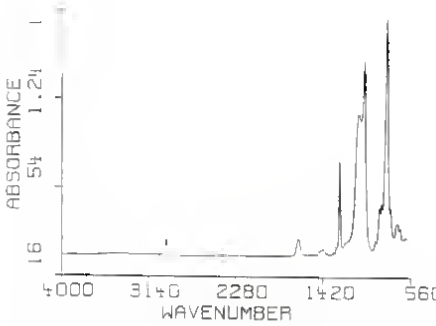

Figure 2 45 FTIR/ATR spectrum of NVP g PDMS using the two step process (15% NVP/D 15 Mrad 15% NVP/D 06 Mrad

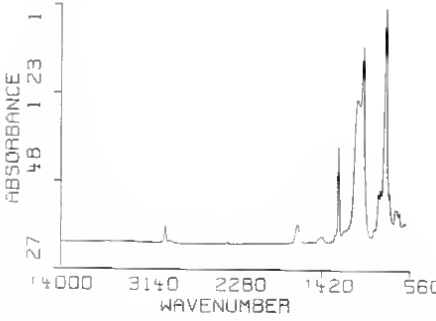

Figure 2 46 FTIR/ATR spectrum of (HA co NVP) g PDMS using the two step process (5%NVP/D 15 Mrad % 6% NVP/ D 4%HA/D 06Mrad)

Table 2 20 Gravimetric analysis and contact angle data for (CMC co NVP) g PDMS using the two step process[1]

CMC %	NVP %	Total Conc %	W gain %	C A (°)	Vis (Cps)
0 0	15 0	15 0	3 0	28	8400
1 0	14 0	15 0	3 0	20	9700
2 0	13 0	15 0	3 2	15	16900
3 0	12 0	15 0	4 4	15	24000
4 0	11 0	15 0	5 5	15	32400
4 0	0 0	4 0	2 3	20	<100
NVP g PDMS (first step only)			2 2	21	9700

[1] First step: Prepeak 48% NVP/60°C/4hrs then transfer to 10% NVP degas and irradiate to 0 15 Mrad at 781 rad/min Wash and dry Second step Transfer to NVP/CMC solutions degass then irradiate to 0 05 Mrad at 701 rad/min

[2] Viscosity was measured at 25°C using a Brookfield viscometer DV 1I (CP 52) at 1 0 s $^{-1}$

(CMC co NVP) g PDMS An increase in graft yield with [illegible] concentration was also observed here The FTIR/ATR spectrum of (CMC co NVP) g PDMS (10% NVP irradiated to 0 15 Mrad at 701 rad/min followed by 4_0% CMC/11% NVP irradiated to 0_06 Mrad at 701 rad/min is Figure 2 47 shows a much more intense peak at 1660 cm^{-1} in comparison with that of NVP g-PDMS (10% NVP irradiated to 0 15 Mrad at 701 rad/min followed by 15% NVP irradiated to 0_06 Mrad at 701 rad/min) in Figure 2 45 This is attributable to contributions from carboxylate groups of CMC XPS analysis of these samples was not performed

The results of gravimetric analysis and contact angle combined with those of FTIR/ATR analysis suggest that HA and CMC are both incorporated into the PVP pregrafts for PDMS

2.4.4 Analysis of HA co NVP and CMC co NVP Polymer Solutions

Although surface grafts may be readily characterized by gravimetric analysis and surface sensitive techniques (i e goniometry, XPS and FTIR/ATR) it is often more difficult to determine their molecular structure and molecular weight To gain some insight in the structure of (HA co NVP) and (CMC co NVP) grafts grafting solutions were analyzed by gel permeation chromatography (GPC)

2.4.4.1 GPC analysis

The molecular weights and molecular weight distributions of grafting solutions were determined using a Perkin Elmer (Series 30 Liquid Chromatograph) HPLC system equipped with a refractive index (RI) detector(RefractoMonitor) and using a column

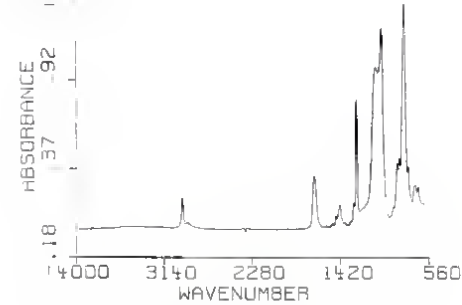

Figure 2 47 FTIR/ATR spectrum of (CMC co NVP) g PDMS using the two step process (15%NVP/0 15 Mrad; 11% NVP/ 4% CMC/0 05Mrad)

by ahndex (TSK Gel) Polyethylene oxide standards were used to generate a calibration curve The mobile phase was HPLC grade water which has been filtered through a 0 45µm Teflon® filters then degassed A 1000 ml Erlenmeyer filtration flask containing 900 ml HPLC grade water was degassed by sonicating under vacuum created by a tap water aspirator for 45 minutes The flow rate was 1 ml/min Typical elution volumes were 12 15 ml The solvent was run through the system for 1 hour to remove air bubbles and impurities

Sample solutions were diluted to a concentration of 0 01% filtered using 0 2µm syringe filters and 50µl injected into the system The MW of the samples were calculated using a Perkin Elmer GPC software (GPC 1)

The results of the MW measurements are given in Table 2 21 The number average MW (Mw) of HA was found to be 9 7x10^5 which is eighty lower than that reported by the manufacturer (12 0x10^5) After gamma irradiation to a dose of 0 1 Mrad at 70l rad/min a significant decrease in the Mw was observed (1 2x10^5) which is indicative of substantial depolymerization This is consistent with oxidative depolymerization of polysaccharides by gamma radiation which has been shown to involve free radicals(11) Phillips (11) has pointed out that these radicals can initiate reactions with vinyl monomers to yield grafted products The broad molecular weight distribution observed (6 7) is probably due to the degradation mechanism which involves random chain cission Polyvynilpyrrolidone (PVP) obtained by irradiating a 10% NVP solution to 0 1 Mrad at 701 rad/min gave a Mw of 19 7x10^5 and a MWD of 4 9 HA/PVP blend was

pregered by mixing solutions of 0.4% HA irradia[illegible] rad/min and 10% NVP irradiated to 0 1 Mrad at 70l rad/min HA/PVP blend gave a Mw slightly lower than that of 10% NVP/ 0 1 Mrad (1.8×10^5) but a number average molecular weight (Mn) significantly lower (2.2×10^5) This may be due to the fact that Mn is more sensitive to the presence of low molecular species (i e , short chains from HA) This difference is also visible from the MWD which was found to be much broader (# 3) than that of PVP prepared with 10% NVP/0 1 Mrad (4 1)

The results obtained for (HA co NVP) (0 4% HA/9 6% NVP 0 1 Mrad 70l rad/min) were significantly different from those obtained for HA/NVP blend The weight average molecular weight Mw for (HA co NVP) is higher compared to that of HA/NVP blend Most importantly, the MWD for (HA co NVP) (5 1) is much narrower than that of HA/PVP blend (# 3) This suggests that (HA co NVP) contains a much smaller population of low molecular species when compared to HA/PVP blend It is possible that during gamma induced grafting free radicals produced in HA which usually cause oxidative degradation may react with NVP or macroradicals in PVP to form graft copolymers as depicted in equation (2 5) of Figure 2 4# NVP may also yield radicals that then abstract hydrogen atoms from the backbone polymer to give additional sites for grafting as depicted in equation (2 8) of Figure 2 4#

It is important to note also that (HA co NVP) (0 4% HA/9 6% NVP 0 1 Mrad, 70l rad/min) gave Mw and Mn values comparable to those of 10% NVP (0 1 Mrad, 70l rad/min) but slightly broader MWD This is

consistent with the results obtained by Eastwood et al. for graft copolymers (p127, Eqset). The macroradicals produced by the reaction of radicals in HA (HA•) with NVP monomer units shown in equation (2.8) in Figure 2.48 may further react with HA or PVP to form partially crosslinked products.

CMC solutions showed similar trends. Gamma irradiation of solution of 4.0% CMC (12LF) resulted in a decrease in Mw from 1.2x10^5 to 8.6x10^5 with concomitant broadening of the MWD (from 3.1 to 6.5) due to depolymerization of CMC. Also, (CMC co NVP) (4.0% CMC/11.0 NVP, 0.1 Mrad, 701 rad/min.) gave higher Mw (22.3x10^5) and narrower MWD (4.8) than CMC/PVP blend prepared by mixing 4.0% CMC irradiated to 0.1 Mrad at 701 rad/min with 15% NVP irradiated to 0.1 Mrad at 701 rad/min. (Mw = 19.4x10^5 and MWD = 5.5). As discussed for HA, this may be due to graft copolymerization of NVP to CMC as depicted in equations (2.6), (2.7), (2.8), and (2.9) in Figure 2.48.

Graft copolymerization of vinyl monomers to polysaccharides (e.g., HA and CMC) using high energy radiation has been well studied (78). Copolymerization is enhanced when performed in homogeneous solution using the simultaneous irradiation techniques such as the method used in this research. The significance of these results however, resides in the fact that the surface modification technique used in this research, which consisted of simultaneous gamma irradiation of PMMA and PDMS substrates in aqueous solutions of NVP/HA and NVP/CMC, may afford hydrophilic grafts to which HA and CMC are covalently attached. This may enhance the biostability of HA and CMC and provide hydrogel like grafts with bioactive properties.

Table 2 21 Molecular weight measurement of [illegible] grafting solutions using GPC

sample	Mw ($x10^5$)	Mn ($x10^5$)	MWD
0 4% HA before irradiation	9 7	2 7	3 6
0.4% HA 0 1 Mrad	1 2	0 2	6 7
15% NVP 0 1 Mrad	19 7	4 1	4 9
HA co NVP 0.4% HA/9 5% NVP 0 1 Mrad	20 1	4 0	5 1
HA/PVP blend[1]	18 2	2 2	8 3
4 0% CMC before irradiation	1 2	0 4	3 1
4 0% CMC 0.1 Mrad	0 6	0 1	6 5
15% NVP 0 1 Mrad	22 1	4 9	4 5
CMC co NVP 4 0% CMC/11 0% NVP 0 1 Mrad	22 3	4 6	4 9
CMC/PVP blend[2]	19.4	3 5	5 6

[1] blend of HA and NVP irradiated separately; prepared by mixing 0 4% HA irradiated to 0 1 Mrad with 10% NVP irradiated to 0 1 Mrad

[2] blend of CMC and NVP irradiated separately prepared by mixing 4 0% CMC irradiated to 0 1 Mrad with 15% NVP irradiated to 0 1 Mrad

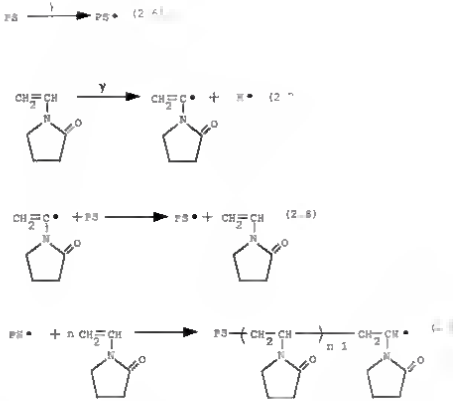

PS: polysaccharide HA or CMC

Figure 2.4: Possible reactions involved during gamma irradiation of (HA co-NVP) and (CMC co-NVP) solutions

2.4.5 In vitro Biological Evaluations of Surface Modified PMMA.

In vitro testing provides a convenient and often useful way to predict the performances of a material in a real clinical situation. Various modified PMMA surfaces were evaluated for their tissue interactions and and their tendency to support cell adhesion and spreading.

2.4.5.1 Corneal endothelial cell damage

For over a decade our laboratories have been involved in the study of tissue-material interfacial adhesion (4,5). It has been shown that during PMMA IOL insertion, fragile ocular tissues can be extensively damaged even upon brief contact with the acrylic IOL surface(6). Damage to the corneal endothelium, a non regenerating tissue responsible for maintaining cornea clarity, can be a major complication in cataract surgery. Tissue protection afforded by various hydrophilic grafts surfaces synthesized in this research was investigated with the cooperation of Paul Martin and Dr. Hiroyuki Hattori using an instrument designed and build in our laboratories(80). The test consisted of contacting rabbit corneas with PMMA stubs (modified or unmodified) under controlled conditions (i.e., weight and surface area). SEM was used to assess the extent and kind of damage caused by such contacts. Three samples were tested for each graft surface.

An SEM micrograph of normal rabbit corneal endothelium displayed in Figure 2.49, reveals the presence of hexagonally shaped cells. An SEM micrograph of the corneal endothelium after contact with an unmodified PMMA surface is shown in Figure 2.50. The damage

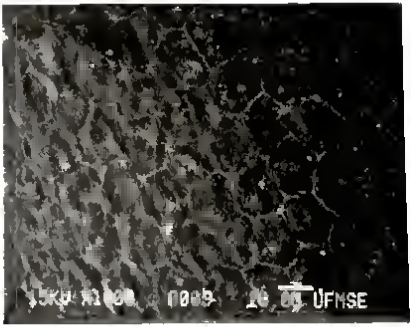

Figure 2 49 SEM micrograph of normal rabbit corneal endothelium showing hexagonally shaped cells

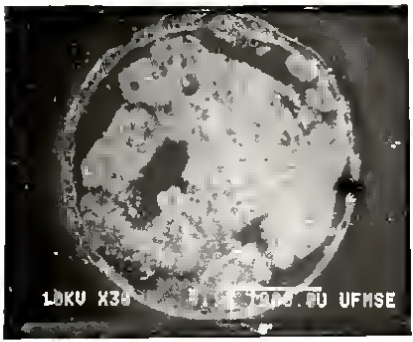

Figure 2 50 SEM micrograph of corneal endothelium after contact with unmodified PMMA showing extensive damage (80 % light areas)

caused by the hard hydrophobic surface of PMMA is shown by [illegible] white areas this damage is estimated to be ca 80% A higher magnification SEM micrograph of the damaged areas (i.e , white areas) is shown in Figure 2 51 In contrast to a normal endothelium the damaged endothelium consisted of areas where the endothelial cells were completely removed The protective effect of a (HA co NVP) graft surface is illustrated in Figure 2 52 which shows an SEM micrograph of the corneal endothelium after contact with an (HA co NVP) g PMMA surface. Significantly less damage was observed (10%) as indicated by the white areas (CMC co NVP) g PMMA showed virtually no corneal endothelial cell damage as shown by the absence of white areas in Figure 2 53 These studies suggest that substantial protection of the corneal endothelium is afforded by these hydrophilic surface graft modifications.

2.4.5.2.In vitro adhesion and spreading of rabbit lens epithelial Cells

Rabbit lens epithelial cell adhesion and spreading were qualitatively investigated for different modified PMMA surfaces using F Hofmeister's cell culture method described in section 3 1 2 5 7 These studies were conducted with the assistance of Paul Martin Unmodified PMMA surfaces normally exhibit extensive cell adhesion and spreading as shown in Figure 2-54

In contrast to unmodified PMMA, (y-PVP/NVP) g PMMA prepared using a y PVP/NVP total concentration of 10% with a y PVP NVP ratio of 1 3 (0 15 Mrad 701 rad/min) (Figure 2 55), showed virtually no adherent cells This is consistent with the previously observed

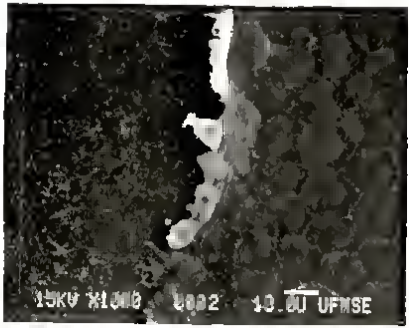

Figure 2 51 Higher magnification SEM micrograph of damaged area of endothelium after contact with unmodified PMMA

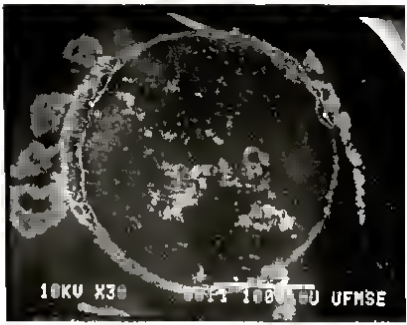

Figure 52 SEM micrograph of corneal endothelium after 1 hr in contact with (HA co NVP) g PMMA surface (no damage)

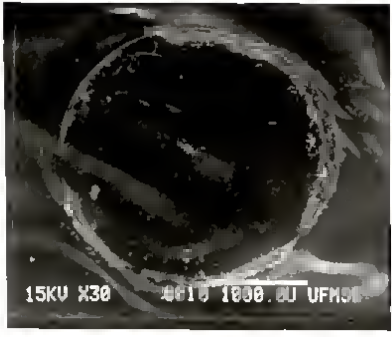

Figure 2.53 SEM micrograph of corneal endothelium after being in contact with (CMC co HVF) g PMMA surface (<5% damage)

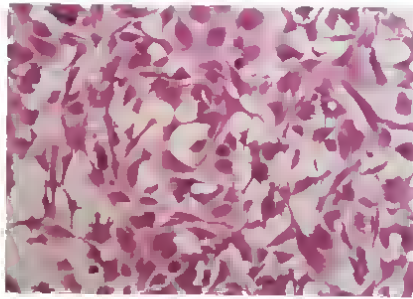

Figure 2 54— Optical micrograph of rabbit lens epithelial cells on unmodified PMMA (24 hour cell culture)

Figure 2 55— Optical micrograph of rabbit lens epithelial cells on (γ PVP/NVP) g PMMA (10% total concentration 1:3 γ PVP NVP ratio, 0 25 Mrad/701 rad/min) (24 hr cell culture)

behavior of PVP modified PMMA surfaces in our group(79) This result is not exclusively due to the hydrophilicity of these surfaces but to a combination of surface chemical and mechanical properties The PVP hydrophilic polymers are mechanically soft with a high water content and do not readily support protein cell pseudopod scaffolding because of the presence of the flexible highly hydrated chains(48)

However, adhesion of rabbit lens epithelial cells to an anionic hydrogrsft (SSA g PMMA) (Figure 2 56) showed a moderate level of cell adhesion and spreading Negatively charged surfaces should generally inhibit adhesion of negatively charged cells through electrostatic repulsion(86) However the presence of counterions in the physiological medium can reduce such forces to allow cells to come in contact with the substrate SSA g PMMA surfaces have been shown to adsorb high albumin concentrations which promotes cell adhesion and spreading(54)

Therefore (PSSA g PMMA) may not be suitable for IOL applications where adhesion and spreading of lens epithelial cells is undesirable
However, these surfaces might be potentially useful as nonthrombogenic lining of endothelial cells in vascular prostheses

A different behavior was observed for (SSA co NVP) g PMMA as shown in Figure 2 57 Fewer cells adhered to these surfaces but did not spread The charge density is probably lowered by the copolymerization of SSA and NVP which may account for less cell adhesion Adhesion has been shown to decrease with decreasing negative surface charge density The lack of spreading may be caused

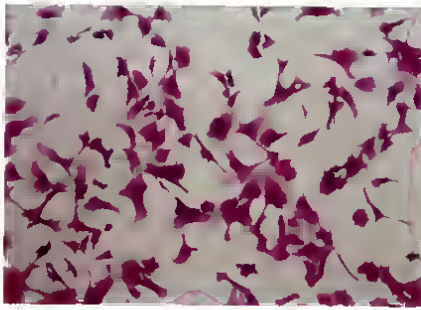

Figure 2 56 Optical micrograph of lens epithelial cells on SSA g PMMA with gresoak 40%NVP/60°C/4hrs (20% SSA 0.15 Mrad 701 rad/min) (24 hour cell culture)

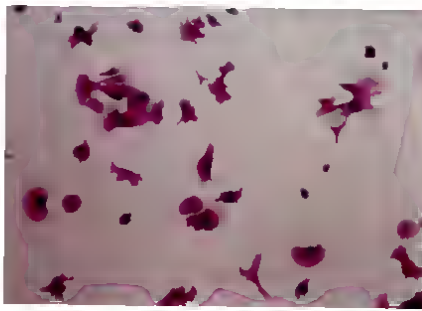

Figure 2 57 Optical micrograph of lens epithelial cells on (SSA ce NVP) g PMMA with gresoak 40%NVP/60°C/4hrs (40% SSA NVP ratio of 1 1, 0 15 Mrad, 701 rad/min) (24 hour cell culture)

by reduced protein adsorption and increased chain flexibility induced by the presence of PVP

Adhesion of lens epithelial cells to (AMPSA co NVP) p PMMA is shown in Figure 2 58 These samples support virtually no cell adhesion It is possible that (AMPSA co NVP) p PMMA surfaces may exhibit increased chain flexibility in contrast to (PSA co NVP) p PMMA where the aromatic structure of SSA provides the copolymer hydrogel (i e , PSSA co PVP) with increased stiffness (67)

A striking similarity to SSA p PMMA was observed for KSSA p PMMA ic Figure 2 59 Cells adhere and spread readily on such surfaces High charge density and increased protein adsorption may account for such behavior A drastic decrease in the number of adhered cells was observed when NVP and KPPA where copolymerized onto PMMA as shown in Figure 2 60 Adhesion and spreading of lens epithelial cells were not investigated on AMPSA p PMMA SPMA p PMMA or (SPMA co NVP) p PMMA because of the grafting levels obtained for these samples

Finally, (HA co NVP) p PMMA and (CMC co NVP) p PMMA did not support any significant amount of cell adhesion as can be seen in their respective photomicrographs shown in Figures 2 63 and 2 64

2.5 Conclusions

1 Hydrophilic polymer grafts on PMMA and PDMS were prepared by a simple one step gamma radiation polymerization process using aqueous polymer/monomer solutions (i e K90 PVP/NVP and γ PVP/NVP)

2 This method afforded uniform hydrophilic grafts as evidenced by low

Figure 2.58 Optical micrograph of lens epithelial cells on (AMPSA co NVP) g PMMA prepared with prerosk 40%NVP/80°C/4hrs (40% AMPSA NVP ratio of 1 4. 0.05 Mrad 701 rad/min) (24 hour cell culture)

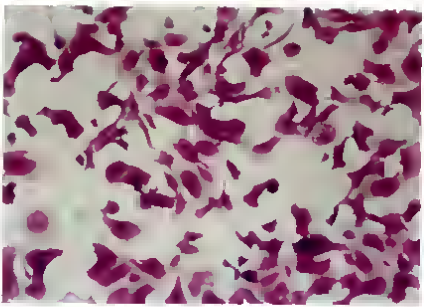

Figure 2.59. Optical micrograph of lens epithelial cells on KSPA g-PMMA prepared with prerosk 40%NVP/80°C/4hrs (10% 0.15 Mrad 701rad/min) (24 hour cell culture)

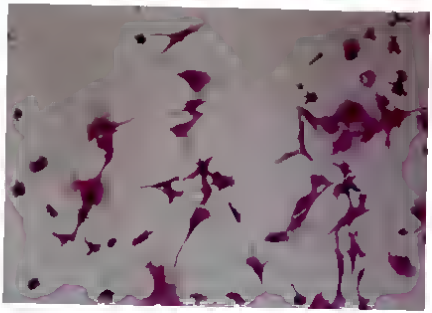

Figure 2 60 Optical micrograph of lens epithelial cells on (KSPA cc NVP) g PMMA prepared with pressak 46%NVP/60°C/4hrs (30% KSPA NVP ratio of 2 1, 0 15 Mrad 701 rad/min) (24 hour cell culture)

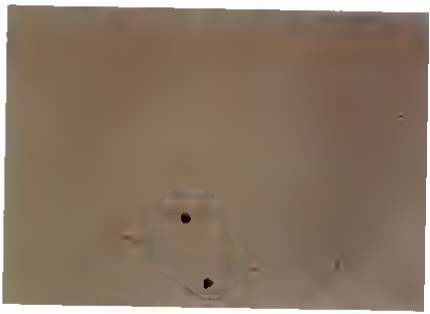

Figure 2 61 Optical micrograph of lens epithelial cells on (HA cc NVP) g PMMA prepared using the two step process (15% NVP/0 59 Mrad followed by 9 6% NVP/3 4% HA)/0 05 Mrad) (24 hour cell culture)

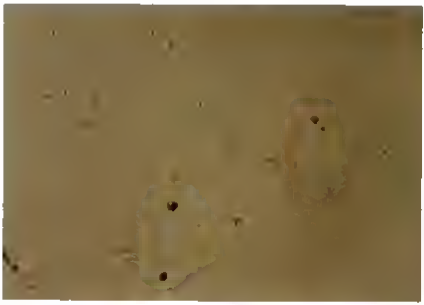

Figura 2.62 Optical micrograph of lens epithelial cells on (CMC-co-NVP)-g-PMMA prepared using the two step process (15% NVP/0.09 Mrad followed by 11% NVP/4% CMC)/0.06 Mrad) (24 hour cell culture)

contact angles (<20°) and SEM

3 Graft thickness measurements using staining techniques and light microscopy showed that grafts prepared using NVP solutions with presoaking in 40% NVP at 60°C for 4 hours (0 15 Mrad 701 rad/min) have a diffuse IPN-like structure within the substrate Thickness for PMMA grafts was 180±2P µm and 50±15µm for PDMS grafts However,grafts prepared with K8P PVP/NVP and γ-PVP/NVP aqueous solutions with the same dose and dose rate (P 15 Mrad 7P1 rad/min) showed a slight bluish color on the surface but little substrate penetration

4 FTIR/ATR with a depth of penetration of 0 66 µm showed the presence of comparable amounts of PVP in both grafts prepared using NVP solutions with monomer presoak (40% NVP/60°C/4 hours, 0 15 Mrad 7P1 rad/min) and those prepared using polymer/monomer aqueous solutions (i e , K8P PVP/NVP and γ PVP/NVP) with the same dose and dose rate (P 15 Mrad 701 rad/min)

XPS analysis with a depth of penetration of 5P Å revealed the presence of higher nitrogen content for grafts prepared with polymer/monomer solutions This further suggests that grafts prepared using polymer/monomer mixtures tend to remain at the uppermost surface, in contrast to those prepared with NVP monomer alone using the NVP presoak method in which monomer diffuses into the substrate

5 Aging of PDMS grafts in air at 60°C for 4 weeks resulted in 12° increase in contact angle and P P% decrease in nitrogen at the surface for NVP γ-PDMS prepared using NVP presoak (40% NVP/5P°C/4

hours. 0.2 Mrad, 701 rad/min). Grafts prepared using polymer/monomer mixtures (i.e., K90 PVP/NVP and γ PVP/NVP) with no NVP present using the same dose and dose rate (0.2 Mrad 701 rad/min) gave 6° increase in contact angle and 0.5% decrease in nitrogen for K90 PVP/NVP (10%, K90 PVP:NVP of 1:4). Grafts obtained using γ-PVP/NVP mixtures (10%, γ-PVP:NVP of 1:3) gave no significant increase in contact angle (3°) and only about 0.3% decrease in nitrogen elemental composition of the surface. These results suggest that grafts prepared using polymer/monomer mixtures (i.e., K90 PVP/NVP and γ PVP/NVP) may be more stable to molecular reorganization of the PDMS substrate than those obtained with NVP monomer solution alone using NVP presoak.

6. SEM surface morphology studies showed PMMA grafts prepared using polymer/monomer mixtures to be smooth and homogeneous.

7. PMMA surface grafts prepared using K90 PVP/NVP and γ PVP/NVP aqueous solutions supported virtually no lens epithelial cell adhesion and may be suitable for IOL surface modification especially for foldable IOL materials (e.g., PDMS).

8. Anionic grafts on PMMA and PDMS were prepared by gamma radiation induced polymerization of sulfonic acid group containing vinyl monomers including styrene sulfonic acid (SSA), acrylamido methyl propane sulfonic acid (AMPSA), potassium sulfopropylacrylate (KSPA), and potassium sulfopropylmethacrylate (SPMA). Monomer concentrations were varied from 5% to 30% and radiation doses from 0.05 Mrad to 0.5 Mrad the dose rate was 701 rad/min. Presoaking in 40% NVP at 60°C for 4 hours was shown to enhance grafting of SSA to PMMA as evidenced by greater weight gains

and lower contact angles

9 Hydrophilic grafts of sulfonic acid monomers copolymers with NVP on PMMA and PDMS substrates were also prepared using the presoak method (40% NVP/50°C/4hours) and comonomer concentrations varying from 10% to 40% with sulfonic acid monomer:NVP ratios of 1:4 to 4:1 For PSA, AMPSA, and KSPA grafting on both PMMA and PDMS was enhanced by copolymerization with NVP

10 PPA and KSPA modified PMMA surfaces supported substantial epithelial cell adhesion and spreading Such grafts may be of interest in designing surfaces which support cell proliferation such as endothelial cell linings of synthetic vascular prostheses

12 Radiation graft copolymerization of anionic sulfonic acid vinyl monomers with NVP produced surfaces with greatly reduced cell adhesion and spreading

13 Hydrophilic grafts containing hyaluronic acid (HA) and carboxymethylcellulose (CMC) on PMMA and PDMS were synthesized using a two step gamma radiation induced polymerization process The first step consisted of preparing hydrophilic PVP pregrafts using relatively lower radiation doses (0 05 Mrad for PMMA and 0 15 Mrad for PDMS) The second step consisted of gamma grafting HA/NVP and CMC/NVP mixtures using lower radiation doses (0 05 Mrad) Hydrophilic surfaces were obtained for both PMMA and PDMS (contact angle values less than 20°)

14 For PMMA and PDMS substrates grafting yield was found to increase with increasing HA and CMC concentrations For PMMA substrates, graft yields varied from 2 3 to 3 8% for HA and from 2 5%

to 5.3% for CMC. For PDMS substrates, graft yields varied from 3.0 to 4.2% for HA and from 3.8 to 5.5% for PDMS.

FTIR/ATR and XPS showed the presence of (HA-co-NVP) and (CMC co-NVP) grafts on PMMA and PDMS substrates.

15. Molecular weight analysis of grafting solutions (i.e. (HA co NVP) and (CMC co-NVP) solutions after gamma irradiation) by GPC suggested that HA and CMC are may be covalently bound to PVP in the grafts.

15. Corneal endothelium damage tests revealed that HA modified PMMA surfaces cause substantially less adhesion induced damage to the corneal endothelial cells (10% damage) in comparison to unmodified PMMA surfaces (80% damage). CMC modified PMMA surfaces caused virtually no damage (<5% damage).

16. HA and CMC modified PMMA surfaces supported no lens epithelial cell adhesion or spreading and may be of interest for IOL surface modification.

CHAPTER 3

TISSUE PROTECTIVE HYDROPHILIC POLYMER SOLUTIONS AND MEMBRANES

3.1 Introduction and Background

The use of hydrophilic polymer solutions in the biomedical field can be traced back to 40's. During World War II, polyvinylpyrrolidone (PVP) solutions were used as plasma expander with surprisingly few significant adverse reactions. Over the past fifty years, hydrophilic polymer solutions of natural and synthetic origins have been the subject of extensive research (114). With the new interests in biomedical and pharmaceutical industries, considerable research has been directed toward natural polymers which are water soluble or can be rendered water soluble by chemical modification. Dextran solutions have been used as plasma expander but have been shown to have some adverse physiological behavior (i.e., inhibition of clotting). The use of hydroxyethyl starch solutions for regulation of osmotic pressure in blood substitutes has also been reported (115).

The biocompatibility and versatility of hydrophilic polymer solutions have prompted interest in their potential use in surgery. This research dealt with the preparation, characterization and evaluation of hydrophilic polymer solutions as tissue protective devices. The use of such solutions in ophthalmic and abdominal surgery and related applications was addressed in some detail.

3.1.1 Hydrophilic Polymer Solutions in Ophthalmic Surgery

The introduction of hydrophilic polymer solutions as surgical tools has had a significant impact on the practice of ophthalmic surgery. These viscoelastic substances are mainly used to protect fragile ocular tissues during surgery and facilitate tissue manipulation.

The concept of using a viscous material in eye surgery goes back to the early 50's when Faufique and Sheffer used human cadaver vitreous to manipulate the detached retina (116,117). The search for a substitute to the natural vitreous which may be used as a surgical tool immediately followed. In 1958, Balazs suggested the use of hyaluronic acid (HA) solutions for this purpose (118) and considerable efforts were directed toward producing purified and noninflammatory preparations of HA.

The use of so-called viscoelastic solutions in cataract surgery to prevent tissue damage during IOL implantation was pioneered by Miller and Stegmann (119,120). The term viscosurgery was coined during the first film festival on IOL implantation in Cannes to designate the use of viscoelastic materials in ophthalmology (121). These substances have since been used in a wide range of surgical procedures and have become an invaluable surgical tool in ophthalmic surgery (122,123,124).

No one substance may be ideal for all ocular applications. The growing number of viscosurgical procedures requires viscoelastic materials with a wide range of physical properties. In this age of viscosurgery, a better understanding of the structure property relationships is needed to design improved viscoelastic solutions with desired properties.

3.1.1.1 Clinical use and properties of viscoelastics

The rheological properties of aqueous viscoelastic polymer solutions [illegible] the essence of their usefulness as surgical tools in ocular surgery Their performance is a function of solution viscosity shear behavior elasticity and tissue affinity Under static conditions, zero shear viscosity is an important characteristic of viscoelastics High zero shear viscosities will help support the weight of implants and instruments and thereby inhibit direct contact with fragile ocular tissues and reduce adhesion induced damage (125) Highly viscous solutions usually maintain space between tissues and allow easy manipulation within small cavities In ophthalmic surgery when the eye is opened the aqueous humor flows out of the eye and the anterior chamber tend to collapse making further manipulations such as IOL insertion a difficult task (126) One of the reasons for the use of viscoelastics in ocular surgery is their ability to maintain space within the anterior chamber and allow easy insertion and positioning of the IOL The pseudoplastic behavior of aqueous viscoelastic polymer solutions is also a major factor in their practical use During ocular procedures, Shear rates vary from 0 sec^{-1} at rest to perhaps 15000 sec^{-1} when the solution is rapidly extruded through a fine 25 gage needle (127) Viscoelastics which shear thin to a large extent exhibit a low viscosity when pushed through a small gauge cannula and are therefore easily delivered to specific surgical sites using a syringe

3.1.1.2 Protection of the corneal endothelium

A significant amount of damage to fragile ocular tissues may occur in any ophthalmic surgical procedure Considerable efforts are directed

toward preventing such damage especially to the corneal endothelium because it does not regenerate. The permanent loss of endothelial cells can be a source of major postoperative complications such as corneal edema and opacification. As discussed in chapter 2, these problems may be inhibited by hydrophilic surface modification of implant materials. The use of hydrophilic polymer solutions as adjuvants can also help minimize excessive trauma to the corneal endothelium.

Viscosurgical techniques were first applied to intracapsular cataract extraction (ICCE) and several studies showed a drastic reduction in endothelium damage (128,129). In the past decade extracapsular cataract extraction (ECCE) has become the cataract procedure of choice because of lower risk of surgical complications and the introduction of phacoemulsification devices which allow the preservation of the posterior lens capsule and extraction through small incisions. However, phacoemulsification may induce considerable damage to the endothelium and to other ocular tissues (130). This damage has been significantly reduced by the use of viscoelastics (131,132,134).

The protection of the corneal endothelium afforded by the viscoelastic solutions is due to a combination of properties which are unique to these materials. Their ability to prevent the anterior chamber from collapsing and maintain space between tissues reduces the risk of adhesion-induced damage significantly. Direct contact of endothelial cells with surgical instruments and implants is also reduced due to the ability of these solutions to coat the corneal endothelium.

However, the corneal endothelium is subjected to compression forces transmitted through viscoelastic substances. Highly elastic materials absorb the mechanical impact of instruments and implants and

transmit less compressive forces. Arshinoff has also reported endothelial damage due to drag forces caused by high viscosity viscoelastics (135). A high viscosity solution such as 1% HA can cause endothelial damage via the drag force phenomenon (136).

The ability of viscoelastic solutions to coat tissue surfaces has also been implicated in their effectiveness to protect the endothelium. It is believed that solutions with better tissue wettability which readily spread on the endothelial surface may provide enhanced protection (137). However, some question have been raised concerning the validity of the experimental methods used in these studies (138). It is still unclear whether the difference in endothelial cell protection afforded by various viscoelastic is truly related to their tissue coating ability. In addition, the factors influencing the wetting behavior of viscoelastics are yet to be investigated and only few studies have been directed toward wettability. Harrison et al. have suggested that anionic viscoelastics such as those based on HA and CS might have greater affinity for tissue surfaces and hence superior wetting properties (139).

3.1.1.3 Intraocular Pressure (IOP) rise

One major drawback to the use of viscoelastics is their apparent tendency to induce an increase in IOP (140, 141, 142). The relationship between IOP rise and viscoelastic use can be further appreciated by understanding the dynamics of aqueous humor.

The aqueous humor is a transparent fluid that is produced by the ciliary processes. It enters the eye in the posterior chamber, passes through the pupil into the anterior chamber, flows through the

trabecular meshwork, and enters the Schlemm's canal before draining into the episcleral vein. This flow pattern is shown in Figure 3.1.

The trabecular meshwork functions like a one way valve that permits aqueous humor to leave the eye but limits backflow in the other direction. IOP is determined by the rate of aqueous humor formation, the rate of its outflow trough the trabecular meshwork, and the pressure of the episcleral vein via the following equation:

$$IOP = (F/C)+P$$

where: F is the rate of aqueous formation in µl/min

C is the facility of outflow in µl/min/mmHg

P is the episcleral venous pressure

The normal rate of aqueous flow is 2 to 3 µl/min. Aqueous inflow decreases with inflammation, surgery or trauma to ocular tissues. The IOP in normal eyes ranges from 10 to 21 mmHg and higher values can cause glaucoma and optic nerve damage.

There are contractile elements within the trabecular meshwork and ciliary body, so the clearance of viscoelastics from the anterior chamber is probably dynamic (143). The increases in IOP associated with the use of viscoelastic is complex and research has been conducted in order to elucidate the properties of viscoelastics involved in this particular complication (144,145).

Viscoelastic substances are cleared from the anterior chamber through the trabecular meshwork. This can interfere with the normal outflow of the aqueous humor and cause a pressure increase. HA was

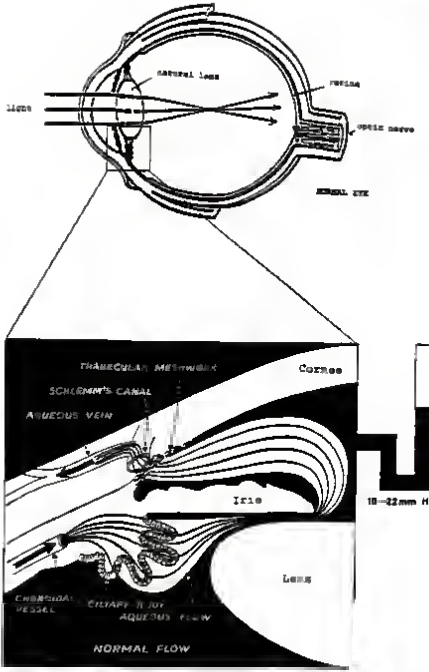

Figure 3 1— Flow pattern of aqueous humor in the human eye

found to cause 85% of the outflow facility in enucleated human eyes (148). The tendency of a given substance to increase IOP may be related to its rate of clearance through the trabecular meshwork. The chemical structure, molecular weight, molecular conformation and metabolic degradation of viscoelastics are primary factors which can govern the rate of clearance.

The increase of IOP associated with HA has been reviewed (147,148). In animal studies, an increase in IOP was observed only when the concentration of HA in the aqueous humor at any time after injection was greater than 2 mg/ml. Henriger et al. have shown that if the concentration of HA is kept constant in the aqueous humor, lower molecular weight HA causes a higher IOP. This was explained by the fact that low molecular weight HA is easily diluted in the aqueous humor and flows rapidly into the angle structure causing obstruction and high transient IOP.

Other in vivo studies found that the recovery from the transient IOP was not dependent on the molecular weight or concentration of HA solutions (148). An artificial model of the trabecular meshwork also suggested that pressure is directly related to the molecular size, rigidity and charge of the macromolecules (150).

Viscoelastics which have been claimed to cause moderate increase in the IOP even when left in the eye postoperatively due to the use of relatively low molecular weight polymers such as mixtures HA and CS have been investigated with regard to their tendency to induce IOP increase. Reports on this subject are contradictory and several animal and clinical studies failed to support these claims (151,152). A comparative study of the clearance rate of HA, CS, and methylcellulose

(MC) viscoelastics from the anterior chamber and its impact on IOP have shown that all of these solutions induced a transient IOP increase 6 hours postoperatively (153) The IOP increase was considerably higher for MC and was attributed to its molecular weight (0.6×10^6) and lack of degradation in the AC HA of similar molecular weight exhibited much lower IOP and shorter time of recovery and was shown to degrade enzymatically by hyaluronidase present within the iris and corneoscleral junction Chondroitin sulfate, exposed to extracts from the same tissues, did not degrade and caused slightly higher IOP increase than HA of much higher molecular weight (153) However in normal cataract surgery it has been reported that transient IOP rise can occur even when no viscoelastic was used

The research reported here involved the preparation and characterization of hydrophilic polymer solutions based on carboxymethylcellulose (CMC) i e polysaccharide similar to hyaluronic acid but of much greater stability The rheological properties of these solutions were investigated as function of purification processing (filtration autoclaving) in order to understand the structure property relationships of CMC solutions and to enable preparation of improved viscoelastic solutions

1.1.2 Hydrophilic Polymer Solutions for Surgical Adhesion Prevention

1.1.2.1 Formation of surgical adhesions

The formation of postoperative adhesions can be a serious complication in all surgical procedures which involve handling of internal organs Postsurgical adhesions are the main cause of intestinal obstruction in abdominal surgery infertility in pelvic

surgery and higher mortality in cardiac surgery (154).

It is widely accepted that adhesions result from an inflammatory response caused by surgical trauma, drying of tissue, ischemia (i.e., temporary obstruction of blood flow), and the presence of foreign bodies (155). The formation of adhesions is schematically shown in Figure 3.2. Initial surgical insult to tissue surfaces leads to the formation of fibrin exudate containing inflammatory cells (i.e., neutrophils, monocytes, and macrophages) within the first day after surgery. Fibrin is the "glue" responsible for adhesion of surfaces and subsequently serves as matrix for fibroblasts. Collagen is secreted by fibroblasts which leads to connective tissue formation bridging adjacent tissues as depicted in Figure 3.2 (155).

3.1.2.2 Prevention of surgical adhesions

The prevention of surgical adhesions has attracted increasing attention in recent years. A variety of therapeutic agents and surgical techniques have been investigated. The pharmacological approach has been to study agents capable of reducing the inflammatory response decreasing fibroblast migration, or enhancing fibrinolysis. Antiinflammatory compounds such as corticosteroids, non steroidal antiinflammatory drugs (NSAID's) have been shown to reduce adhesion formation when administered topically (157). Recent evidence suggests that oxygen derived free radicals (ODFRs) produced by inflammatory cells are also responsible for extensive tissue damage (158). The use of antioxidants and free radicals scavengers such as superoxide dismutase (SOD) and catalase to prevent adhesion formation has also shown some promising results.

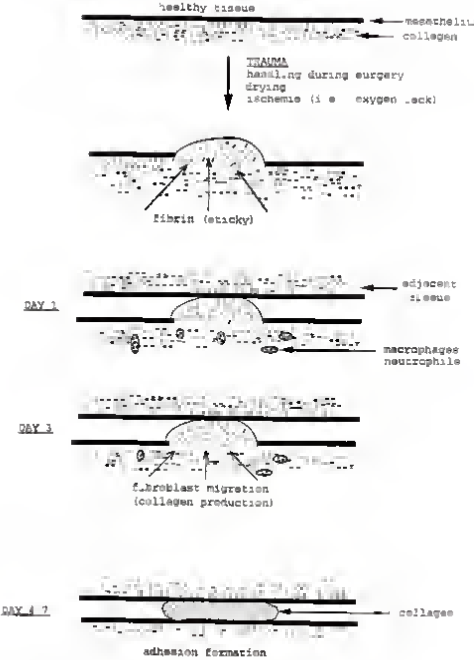

Figure 3 2 Schematic drawing of peritoneal adhesion formation mechanism

Other strategies have involved the use of fibrinolytic agents capable of dissolving the fibrin matrix which supports fibroblast proliferation. Tissue plasminogen activator, an enzyme which converts inactive plasminogen to a potent fybrinolytic agent called plasmin, has been reported to be useful (158).

Other pharmacological agents include those capable of decreasing fibroblast migration and collagen production (e.g., corticosteroids). These substances, however, can interfere with healing of the incision wound and hence result in weak tissue repair, risk of infection.

3.1.2.3 Hydrophilic polymer solutions in surgical adhesion prevention

A variety of synthetic and natural hydrophilic polymer solutions have been investigated for the prevention of surgical adhesions. These solutions were usually instilled at the surgical sites at the completion of the surgical procedure. Dextran solutions of various concentrations were reported to show promising results (160). However, recent clinical studies have indicated that the use of dextran does not significantly reduce adhesion formation (161). In addition, such solutions have been implicated in severe allergic reactions and excessive peritoneal fluid accumulation (162). A number of other hydrophilic polymer solutions have been studied with varying reported success. These include PVP block copolymers of PEO and PPO (Polaxomer), methylcellulose, CMC, and HA (163,164,165).

Elkins et al. reported CMC to exhibit some effectiveness in reducing adhesion formation in rats (166). These results were further confirmed by Diamond (167) and Fredericks (168). The effectiveness of CMC in reducing the incidence and severity of surgical adhesions was

attributed to superior tissue contability which prevented direct apposition of traumatized tissues. Slow absorption from the peritoneal cavity was also believed to afford prolonged protection. Solutions reportedly afford physical tissue separation enhanced by their lubricating properties.

This effect is often described in the literature as a "siliconizing" effect (169,170). These solutions may also draw fluid to the surgical sites via a "hydroflotation" effect which helps prevent dehydration of traumatized tissues (171).

Although these solutions, applied at the conclusion of surgery are believed to remain in surgical sites for prolonged periods of time thereby acting as physical barrier which separate traumatized tissue and allow them to heal without adhering to each other, there is no compelling evidence that they are truly effective and there has therefore been no general clinical use of these agents.

3.1.2.4 Prevention of adhesion formation by preventing tissue damage

As discussed earlier, adhesion prevention studies generally involved instilling polymer solutions after completion of the surgical procedure. However, Goldberg et al. have shown that a contact adhesion phenomenon similar to that observed for the corneal endothelium discussed in the first part of this research, may be responsible for extensive tissue damage which triggers adhesion formation (172). Such damage can be caused by manipulation of internal organs, inadvertent contact with surgical instrument, and drying of tissues. Therefore they suggested the use of hydrophilic polymer solutions as protective coatings applied to tissue surfaces and surgical instruments prior to

any surgical manipulation (173) The use of hydrophilic polymer solutions as protective coatings to prevent tissue damage has now been proven to reduce the incidence and severity of adhesions significantly by minimizing surgical tissue damage (174 175 176)

A portion of this research was therefore devoted to the preparation and evaluation of hydrophilic polymer solutions for use as tissue protective coating in abdominal surgery The stability and oxidative degradation of HA and CMC solutions which might occur at injury sites via oxygen derived free radicals (ODFRs) produced by polymorphonuclear leucocytes was also investigated

3.1.2.5 Polymer membranes in the prevention of surgical adhesions

Adhesion prevention polymer membranes have been studied to mechanically separate damaged tissues allowing them to heal without adhering to each other The main advantage of the mechanical barrier approach is the prolonged separation afforded by such materials A variety of natural and synthetic materials have been investigated for this purpose

Microporous polytetrafluoroethylene (PTFE) thin films as surgical membranes has been reported by Boyers and Jansen (177) Reports on the efficacy of these materials are contradictory and their use for the prevention of adhesions is hampered by the fact that PTFE is not biodegradable and these membranes need to be retrieved surgically (178)

An oxidized regenerated cellulose membrane INTERCEED® (TC7) has also been reported to reduce adhesion formation (179) TC7 is a resorbable woven fabric which is applied directly to tissues and does not require suturing One major disadvantage of TC7 is the fact that

its ability to inhibit adhesions is compromised by the presence of blood (IBP). Additionally studies in this laboratory suggest that TC 7 can promote adhesion formation under some conditions. The use of some substances to control bleeding prior to the use of TC7 has shown little success. Hyaluronic acid membranes, which biodegrade in 3 4 days, developed by the Genzyme corporation have also shown some effectiveness in reducing adhesion formation.

In this context, the preparation and evaluation of resorbable adhesion prevention barrier membranes based on carboxymethylcellulose (CMC) was investigated. Methods for insolubilizing CMC films were studied and a novel thermal insolubilization technique has was developed in this research for the preparation of CMC membranes with a wide range of physical properties (e.g., water uptake, degradation time in physiological media).

3.1.3 Rheology of Polysaccharide Solutions

The purpose of this section is to discuss the flow properties of polysaccharide solutions in general but with emphasis on CMC and HA solutions. Major departures from conventional polymer solution properties, which impart some unique rheological properties to these materials, are discussed.

3.1.3.1 Conformational considerations

The behavior of polymers in solution is directly related to the chain conformation and to the extent and nature of intermolecular interactions. Polysaccharides including HA and CMC usually assume disordered solution conformations since polymer solvent interactions provide only a small contribution to the entropy of mixing making polymer dissolution thermodynamically unfavorable. The disordered

solution state. generally described as random coil state. provides the required entropy contribution to the free energy of mixing. The coil flexibility can be expressed in terms of a parameter S and the ionic strength (I) according to the equation (181):

$$S \sim S\,([\eta]_{0.1})^{1.3} \qquad (3.1)$$

where S is the slope of the plot $[\eta]$ vs $I^{1/2}$ and $[\eta]_{0.1}$ is the intrinsic viscosity at ionic strength of 0.1 N. At high ionic strength charge screening reduces the influence of coulombic interactions on the polymer conformation. At low ionic strength, these interactions become important and do effect the conformation. The overall coil dimension are mainly determined by the shape of the monosaccharide residues and the rotational freedom around the glycosidic linkages. As shown in Figure 3.3, the restricted coil flexibility of CMC is due to its trans (1,4β) linkages between repeating units which significantly restrict the rotation of glycosidic linkages (182). The presence of carboxylic groups has also been implicated in the restriction of such movements (183). The structure of HA is also shown in Figure 3.3. The linkages between residues in HA consist of alternating trans (1,4β) and cis (1,3β) which is expected to allow a higher degree of freedom of rotation around glycosidic bonds. Therefore, according to its structure, the HA random coil should be somewhat more flexible than that of CMC. However HA chains have been shown to be much stiffer than CMC chains. Morris et al. have suggested that this discrepancy is may be due intramolecular hydrogen bondings which provide HA molecules with additional stiffeness (184).

Carboxymethylcellulose

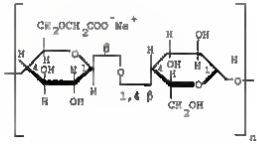

1 4 β linkages

Hyaluronic Acid

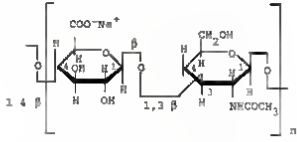

Alternating 1,4 and 1,3 β linkages

Figure 3 3 Chemical structures of CMC and HA showing linkage type between monosaccharide units

The chain conformation is directly related to the size of the interresidue hydrogen bonding which provides HA molecules with additional stiffeness (184) The chain conformation is directly related to the size or hydrodynamic volume of the random coil which in turn effects flow parameters of the polymer solution including concentration and sheer behavior

3.1.3.2 Flow behavior of polysaccharide solutions

Polysaccharides solutions exhibit a variety of rheological properties, ranging from Newtonian to various type of non Newtonian behavior (185) The solution behavior of random coil polymers is influenced by the extent to which individual polymer molecules interact with each other and by the nature of these intermolecular interactions By considering the concentration at which individual chains overlap as a critical concentration three concentration regimes can be distinguished for polymer solutions as shown in Figure 3 4.

(i) c < c* dilute concentration where the polymer chains exist as isolated, hydrodynamically non-interacting species

(ii) c = c*, concentration where coil overlap or entanglement occure

(iii) c > c* concentration solution regime where considerable coil overlap occure.

The critical concentration c* is usually obtained from double logarithmic plots of specific viscosity ve concentration There is a pronounced increase in the slope of log-log plots of viscosity versus concentration above c* which indicate the transition from dilute to concentrated solutions The value of c* is a function of the polymer/solvent interaction, the temperature and the molecular weight

Figure 3 4: Schematic drawing of different concentration regimes in polymer solutions

and is proportional to the hydrodynamic volume occupied by the isolated polymer coils according to the equation

$$c^* = S/[\eta] \qquad (3.2)$$

Where S represent the extent of chain overlap and $[\eta]$ is the intrinsic viscosity which is proportional to the molecular weight according to Mark-Houwink relationship

$$[\eta] = K M^{\alpha} \qquad (3.3)$$

The constant K is related to the polymer backbone stiffness, and the exponent α reflects the degree of molecular expansion

A more convenient way to relate the molecular structure to the flow behavior is usually achieved by using the coil overlap parameter $c[\eta]$ This dimensionless parameter is a measure of the total volume occupied by all coils within a polymer solution regardless of their type and molecular weight (186). Generalized behavior of polymers are often described in term of $c[\eta]$

A major difference between flexible non ionic synthetic polymers and ionic polysaccharides is the fact that the onset of the concentrated regime occure at much lower concentration and coil overlap parameter due to the unusually high hydrodynamic volume of the polysaccharides This difference originates from the fact that ionic polysaccharide molecules are much less flexible and therefore adopt considerably more expended coil geometry (187). This allows coil overlap at lower concentrations and very high viscosities For CMC and HA the terms "concentrated" and "dilute" will be used to denote concentration above and below c^*

This research was primarily concerned with the rheology of CMC in the concentrated regime HA was used for comparison since it is the

most important hydrophilic polymer clinically used for ophthalmic viscoelastic solutions and other biomedical uses

3.1.3.3 Rheology of concentrated polysaccharide solutions

In dilute polymer solutions, polymer solvent interactions predominates and the flow behavior is dictated by intramolecular interactions. When the concentration is increased considerable coil interpenetration occurs and the motion of the polymer chains is influenced by intermolecular interactions in addition to intramolecular interactions. For synthetic polymers, Fethrick showed that topological entanglements in concentrated solutions form typically at c[η] values of 10 (188). In polysaccharide solutions, however significant coil interpenetration occurs at c[η]=4. and zero shear viscosity increases sharply with increasing coil overlap parameter (i e with increasing concentration for a fixed molecular weight) (189). Polysaccharides are usually used as gelling agents, and the mechanism of gelation of these systems has been shown to involve the formation of stable molecular "junction zones" between structurally and conformationally regular chains sequences which act as physical crosslinks(190). Several studies showed that analogous ordered structures may be adopted in concentrated solutions of polysaccharides and may explain departures from the flow behavior of purely synthetic polymers (191). The essence of this model is the fact that each chain has sufficient length and flexibility to participate in several junction zones simultaneously thereby allowing a certain degree of " crosslinking". Most of the polysaccharides which exhibit such behavior in solution possess random coil geometry and exhibit unusual rheology (192).

Among the anomalies observed for such substances are the sharp increase of "zero shear" viscosity with increasing concentration and a pronounced shear thinning (133) Morris et al have also shown that the onset of shear thinning is observed at relatively lower shear rates which has been attributed to a longer time scale intermolecular associations (134) Further evidence of the "junction zone model" was provided by Welsh et al who showed that the network properties of some polysaccharides can be inhibited by the addition of short chains of well characterized length (135) He suggested that such short chains compete with longer chains for the junction zones and do not participate in a sufficient number of these junctions to allow physical "crosslinking"

The effect of shear rate on polysaccharide solutions is not solely governed by the time scale of disentanglements and formation of new non-specific intermolecular associations as in synthetic polymers (136) Additional contributions from the specific associations (i e junction zones) have to be taken into consideration This gives polysaccharide solutions such as CMC and HA unique rheological properties

The research reported here dealt with the preparation and characterization of purified CMC solutions for use as viscoelastic materials in ophthalmology and as tissue protective devices in surgery This investigation of rheological properties has led to the development of empirical equations which describe concentration dependence of shear viscosity and pseudoplastic behavior of these solutions A unique purification method which include filtration and autoclave sterilization was also developed based on the unusual rheology of CMC solutions

3.2 Materials and Methods

3.2.1 Materials

3.2.1.1 Carboxymethylcellulose (CMC) and hyaluronic acid (HA)

Pharmaceutical grade carboxymethylcellulose (CMC FPH) of molecular weight ranging from 8.0×10^4 to 1.0×10^6 used for this research were obtained from Aqualon (Wilmington, DE). The specifications of CMC grades used are given in Table 3.1. Hyaluronic acid (HA) with molecular weight ranging from (1.2×10^6 to 2.8×10^6) was generously provided by the Genzyme Corporation. Balanced salt solution (BSS) was obtained from Alcon surgical Inc. (Fort Worth, TX).

3.2.1.2 Antioxidants and other reagents

Ferrous sulfate, Calcium chloride heptahydrate, dimethylsulfoxide (DMSO), and catalase from Fisher. Ethylenediaminetetraacetic acid (EDTA), D-Mannitol, α-tocopherol (vitamin E), glutathione (reduced form), and sodium salt of L-ascorbic acid obtained from Aldrich. L-histidine, acetylsalicylic acid (aspirin), and Ibuprofen obtained from Sigma.

3.2.2 Methods

3.2.2.1 Viscosity measurements

Viscosity is a measure of the internal friction of a liquid or a measure of its resistance to flow. This definition can be better visualized if one considers the movement of a liquid contained between two infinite parallel plates as shown in Figure 3.5. If one plate is fixed and the other one is moving with a constant speed V. The sheer rate is defined to be the plate velocity divided by the spacing h. In this case, four components of the stress tensor are nil and the

Table 3 1 Specificetions of CMC grades used for this research

grade	DS[1]	Mw	DP[2]
7LDH	0 7	90 000	400
7MPH	0 7	350 000	1100
7HPH	0 7	900 000	3200
7H4F	0 7	1,000 000	

[1] Degree of substitution of carboxylic group

[2] Degree of polymerization

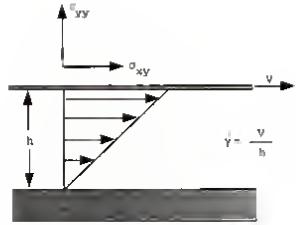

Figure 3 5 Simple shearing flow between two plates

remaining five can be written as follows:

$$\sigma(a) = \sigma_{xy} \qquad (3\ 1)$$

$$N_1(a) = \sigma_{xx} - \sigma_{yy} \qquad (3\ 2)$$

$$N_2(a) = \sigma_{yy} - \sigma_{zz} \qquad (3\ 3)$$

Where a is the shear rate, N_1 and N_2 are the first and second stream differences respectively. Shear viscosity is defined according to the following equation:

$$\eta = \sigma(a)/a \qquad (3\ 4)$$

A variety of methods, based on various geometries, have been used to measure shear viscosity. These methods include concentric cylinders, parallel plates, sliding plates, sliding cylinders, and cone and plate. In this research the shear viscosity was measured with a viscometer based on a cone & plate geometry as shown in Figure 3.6. The plate is fixed while the cone is rotated with a constant angular velocity ω. The velocity at any point of the two surfaces is proportional to its distance from the axis. The separation of the surfaces at any point is proportional to the same radius. If the cone angle is small enough, the shear rate defined as the ratio of velocity to the gap width is therefore constant. The cone angle is made very small ($<4^\circ$) to obtain a constant shear rate over the cone surface. The viscosity can be obtained from the following equations:

$$\eta = \tau / a \qquad (3\ 5)$$

$$\tau = \frac{T}{2/3\,\pi r^3} \qquad (3\ 6)$$

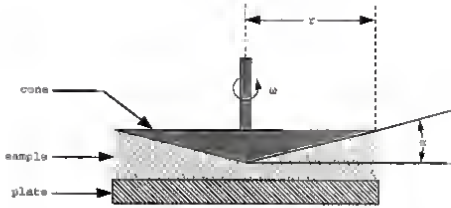

Figure 3 6 Schematic drawing of the cone and plate geometry

$$\dot{\epsilon} = \frac{\omega}{\sin \theta}$$

Where

η = viscosity in Centipoise (Cps)

τ = shear stress in dyne cm

$\dot{\epsilon}$ = shear rate in s-1

T = percent full scale torque in dyne cm

r = cone radius in cm

ω = cone angular velocity

θ = cone angle in degrees

Cones of different dimensions and configurations (i.e , r and α) allow measurements over a wide range of viscosities Low viscosities are usually measured using high radius cones (e g , CP 40 or CP 41) and higher viscosities are better obtained with smaller cones (e g , CP 51 or CP 52) The viscosity can be measured under various conditions of shear rate by varying the rotational speed of the plate Shear behavior of solutions can be evaluated by measuring the viscosity at different rates of shearing

The instrument used for this research was a cone and plate Brookfield digital viscometer model DV II equipped with jacketed plate (Stoughton MA) A constant temperature water bath was used to control the sample temperature during measurements Calibration was performed using Brookfield calibration standard fluids (1000 100 000 Cps)

3.2.2.2 Solution preparation

Numerous studies have reported some difficulties associated with the dissolution in water of polysaccharides such as CMC and HA

CMC and HA tend to agglomerate and form heterogeneous solutions in the presence of water Several methods have been suggested to facilitate dissolution and obtain homogeneous solutions The powderous material can be wetted with a nonswelling solvent such as acetone or methanol in the case of CMC prior to adding water (197) Another method consists of using specially designed mixing devices using high velocity water jets which allow particle wetting prior to dissolution (197)

In this research CMC solutions were prepared in a dust free hood using a mechanical paddle stirrer equipped with Teflon® paddle stirrers (Caframo model RZR paddles from Cole Parmer Inc) Desired amount of solvent (i e, PBS, PBS or water) was poured into a 100 ml Erlenmeyer flask and vigorously stirred at 5000 rpm to create a vortex The powder was gently sifted inside the vortex slowly enough to permit complete wetting of the individual particles but fast enough to avoid rapid viscosity build up which limits the rate of dissolution Solutions were stirred at 5000 rpm for the first 15 minutes then the flask was covered, and the solution allowed to stir at 1000 rpm for 12 hours The flasks were finally removed, tightly covered, and allowed to sit at room temperature for 24 hours prior to viscosity measurements In spite of their light and temperature stability, CMC solutions are prone to bacterial attack (197) Special care should be taken to avoid solution contamination

Due to their thixotropic behavior, CMC solutions are sensitive to shear history The time and speed of mixing were kept the same for all of the test solutions All of the solutions used in this research were systematically prepared as described above

1.2.2.3 Solution filtration

Filtration of viscous solutions through small diameter filters is difficult. This is usually best achieved by decreasing the viscosity using elevated temperatures. However, increasing the temperature in the case of HA or CMC solutions may cause some degradation. CMC solutions "shear-thin" and viscosity is substantially reduced at high shear rates. This behavior can be used to facilitate filtration of such solutions.

The filtration apparatus used is schematically shown in Figure 3.7. The actual filter consisted of a small disc 10mm in diameter cut from a 10μ Teflon filter mesh (Spectra Mesh, LA, CA) obtained from Fisher. The filter was sandwiched between two circular stainless steel screens (10mm diameter), of 200μ pore size. These screens were used to keep the membrane filter flat and ensure an even distribution across the filter surface. To increase shear rate further a PTFE disc (10 mm diameter) with an opening of 2 mm was added adjacent to the first screen as described in Figure 3.7. The filter screens and PTFE disc were housed in a high pressure stainless steel filter housing (13mm, Fisher) having a female locking luer inlet and a male luer slip outlet. The filter housing is especially designed to accommodate a syringe with luer fitting. Solutions were loaded in a 3 cc syringe (Monoject®) with a 9.7 mm plunger and a 4 mm orifice, and extruded through the filter. For higher viscosity solutions (>30 000 Cps), 1cc syringes (Monoject®) with a 4.7 mm plunger and 4.0 mm orifice were found to work better. Filtered solutions were allowed to sit at room temperature for 24 hours prior to viscosity measurements or ultracentrifugation.

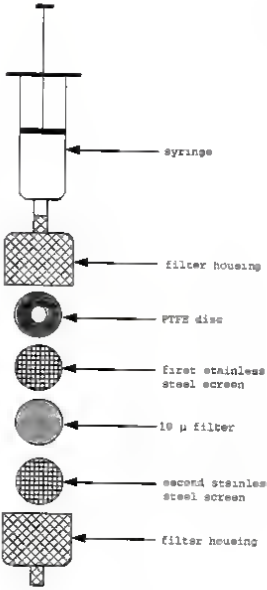

Figure 3.7 Schematic drawing of the filtration apparatus used to filter CMC solutions.

3.2.2.4 Solution autoclaving

Autoclave sterilization was at 240° F for 20 minutes with 8 minutes heating and cooling ramps using a Market Forge Sterilmatic autoclave. Solutions were loaded in 50 ml glass vials with Teflon® screw caps, autoclaved at a slow cycle and allowed to sit at room temperature for 24 hours prior to viscosity measurements.

3.2.2.5 In vitro degradation of HA and CMC and the evaluation of antioxidant stabilizers

The purpose of this experiment was to investigate the effect of oxygen derived free radicals (ODFR's) produced in vitro, on CMC and HA solutions. HA (1.5×10^6) was dissolved to 0.4% in PBS, allowed to stir for 12 hours and then stored at 4°C until use. Carboxymethylcellulose (CMC 7HFPH) was dissolved to 0.5% in PBS as described in section 3.2.2.2. An aqueous solution of equimolar ratio of EDTA to ferrous sulfate (50mM:50mM) was prepared shortly before running the experiment. Aliquots of 10ml of test solutions were transferred to separate test tubes and antioxidants were added to desired concentration. Samples were then shaken for a few minutes to insure homogeneous solutions. Free radicals were produced by adding 50µl of the Fe/EDTA solution to each test solution. Samples were then kept at room temperature for 6 hours. Viscosities were measured before and after adding the Fe/EDTA solution.

3.2.2.6 CMC film preparation and modification

3.2.2.6.1 CMC film (CMC-F) preparation

A preliminary study was first conducted to find appropriate viscosities for casting. A solution of 1% CMC-7HPH filtered through a 10 µ filter was found to yield a good viscosity (1200 Cps) for this

application CMC films were cast on clean glass plates (8x8cm) A doctor blade was used to control film thickness Drying at room temperature for extended periods of time resulted in films with poor optical properties On the other hand when the films were oven dried at higher temperatures some shrinkage occurred and the resulting films were brittle The apparatus used for film drying is schematically shown in Figure 3 8 An acrylic chamber with two lateral openings was used to shield the cast solutions from dust particles A blow dryer was used to create a hot air convection current which allowed the solutions to be dried without effecting their surfaces CMC-F were dried for 12 hours peeled off the glass plates and stored in a desiccator until use

3.2.2.6.2 Treatment with calcium chloride

Treatment in aqueous solution of calcium chloride was conducted by soaking dry CMC-F in saturated aqueous solution of calcium chloride ($CaCl_2$) for 12 hours The films were then rinsed with distilled water and finally dried for 12 hours as described in section 3 3 2 2 1 CMC-F treated with aqueous calcium chloride solutions were weak and difficult to handle (i.e., easily torn) The fact that the CMC films were introduced to calcium ions through an aqueous phase affected the integrity of these films

To minimize film swelling and tearing, throughout the crosslinking reactions a mixture of aqueous calcium chloride and acetone was used Calcium chloride in its crystalline form is not soluble in acetone However aqueous solution of Calcium chloride combined with acetone form a two phase system A saturated aqueous solution of $CaCl_2$ was mixed with acetone in ratio of 1:1 The two phases were dispersed by sonication and the resulting mixture was allowed to phase separate in a

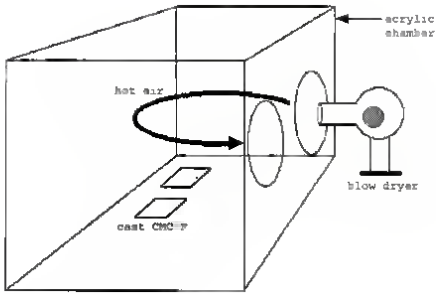

Figure 3.8. Drying apparatus used to prepare CMC-P.

seperatory funnel The acetone-rich phase (upper phase) was collected and used to crosslink CMC films CMC films were soaked in the acetone rich phase for 12 hours rinsed with a 1 1 mixture of acetone and water then dried for 12 hours

3.2.2.6.3 Insolubilization by thermal treatment of CMC F

Heat treatment was conducted in air or in a carbon dioxide atmosphere, at temperatures ranging from 140 to 190°C for a few minutes to 24 hours Dry CMC F were individually deposited on glass dishes and heat treated in air in an oven equipped with internal thermocouple Heat treatment in CO_2 was achieved as follows CMC F were individually put inside glass vials and vacuum degassed for 10 minutes The vials were then backfilled with CO_2 tightly closed with teflon screw caps and heat treated as described above; Thermally treated CMC F were removed and immediately stored in a dessicator until use

3.2.2.6.4 CMC F swelling and solubility

CMC F were soaked in PBS at room temperature for 5 hours and water uptake was measured as percent swelling using the following relationship:

$$\text{Percent Swelling} = \frac{\text{Weight (wet film)} - \text{Weight (dry film)}}{\text{Weight (dry film)}} \times 100$$

The rate of dissolution of CMC films heat treated under different conditions was qualitatively evaluated by immersing the samples in individual test tubes in PBS at 70°C Films were inspected visually every hour until complete dissolution

3.2.2.7 In vitro rabbit endothelium wetting properties of various viscoelastics

This experiment was conducted with the assistance of Dr Hiroyuki Nattori and Mr Paul Martin New Zealand White rabbits were euthenized using sodium pentobarbitol via the marginal ear vein Eyes were enucleated and immediately placed in BSS The corneas were then carefully removed and 9mm diameter corneal buttons were cut and glued flat with cyanoacrylate glue on glass slides The corneas were kept in BSS until contact angle was measured The contact angle measurements were performed on endothelium surfaces using a Ramé Hart goniometer Wetting contact angles on water free endothelium surfaces were obtained as follows : Corneal buttons were removed from the BSS one at time shaken twice to remove excess BSS and a drop of the test solution of approximately 10µl was gently deposited on the endothelium surface The contact angles on both sides of the same bubble were recorded and their respective values averaged Contact angles on moistened endothelium surfaces were obtained by wetting the endothelium surface with a drop of BSS prior to depositing the test solution samples were run in triplicate

The viscoelastic solutions used for this study were a solution of 1% HA (Healon®) obtained from Pharmacia Viscoat® from CooperVision CILCO is a solution of 3% HA / 4% C6S, C6S with a molecular weight of 22,500 and HA with a molecular weight of 500,000; CMC V1 a sterile solution of 1.85% CMC 7HFPH (800,000); and CMC V2 a sterile solution of bimodal CMC blend (4.8% 7HFPH 7LP of 2:3) The viscosity was measured at 25° C using a cone and plate Brookfield Viscometer RVT DVII with a spindle CP-52

3.3 Results and Discussion

The rheological properties of polymer solutions are of considerable scientific and technological interest and a number of theories have been developed to relate flow properties to molecular behavior. These theoretical treatments, however, normally relate to narrow molecular weight distributions of polymer chains interacting only by topological entanglement, and experimental verifications have been largely confined to synthetic polymers in nonaqueous solutions or as polymer melts.

Due to their biocompatibility, stability, and solutions properties, CMC solutions appear to be promising for use as viscoelastics in ophthalmology, or as tissue protective coatings for the prevention of surgical adhesions. In the present work a systematic investigation of the rheology of a modified cellulosic polysaccharide carboxymethylcellulose (CMC) was conducted. These studies have been confined to flow behavior under lateral shear, since this is the most widely used form of viscosity measurement.

3.3.1 Rheology of CMC Solutions

3.3.1.1 Effect of concentration on 'zero shear' viscosity

In comparison with neutral synthetic polymers, CMC imparts unusually high solution viscosities at relatively low concentrations. Zero shear viscosity (η_0) is a complex function of concentration and molecular weight. The viscosity of aqueous CMC solutions increases exponentially with increasing concentration as shown in Figure 3.9. This increase in viscosity is much more pronounced than in the case of most neutral synthetic polymers of similar molecular weight.
This behavior is probably due to additional intermolecular electrostatic

repulsions, hydrogen bonding, and chain stiffness and will be discussed in details in the next section.

It appears from Figure 3.9 that the concentration dependence of η_0 can be represented by a power law of the form

$$\eta_0 = Ac^m \qquad (3.7)$$

where A and m are two constant which can be empirically determined from double logarithmic plots of η_0 vs c according to the equation:

$$\log \eta_0 = \log A + m \log c \qquad (3.8)$$

m is the slope of the logarithmic plot and A is the intercept with the y axis. Double logarithmic plots for CMC of various molecular weights are shown in Figure 3.10. Values of A and m are summarized in Table 3.2. These empirical equations can be useful in predicting approximate values of shear viscosity for a given concentration under the same conditions used in this research. These include ionic strength, pH, temperature and mixing conditions.

In order to gain some understanding of the molecular origin of the flow behavior of CMC solutions, the effect of conformation and segmental mobility of isolated molecules should be distinguished from that of intermolecular associations. The two principal factors which determine the hydrodynamic volume of isolated molecules are molecular weight and chain stiffness[198]. CMC is a very rigid molecule and therefore adopts a large expanded coil geometry. The origin of such large coil dimensions can be explained in terms of conformational restrictions due to intramolecular interactions between adjacent residues and the linkage geometry of these residues which limit the chain flexibility.

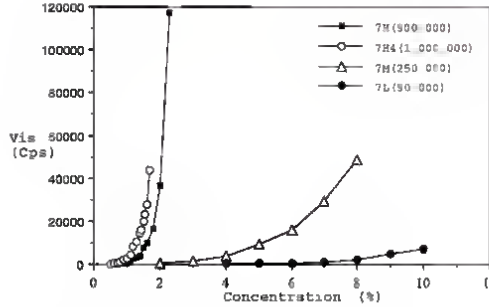

Figure 3.9. Viscosity of CMC solutions versus concentration for various molecular weights at 1.0 s^{-1}

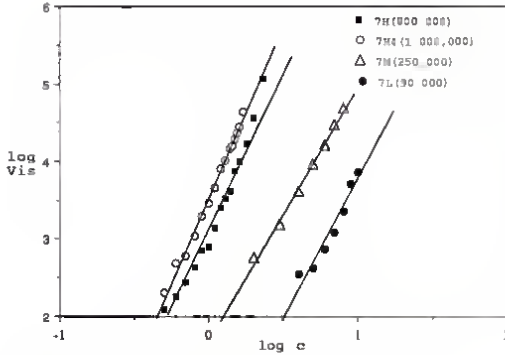

Figure 3.13 Log-log plots of viscosity versus concentration for various MW CMC.

Table 3.2 Empirical equations for zero shear viscosity of various MW CMC.

CMC	MW(x10^5)	m	A	R^2	$\eta_0=Ac^m$
7H4F	10	4.3	3400	0.98	$\eta_0=3400\ c^{4.3}$
7HFPH	9.0	4.2	1350	0.97	$\eta_0=1350\ c^{4.2}$
7MF	3.5	3.3	50	0.98	$\eta_0=50\ c^{3.3}$
7LP	0.9	3.2	8	0.95	$\eta_0=8\ c^{3.2}$

R is the correlation factor
c is the concentration in %S
η_0 is the shear viscosity at 3.75 s^{-1} for viscosities lower than 1000 Cps, and at 1.0 s^{-1} for viscosities higher than 1000 Cps measured at 25°C

In CMC anhydroglucose residues are linked thru trans (1,4)

bondings which significantly hinder molecular mobility Additional chain stiffening is due to a high degree of steric crowding and possible intermolecular hydrogen bondings between hydroxyl groups and carboxyls or oxygen O(6)

The high viscosity obtained for CMC solutions at relatively low concentrations is partially due to its unusual large coil dimensions Significant coil overlap and entanglies occur at relatively low concentrations In addition, the slopes of the log-log plots are significantly higher than those obtained for high MW nonionic synthetic polymers of similar MW s This indicates that flow behavior of CMC solutions is due to other molecular interactions in addition to topological entanglements seen in synthetic polymers

The polyelectrolyte character of CMC is clearly partially responsible for the high viscosity displayed by aqueous solutions Polyelectrolyte polymer solutions show significantly enhanced viscosity due to electrostatic interactions In the following section the effect of electrostatic forces on shear viscosity of CMC solutions was investigated

3.3.1.2 Effect of salt on zero shear viscosity

The electrostatic effects were studied by increasing the ionic strength of CMC solutions CMC solutions of 1 2% and 1 5% 7HFPH (900 080) were selected for this experiment Test solutions were prepared in 100 ml flasks as described in section 3 3 2 2 and allowed to sit at room temperature for 24 hours Aliquots of 50 ml test solutions were transferred to 50 ml flasks and NaCl added to the desired concentrations (1 to 40%) Solutions were then stirred for 6 hours at room temperature in a dust free hood tightly covered and allowed to sit

at RT for at least 24 hours before viscosity measurements Zero shear viscosity was measured at 25°C using a Brookfield digital viscometer model DV II

The effect of increasing monovalent salt (NaCl) concentrations on zero shear viscosity is shown in Figure 3 11 The zero shear viscosity of aqueous CMC solutions appears to be only slightly effected For 1 2% 7HFPH(800 000) the viscosity decreased from 2560 cps at 0% NaCl to 2160 at 40% NaCl which corresponds to a reduction of 15% in zero shear viscosity For 1 5% 7HFPP(900,000), a reduction of 9% in zero shear viscosity was observed This suggests that high ionic strengths of monovalent ions have only a modest effect on the flow behavior of CMC at concentrations above c*

This departure from the generalized behavior of polyelectrolytes polymer solutions (e g significant decrease in viscosity of polyacrylic acid solutions in the presence of high salt concentrations) can be attributed to specific intermolecular interactions such as that reported for certain polysaccharides solutions such as locust bean gum and guar gum (181) A similar behavior, termed "hyperentanglement" was also reported for poly(n butylmethacrylate) solutions where entanglement coupling is intensified by specific attractive forces (199)

It is interesting to note that all of the polymers which display such behavior form gels or precipitates under acidic conditions The gel formation involves the formation of "physical" crosslinks which are believed to be local regions of intermolecular organization and the formation of such network structures in solution

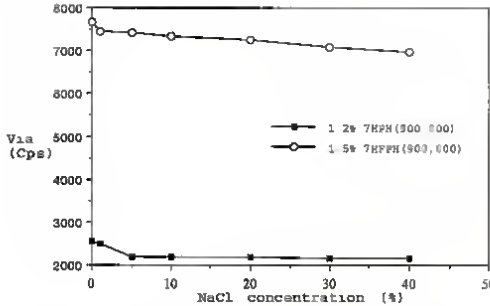

Figure 3-11 Effect of increasing salt (NaCl) concentration on zero shear viscosity of 1.2% and 1.5% CMC (7HFPH 900 000) aqueous solutions. Brookfield RVT DVII, CP 52 @ 1.0(s^{-1}) 25°C

It is possible then that the unusually high viscosity displayed by CMC solutions can be explained by the formation of organized intermolecular chain segments similar to those seen for gels but of lower density and shorter organization time scales as depicted in Figure 3-12. However, the existence of these organized domains (i.e., junction zones) in aqueous CMC solutions needs to be further examined using differential scanning calorimetry, solution viscosity measurements, and neutron scattering.

3.3.1.2 Shear-thinning of CMC solutions

During surgical use, due to mechanical manipulation, hydrophilic polymer solutions are subjected to a wide range of shear rates varying from zero at rest to 10000 s^{-1} when the solution is pushed rapidly through a fine gage cannula. Therefore, the performance of these viscoelastics may often be related to their shear behavior. The viscosity at high shear rates is of importance, for example, when considering the force required to push a solution through a small gauge syringe. In such circumstances, the viscosity should be low to allow easy handling of the solution. The shear thinning or pseudoplastic behavior of viscoelastic solutions therefore facilitates their use as surgical tools. They possess the viscosity necessary to maintain space between tissues but can be easily delivered through small gauge needles. The shear behavior of CMC solutions was therefore investigated and is discussed here. Shear thinning behavior of CMC solutions of various concentrations is shown in Figure 3-13 (a) and (b). The viscosity is significantly reduced with increasing shear rate. It appears that shear thinning behavior of CMC solutions can also be described by a power law

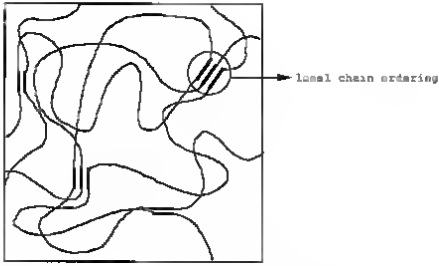

Figure 3-12 Schematic drawing of intermolecular organization of chain segments which may explain network properties of CMC solutions.

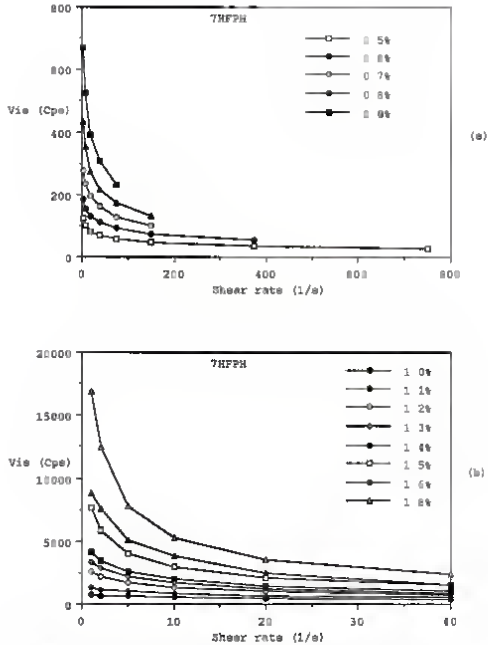

Figure 3-13 Sheer thinning behevior of CMC 7HFPH (800_000) solutions Viscosities were measured at 25° C using a Brookfield viscometer RVT DVII
(a) Viscosities measured using a CP40 cone and plate
(b) Viscosities measured using a CP52 cone and plate

relationship of the form

$$\eta = B\dot{\epsilon}^{n} \qquad (3\ 9)$$

where η is the viscosity, $\dot{\epsilon}$ is the shear rate, B is a constant, and n is the exponent. The exponent n can be obtained from the slope of double logarithmic plots of η vs $\dot{\epsilon}$ showed in Figure 3.14, and B is the intercept of the log plots with the y axis or zero shear viscosity (i.e., viscosity at shear rate of $1.0\ s^{-1}$). Shear thinning can be characterized independently of zero shear viscosity using the exponent n.

Log log plots of η vs $\dot{\epsilon}$ for various CMC concentration are shown in Figure 3.14. Values of n for different concentrations are summarized in Table 3.3. Inspection of equation (3.9) reveals that high absolute values of n are indicative of pronounced shear thinning, while low values are characteristic of more moderate pseudoplastic character. As shown in Table 3.3, the absolute value of n increases with increasing concentration which indicates that the shear thinning behavior is more pronounced for concentrated solutions. For dilute solutions the reduction in viscosity with increasing shear rate is relatively minor and arises from alignement of molecules in the direction of flow. For concentrated solutions, however, the shear thinning is much more dramatic and arises from different mechanisms due to specific segmental interactions discussed in section 3.3.1.2, in addition to topological entanglements generally observed for high polymers. Interpenetration of polymer coils in concentrated CMC solutions under shear deformation can be viewed as a dynamic entangled network where intramolecular interactions are continuously disrupted and new ones formed

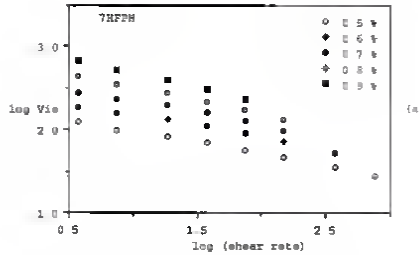

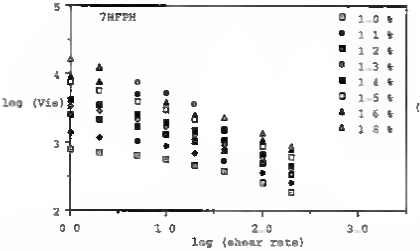

Figure 3 14 Log log plots of viscosity versus shear rate for CMC 7HFPH (500,000) solutions Viscosities were measured at 25°C using a Brookfield viscometer HVT DVII
(a) Viscosities measured using a CP40 cone and plate
(b) Viscosities measured using a CP52 cone and plate

Table 3 3 Power law equations for shear thinning behavior of CMC 7HFPH solutions (equation 3 9)

Concentration (%)	n	E	R^2	$\eta = E\dot{\gamma}^n$
0 5	0 27	177	0 98	$\eta = 177\dot{\gamma}^{0\ 27}$
0 6	0 27	261	0 99	$\eta = 261\dot{\gamma}^{0\ 27}$
0 7	0 27	392	0 98	$\eta = 392\dot{\gamma}^{0\ 27}$
0 8	0 32	680	0 98	$\eta = 680\dot{\gamma}^{0\ 32}$
0.9	0 35	705	0 96	$\eta = 705\dot{\gamma}^{0\ 35}$
1 0	0 35	786	0 97	$\eta = 786\dot{\gamma}^{0\ 35}$
1.1	0 36	1380	0 99	$\eta = 1380\dot{\gamma}^{0\ 36}$
1 2	0 38	2880	0 99	$\eta = 2560\dot{\gamma}^{0\ 38}$
1 3	0 40	3340	0 99	$\eta = 3340\dot{\gamma}^{0\ 40}$
1 4	0 42	4120	0 99	$\eta = 4120\dot{\gamma}^{0\ 42}$
1 5	0 48	7660	0 99	$\eta = 7680\dot{\gamma}^{0\ 48}$
1 8	0 55	16800	0 98	$\eta = 16800\dot{\gamma}^{0\ 55}$

η is the shear viscosity measured at 25°C using Brookfield viscometer RVT-DVII

$\dot{\gamma}$ is the shear rate in s^{-1}

R is the correlation factor.

E is the shear viscosity at shear rate of 1 0 s^{-1}

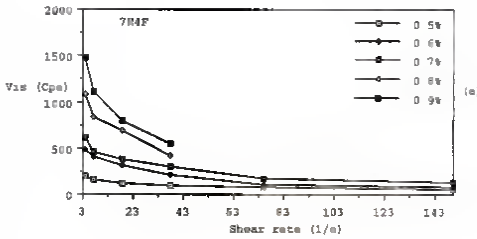
7H4F
0.5%
0.6%
0.7%
0.8%
0.9%
Vis (Cps)
2000
1500
1000
500
0
3
23
43
63
83
103
123
143
Shear rate (1/s)

(a)

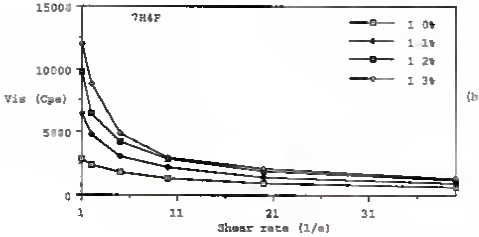
7H4F
1.0%
1.1%
1.2%
1.3%
Vis (Cps)
15000
10000
5000
0
1
11
21
31
Shear rate (1/s)

(b)

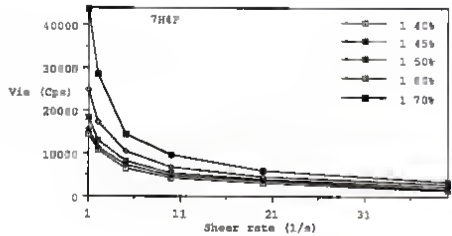

Figure 3 15 Shear thinning behavior of CMC 7H4F (10^{6}) solutions. Viscosities were measured at 25° C using a Brookfield viscometer RVT DVII.
(a) Viscosities measured using a CP40 cone and plate
(b) and (c) Viscosities measured using a CP52 cone and plate

Table 3 4 Power law equations for shear thinning behavior of CMC 7H4P solutions (equation 3 8)

concentration (%)	n	θ	R^2	$\eta = \theta\dot{e}^{n}$
0 5	−0 35	202	0 90	$\eta = 202\dot{e}^{-0\ 35}$
0 6	−0 38	480	0 98	$\eta = 480\dot{e}^{-0\ 38}$
0 7	0 38	608	0 08	$\eta = 608\dot{e}^{-0\ 38}$
0 8	0 40	1090	0 00	$\eta = 1080\dot{e}^{-0\ 40}$
0 9	0 42	2430	0 00	$\eta = 2430\dot{e}^{-0\ 42}$
1 0	0 44	2940	0 00	$\eta = 2840\dot{e}^{-0\ 44}$
1 1	−0 54	6530	0 00	$\eta = 6530\dot{e}^{-0\ 54}$
1 2	−0 57	8820	0 00	$\eta = 9820\dot{e}^{-0\ 57}$
1 3	−0 61	12000	0 99	$\eta = 12000\dot{e}^{-0\ 61}$
1 4	0 62	14500	0 97	$\eta = 14500\dot{e}^{-0\ 62}$
1 5	0 62	18300	0 00	$\eta = 18300\dot{e}^{-0\ 62}$
1 6	0 62	24800	0 00	$\eta = 24800\dot{e}^{-0\ 52}$
1 7	0 70	43800	0 00	$\eta = 43800\dot{e}^{-0\ 70}$

η is the shear viscosity measured at 25°C using Brookfield viscometer RVT-DVII

$\dot{e}$ is the shear rate in s^{-1}

R is the correlation factor

θ is the shear rate viscosity at 1 0 s^{-1}

The response of such networks to shear deformations is governed by the time scale of these intermolecular interactions. At low rates of shearing, those interactions which are disrupted by the imposed deformation are progressively replaced by new ones between different chains, i.e., the reciprocal shear rate is longer than the time required for entanglement. The overall density of these interactions is only slightly effected and hence the viscosity is not reduced. At high rates of shear the rate of externally imposed movement becomes greater than the molecular relaxation times hence the rate of formation of new intermolecular interactions. The "crosslink density" is reduced and the molecules are able to orient in the flow direction with less resistence which results into reduced viscosity.

As the concentration increases, the freedom of movement of individual chains is progressively restricted with consequent increase in the time required to form new entanglements. Thus as shown in Tables 3.3 and 3.4, the extent of shear thinning is higher for concentrated solutions.

3.3.1.3 Effect of filtering and autoclaving

3.3.1.3.1 Effect on zero shear viscosity

The purity of any polymer solutions considered for surgical use is of paramount importance. This is especially important for those hydrophilic polymer solutions to be used for ophthalmic surgery. A surgical solution should be free of foreign particles.
For example, for viscosurgical solutions, the presence of undesirable structure such as residual fibrous material from processing, or gel particulate can clog the trabecular meshwork and cause IOP increase. A commercially available polyacrylamide viscoelastic has been recently

found to cause serious IOP rise due to the presence of such gel particulates which had not been properly removed. Therefore it is critical to ensure that surgical polymer solutions are free of any particulate contamination.

Filtration of viscous polymer solutions is difficult because of the force required to push entangled molecules through small diameter filters. The feasibility and ease of filtration is governed by the filter size and the viscosity of the solution. The pronounced shear thinning behavior of CMC solutions is a significant advantage in the filtration process since the viscosity will be reduced with increasing shear rate.

The effect of high shear rates developed during the filtration process can be detrimental to the polymer solution being filtered. Several studies have reported degradation and irreversible molecular changes induced by filtration of viscous polymer solution due to the high shearing forces required for such processes(200). In this section, studies on the rheology of filtered and autoclaved CMC solutions is discussed for two CMC grades: 7HFPH and 7H4F.

Figure 3-16 shows the effect of filtering and autoclaving on zero shear viscosity for various CMC concentrations. Independent of the grade used and concentration, the viscosity was increased by filtration. However, subsequent autoclaving had a concentration-dependent effect on shear viscosity. For 7HFPH, Figure 3-16 (a) indicates that upon autoclaving, the viscosity was reduced. When the concentration was increased to 1.7 %, the viscosity was higher after autoclaving. The viscosity for 7H4F showed the same trend but the increase of viscosity after autoclaving was observed for a lower concentration (1.45%).

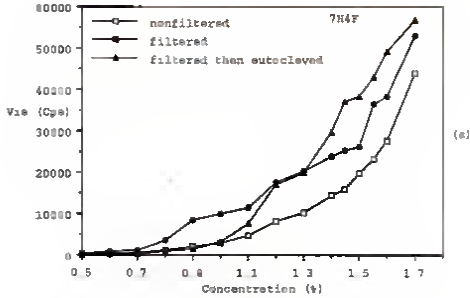
nonfiltered
filtered
filtered then autocleved
7H4F
Vie (Cps)
Concentretion (%)
(a)

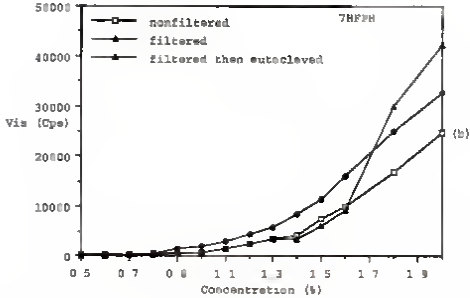
nonfiltered
filtered
filtered then autocleved
7HFPH
Vis (Cps)
Concentretion (%)
(b)

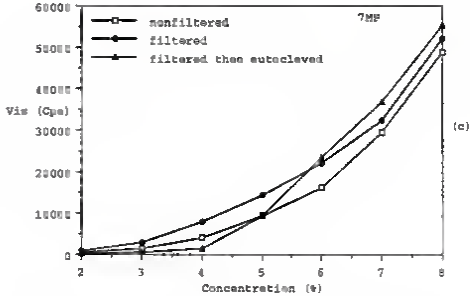

Figure 3.18 Effect of filtering (10μ) and autoclaving (240°F 20 mne) on viscosity of CMC solutions of various MWs

(a) CMC 7H4F(1,000,000)
(b) CMC 7HFPH (800,000)
(c) CMC 7MF (350,000)

The effect of filtering and autoclaving was further investigated by measuring the molecular weight and molecular weight distribution (MWD) of CMC 7HF9H and CMC 7H4F after filtering and autoclaving. Measurements were made at Ping Yu at Genzyme corporation using light scattering GPC. The results summarized in Table 3.5 indicate that no degradation occurred at any stage of the purification process. For CMC-7HFPH, the weight average MW (M_w) of filtered solutions has slightly increased after filtration (ca 10%). The number average MW (Mn) however, showed a more pronounced increase (ca 47%) with concomitant decrease in the MWD from 1.8 to 1.5. Since Mn is more sensitive to low molecular weight species, these results suggest that a higher population of longer chains is present after filtration. CMC 7H4F showed a similar trend. Filtered solutions of CMC 7H4F showed 20% increase in Mw, 46% increase in Mn, and a decrease in PDI from 2.0 to 1.5.

Even when completely dissolved, CMC solutions contain small amounts of ordered structures. These aggregates may be formed by short chains because of greater degree of freedom which allows chain organization and formation of ordered structures. During the filtration process, these low MW aggregates may be retained in the filter. This can affect solution viscosity in a variety of ways. First, a solution with a higher population of longer chains is expected to show enhanced viscosity because of increased entanglement. Second, the depletion of short chains might also affect the viscosity by reduced competitive inhibition of "junction zones".

The essence of the "junction zone" model discussed in section 3.3.1.2 is that CMC chains are long enough to participate in several "junctions" which provides CMC solutions with

Table 3-5 Molecular weight for CMC-7HFPH and CMC-7H4F after filtration (10μ) and after filtration followed by autoclaving measured by light scattering GPC

CMC	Mw (10^6)	Mn (10^5)	PDI = Mw/Mn
7H4F	1.0	0.55	1.8
7H4F filtered	1.2	0.80	1.5
7H4F filtered then autoclaved	1.0	0.66	1.5
7HFPH	0.5	0.45	2.0
7HFPH filtered	1.8	0.88	1.5
7HFPH filtered then autoclaved	0.9	0.60	1.5

a pseudo-crosslinked structure. Shorter chains may compete with high molecular weight species for local segmental interactions which might result in reduced "crosslink" density and hence lower viscosity. This is consistent with other studies by Kahn and Welsh (135) who showed that network properties of some polysaccharide solutions, such as hyaluronic acid, are significantly reduced by the addition of small amounts of low molecular weight species, presumably by inhibiting long chain participation in pseudo crosslinks.

The effect of autoclaving following filtration can also be seen in Figure 3-16. For a given molecular weight, the autoclaving effect on the viscosity is concentration dependent. Viscosities of autoclaved CMC solutions are reduced below a critical concentration and increased above this concentration. For CMC 7HFPH (1.9×10^6), the viscosity was reduced for concentrations below $c^*(7HFPH) = 1.7\%$; above this concentration autoclaved solutions showed an increase in viscosity. Solutions of CMC 7H4F (1.0×10^6) exhibited the same trend but at a lower concentration $c^*(7H4P) = 1.45\%$. For CMC 7MP (350,000), the increase in viscosity upon autoclaving was observed at a much higher concentration, $c^*(CMC\ 7MP) = 5.0\%$. The effect of autoclaving appears to be related to a composite property of molecular weight and concentration which is usually indicative of a property related to the occupancy of space within a polymer solution (188). This can be conveniently characterized by a dimensionless parameter called "coil overlap parameter" $c[\eta]$, which is a measure of the total volume occupied by all chain coils within a polymer solution, regardless of their type and molecular weight.

The coil overlap parameters of various CMC grades were calculated at their respective critical concentrations converted to g/dl.

Intrinsic viscosities were obtained using Mark Houwink Sakurada equation:

$$[\eta] = KM^{\alpha} \qquad (3\ 10)$$

Where M is the number average MW obtained by laser light scattering GPC. $K=1.0 \times 10^{-6}$ dl/g and $\alpha=1.40$ were obtained from Polymer Handbook. The results are shown in Table 3.6. It appears that the increase of viscosity upon autoclaving occurs at comparable values of $c^*[\eta]=364.2$ to 368.4 independent of molecular weight and concentration. Morris et al have reported a general transition behavior from a dilute regime to a concentrated regime for a wide range of natural polymers based on $c[\eta]$ [134]. They showed that the transition occurs at $c[\eta]$ values of about 10 independently of molecular weight and concentration.

A possible explanation for this phenomenon is based on the fact that at relatively lower values of $c[\eta]$, the polymer chains still have enough mobility to rearrange under the influence of thermal energy input during autoclaving, analogous perhaps to thermal annealing processes to enhance crystallization of polymers between Tg and Tm. Intermolecular associations are disrupted to a certain degree and the viscosity is reduced by autoclaving. The disruption of "junction zones" by thermal energy has been reported in the literature and was referred to as "melting" of ordered structures due to intermolecular associations [194]. When $c[\eta]$ is increased, the reduction of the viscosity upon autoclaving is less pronounced. This is probably due to increasingly reduced mobility of the chains due to a higher volume occupied by the polymer coils.

Table 3.6. Coil overlap parameter of various CMC grades at critical concentrations c* at which an increase of viscosity was observed upon autoclaving.

CMC	Mw ($\times 10^6$)	$[\eta]$ [1] (dl/g)	c* [2] (g/dl)	c* $[\eta]$
7H4F	1.0	251.2	1.45	364.2
7HFPH	0.9	216.7	1.70	368.4
7MF	0.35	57.3	6.4	366.7

[1] intrinsic viscosity calculated from Mark Houwink Sakurada $(\eta) = KM^a$ with $K = 10^{-5}$ dl/g and a = 1.40 obtained from Polymer Handbook

[2] concentration at which increase of polymer solution is observed upon autoclaving

A critical value of c[η] is reached where the actual viscosity of the autoclaved solutions is higher than that of their respective starting solutions. Further increase in c[η] appears to cause a more significant increase in the viscosity. This can probably be attributed to enhanced intermolecular interactions.

The significance of these findings resides in the fact that the concentration at which the onset of viscosity increase after autoclaving occurs may be approximated if the weight average molecular weight of the CMC used is known.

3.3.1.3.1 Effect of filtering and autoclaving on shear thinning behavior of CMC solutions

In this section the effect of filtering and autoclaving on pseudoplastic behavior of CMC solutions was reported. Shear thinning behavior of filtered solutions of CMC 7HFPH (990,000 MW) is shown in Figures 3.17 (a) and 3.17 (b). The effect of filtering followed by autoclaving is shown in Figure 3.18(a) and 3.18(b). The effect of filtering and autoclaving on the pseudoplastic profile for some CMC 7H4F (10^5 MW) is shown in Figures 3.19 and 3.20. Filtering and autoclaving do not appear to significantly affect shear thinning behavior of CMC solutions.

3.3.1.4 Rheological properties of CMC blends of different molecular weights

Rheological properties of polymer solutions are strongly influenced by molecular weight distribution. In dilute solutions, where polymer chains do not interact, the polymeric contribution to rheological properties is obtained by simple additive blending laws. In concentrated solutions, the rheological behavior is dominated by topological entanglements and specific intermolecular interactions such as those described here for CMC.

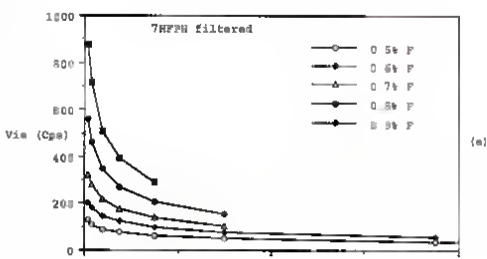

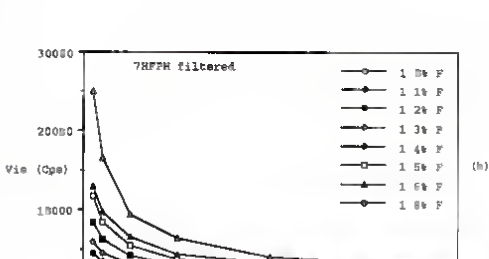

Figure 3.17. Shear thinning behavior of CMC 7HFPH (DD0.000) solutions after filtration through 10µ filter. Viscosities were measured at 25° C using a Brookfield viscometer RVT DVII
(a) Viscosities measured using a CP40 cone and plate
(b) Viscosities measured using a CP52 cone and plate

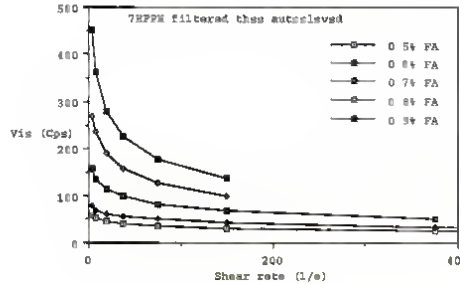

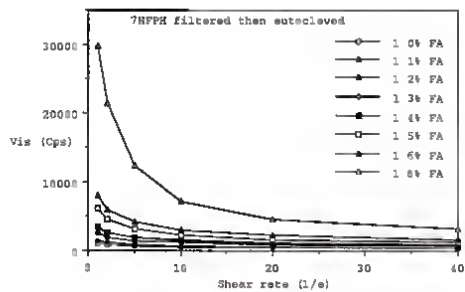

Figure 3-18 Shear thening behevior of CMC 7HFPH (900,000) solutions after filtering then autocleving. Viscosities were measured at 25°C using a Brookfield viscometer RVT DVII
(a) Viscosities measured using a CP40 cone and plate
(b) Viscosities measured using a CP52 cone and plate

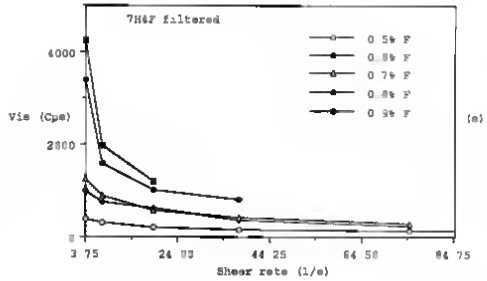

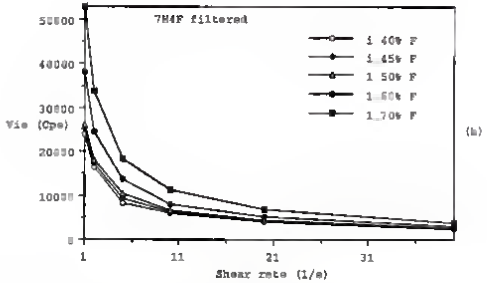

Figure 3-19 Shear thinning behavior of CMC 7H4F ($1\%^{w}$) solutions after filtration through 10µ filter. Viscosities were measured at 25°C using Brookfield viscometer RVT-DVII:
(a) Viscosities measured using a CP40 cone and plate
(b) Viscosities measured using a CP52 cone and plate

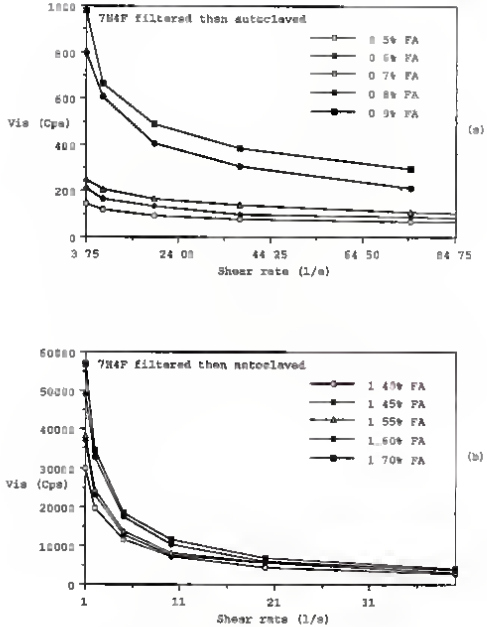

Figure 3-20. Shear thinning behavior of CMC 7H4F (10^6) solutions after filtering then autoclaving. Viscosities were measured at 25°C using a Brookfield viscometer RVT DVII
(a) Viscosities measured using a CP40 cone and plate
(b) Viscosities measured using a CP52 cone and plate

3.3.1.4.1 Effect of MWD and bimodal distribution on the rheology of CMC solutions

The rheological properties of bimodal mixtures of high molecular weight CMC-7HFPH (9.0×10^5) and low molecular weight CMC 7L2P (0.8×10^5) were investigated. Dry CMC powder blends of CMC 7HFPH and CMC 7L2P were mixed in a glass beaker prior to dissolution. The powder blends were then dissolved in BSS according to the method described in section 3.3.2.2. Total concentrations were varied from 2.1% to 6.3%. The results are summarized in Table 3.7. Zero shear viscosities (i.e. viscosities at $1.0\ s^{-1}$) of bimodal blends were plotted against the percentage of the two components in Figure 3.21 (a), (b), and (c). The straight lines in Figure 3.21 are representative of linear additive laws fitting the following equation:

$$y = n\,\eta_1 + (100-n)\,\eta_2 \qquad (3.11)$$

where n is the percent weight of CMC 7L2P

η_1 is shear viscosity of 6% CMC-7L2P solution

η_2 is shear viscosity of (100-n)% CMC-7HFPH solution

It appears from Figure 3.21 that shear viscosity of bimodal CMC blends does not obey a simple linear additive law. The viscosity observed is much lower than that anticipated from equation (3.11). This suggests that significant interactions between CMC polymer chains of different molecular weights. This negative synergistic effect may be explained in terms of the "junction model". The high viscosity of high molecular weight CMC solutions is mainly due to the formation of specific local segmental ordered structures which act as physical "crosslinks" and confer network properties to CMC solutions. In high MW CMC solutions polymeric chains are long enough to participate in several "junction zones" simultaneously and hence increase solution viscosity.

Table 3.7. Viscosity at various shear rates of solutions of bimodel blends of CMC 7HFPH (0.8 x 10^5) and CMC 7L2P (0.9 x 10^5)

Total Conc (%)	ratio 7HFPH:7L2P	Shear rate (1/s) 1	2	5	10	20	40	100	200
2.1	1:6	125	100	90					
2.1	2:5	250	230	225	225	210	130		
2.1	3:4	1100	844	786	830	500	340	254	
2.1	4:3	1970	1730	1510	1310	1020	800	790	
2.1	5:2	3250	3000	2750	2510	2400	2250	2180	2000
2.1	6:1	18100	17400	15700	14700	12000			
4.6	1:3	5450	4870	3500	2740				
4.6	3:5	38600	26700	17400	11200	7500			
4.6	1:1	63500	63700	45000	38500	27400			
5.4	1:5	1160	1040	830	780	630			
5.4	1:2	28600	21500	14100	10000	8030			
5.4	1:1	61600	46400	22400	15400				
5.4	2:1	79200	56400	41400					
8.3	1:6	3750	3040	2750	2130	1740	1120		
6.3	2:7	12300	6650	8010	4200	2650			
6.3	1:2	48700	33200	16600	13500				
6.3	2:5	53400	35800	21600	14400	9300			

VISCOSITY (CPS)

Viscosity was measured at 25°C using Brookfield viscometer model RVT DVII with CP52 cone and plate

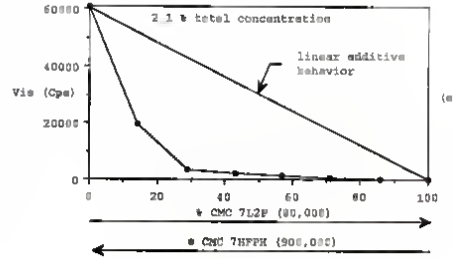
60000
40000
20000
0
Vis (Cps)
2.1 % total concentration
linear additive
behavior
(a)
0
20
40
60
80
100
% CMC 7L2P (80,000)
% CMC 7HFPH (900,000)

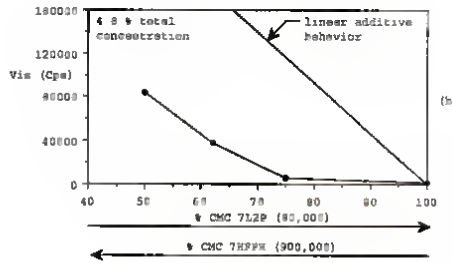
160000
120000
80000
40000
0
Vis (Cps)
4.8 % total
concentration
linear additive
behavior
(b)
40
50
60
70
80
90
100
% CMC 7L2P (80,000)
% CMC 7HFPH (900,000)

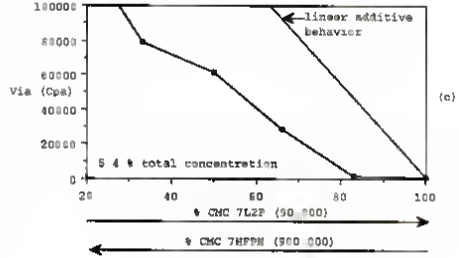

Figura 3.21. Viscosity as function of percent of 7L2P showing a negative synergistic effect in blends of 7HFPH and 7L2P. Brookfield RVT-DVII, CP52, 25°C

(a) 1.2% total concentration
(b) 4.8% total concentration
(c) 5.4% total concentration

In the presence of lower MW CMC, short chains may compete with longer chains for junction zones. Since short chains participate in a limited number of junction zones, the viscosity is reduced.

Shear thinning behavior of some bimodal blends of CMC 7HFPH and CMC 7L2P is shown in Figure 3.22 where viscosity was plotted against shear rate. A solution of 2% CMC 7HFPH filtered and autoclaved which gives a low shear viscosity (viscosity at 1.8 s^{-1}) comparable to that of the 7HFPH/7L2P blend with 4.8% total concentration and a 7HFPH 7L2P ratio of 3.5 (ca. 40,000 Cps) was also included for comparison (dashed line). It appears from Figure 3.22 that solutions of bimodal CMC blends "shear thin" to a lesser extent than those of monodisperse CMC. In spite of comparable low shear viscosities (ca. 40,000 Cps), the decrease in viscosity with increasing shear rate is much more pronounced for 2% CMC 7HFPH than for a 7HFPH/7L2P blend with 4.8% total concentration and a 7HFPH 7L2P ratio of 3.5. This behavior may be explained in terms of the reptation theory of polymer diffusion in solutions. Briefly, this theory assumes that each polymeric chain is forced to move through a tubelike region due to constraints imposed by surrounding chains. For polymer solutions of narrow MW, the diameter of the tube is an intrinsic property of the polymer. The tube is assumed to be fixed and the flow of polymer may take place only by reptation (i.e., one dimensional diffusion of chains along the tube) (201). In bimodal molecular weight systems where the MW of the long chains as well as that of short chains are above the molecular weight of entanglement, reptation is believed to be the dominant mode of molecular motion for both species (202). However, several authors have reported that the tube may dilate in the case of blends of high and low molecular weights. According to the

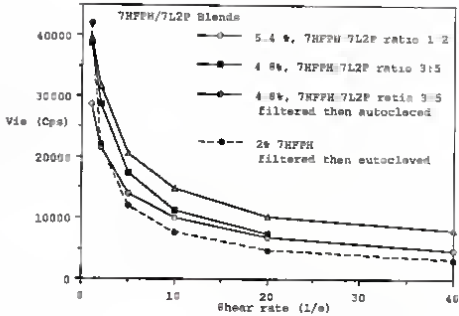

Figure 3 22 Shear thinning behavior of various bimodel blends of CMC 7HFPH and CMC 7L2F Brookfield viscometer RVT DVII, CP 52, 25°C

reptation theory, the macroscopic stress and hence the viscosity is related to the orientation of the chain in the deformed tube (Z81). Doi et al. have proposed that in blends on a short time scale (i.e., high shear rates) tube changes are dominated by short chains (Z83). This suggests that the shear thinning behavior of CMC blends may be dominated by the low molecular weight component which has been shown to shear thin to lesser extent (see section 3.3.1.2).

It is also possible that the junction zones described earlier contribute to this behavior. During shearing of CMC solutions junction zones as well as topological entanglements are disrupted and new ones formed. The time scale of reformation of junction zones is may be longer than that of topological entanglements because of specificity. In the presence of shorter chains, the time scale of junction zone reorganization may be shorter because of higher degree of freedom and the ability of small chains to reorganize readily. At relatively higher shear rate, the time scale of segmental reorganization may be shorter than the shear rate reciprocal and hence the viscosity is not greatly reduced.

The significance of these results resides in the fact that it may be possible to tailor viscoelastic solutions with desired rheological properties (i.e., shear viscosity at rest and shear thinning behavior). Viscoelastic solutions which "shear thin" to a lesser extent (e.g., Viscoat®) have been considered to afford superior endothelial cell protection due to better tissue wetting.

3.3.2 CMC Solution Stability

This experiment was conducted to investigate the stability of CMC solutions during storage. A stock solution of 1% CMC 7HFPH in 0.9% was prepared as described in section 3.3.2.2. Aliquots of 10 ml each were

transferred to glass vials with Teflon® screw caps. Samples of filtered and autoclaved CMC solutions were prepared by transferring 10 ml aliquots of filtered solution (filtration through 10μ according to section 3.3.2.3) to glass vials then autoclaved at 240°F for 20 min. Glass vials were immediately sealed with Teflon® screw caps. Samples were kept at room temperature (25°C) exposed to normal light conditions for a period of 6 months. Viscosities of freshly opened samples were measured every week for the first month and every two weeks thereafter. Samples were discarded after each measurement to avoid bacterial contamination which might occur in contact with air.

Figure 3.23 shows viscosity change with time for 1% CMC 7HFPH which was not filtered or autoclaved and 1% CMC 7HFPH which was filtered and autoclaved. Some changes in viscosity were observed for both solutions during the first 8 weeks. This small change may in part be due to the thixotropic behavior of CMC. The thixotropic behavior of CMC solutions has been attributed to the presence of highly ordered structural units (197). These intermolecular associations are easily disrupted by shearing. In order to give rise to a noticeable thixotropy, the reformation of such associations must be slow.

It is important to note that the thixotropic behavior of CMC viscoelastics may have some clinical implications. For example, during phacoemulsification procedures, the viscosity of CMC viscoelastic solutions may be significantly reduced.

A drastic reduction in viscosity was observed for 1% CMC 7HFPH (nonfiltered, nonautoclaved) after 16 weeks. However, 1% CMC 7HFPH filtered and autoclaved exhibited only a slight decrease in viscosity (4%) after 24 weeks (6 months). The loss of viscosity was likely due to

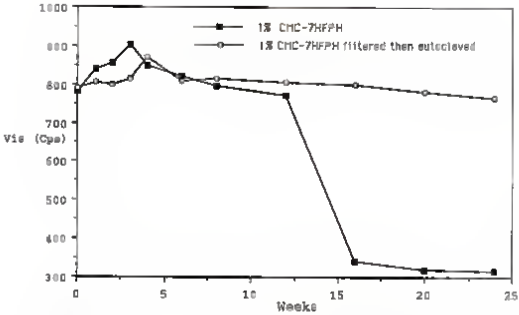

Figure 3.23. Change of viscosity of 1% CMC 7HFPH unfiltred and unautoclaved and 1% CMC 7HFPH filtered then autoclaved with time. Storage at 25°C. Brookfield RTV DVII 25°C, CP 40, ($3.75\ s^{-1}$)

chain scission caused by microbial attack CMC is relatively resistant to chemical and light degradation. The presence of microorganisms however, can cause a rapid loss of viscosity due to oxidation and hydrolytic degradation via cellulase enzymes (197) In addition to being the preferred method of sterilization autoclaving (248°F for 20 minutes) appears adequate to destroy microorganism responsible for CMC degradation. Heating for 30 minutes at 80°C, or for 1 minute at 100°C have been reported to be sufficient to kill microorganisms(197)

3.3.3 Effect of Oxygen Derived Free Radicals (ODFRs) on the Degradation of HA and CMC

Surgical adhesion formation is a result of inflammatory processes At sites of inflammation, polymorphonuclear (PMN) leukocytes generate superoxides which are a very reactive Superoxides can react to generate other ODFRs including singlet and hydroxyl radicals as shown in Figure 3 24 In addition to their damaging effects on tissues, these species can also cause degradation of solutions and membranes used for the prevention of postsurgical adhesion formation This might limit the efficacy of films and solutions to prevent adhesions by decreasing their residence time in the peritoneal cavity. The goal of this research was to identify the reactive species involved in the degradation of CMC and HA and to evaluate some agents capable of inhibiting the detrimental effect of OOFRs The extent of degradation was evaluated by measuring the relative decrease in viscosity after exposure to ODFRs

3.3.3.1 Effect of ODFRs on HA

The protective effect of various antioxidants for HA is shown in Table 3 8 and Figure 3 25 (a) The control sample which consisted of a solution of 0 4% HA in PBS showed a drastic reduction in viscosity after 1 hour exposure to OOFRs generated by autoxidation of iron which is

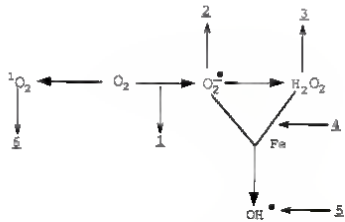

1 inhibiting $O_2^{\bullet}$ formation

2 scavenging $O_2^{\bullet}$ to avoid H_2O_2 and $OH^{\bullet}$ formation

3 scavenging H_2O_2 to avoid $OH^{\bullet}$ formation

4 inhibiting $OH^{\bullet}$ formation

5 scavenging $OH^{\bullet}$

6 quenching $^1O_2$

Figure 3 24 Schematic drawing of ODFR formation and methods of limiting oxidative degradation of CMC and HA

Table 3 8 Effect of various antioxidants on Fe/EDTA induced oxidative degradation of 0.4% HA solutions after 1 hour exposure

antioxidant	concentration (%)	Viscosity (Cps) before Fe/EDTA	Viscosity (Cps) Fe/EDTA exposure (1 hour)
Control 0.4% HA		26	5
SOD	0.01	27	10
	0.05	28	16
mannitol	0.1	26	6
	0.5	27	13
glutathione (reduced)	0.1	26	16
	0.5	26	20
catalase	0.01	26	11
	0.1	26	6
histidine	0.1	26	8
	0.5	27	9
ascorbic acid (vitamin C)	0.1	26	4
	0.5	27	4
Aspirin	0.1	26	17
DMSO	0.5	26	23

Brookfield RVT-DVII, CP 40, 25°C, 375 (1/s)
Viscosities were measured at shear rate at which the percentage torque is greater than 10 %

indicative of a pronounced degradation of HA This degradation is believed to occur by glycosidic bond cleavage (69) Singlet oxygen quenchers such as histidine showed virtually no inhibition of HA degradation This suggests that this particular ODFR does not play a major role in oxidative depolymerization of HA Singlet oxygen is known to be the least reactive of ODFRs and has a limited effect on oxidative depolymerization of polysaccharides in general (69)

Superoxide dismutase (SOD) acts as a superoxide ($O_2^{\cdot-}$) scavenger to prevent the formation of hydrogen peroxide SOD afforded dose related protection against oxidative depolymerization of HA The highest concentration (0 05 %) gave an 50% inhibition of HA degradation The $O_2^{\cdot-}$ species is relatively nonreactive towards polysaccharides especially those containing carboxylic groups such as HA and CMC (69) However, $O_2^{\cdot-}$ is converted to hydroxyl radicals ($OH^{\cdot}$) via H_2O_2 in the presence of trace amount of transition metal (e g , Fe) as depicted in Figure 3 24 The protective effect of SOD is probably due to the fact that less $O_2^{\cdot-}$ is available for these reactions and hence the production of more damaging species is minimized Another ODFR produced in the oxidative process during inflammation is hydrogen peroxide (H_2O_2) which also can lead to the formation of $OH^{\cdot}$ Two H_2O_2 scavengers, catalase and glutathione, were used in this study Catalase showed relatively less degradation inhibition probably because of the fact that it is not very soluble in water Glutathione on the other hand, showed a concentration-related protective effect up to 70% for the highest concentration used (0 5 %) This suggests that scavenging H_2O_2 to prevent the formation of $OH^{\cdot}$ can afford some protection against ODFR degradation of HA

Hydroxyl radical scavengers had different effects on the in vitro degradation of HA. Ascorbic acid showed virtually no degradation inhibition. Mannitol, at relatively high concentration, showed an intermediate protection against the degradative effects of ODFRs. However, DMSO, at a relatively low concentration, showed almost complete inhibition of HA depolymerization.

3.1.3.2 Effect of ODFRs on CMC

The rate of reaction of ODFRs with CMC is much slower than with HA. CMC was therefore exposed to ODFR's for a longer period of time (4hours) to ensure completion of the reaction. Viscosity measurements are shown in Table 3.5 and Figure 3.26. The results were similar to those obtained for HA with the exception of enhanced stabilization by mannitol which appears to afford protection similar to DMSO.

In summary, the results indicate that both HA and CMC are susceptible to degradation by ODFRs although CMC is much more stable. This degradation can be partially inhibited by compounds capable of scavenging H_2O_2 thereby preventing the formation of OH^-. However agents capable of scavenging OH^- were the most effective in preventing the degradation of HA and CMC. It appears that OH^- is the major ODFR which mediates oxidative depolymerization of HA and CMC.

Hydroxyl radicals are very reactive towards polysaccharides in general (204). The main mechanism of degradation involves glycosidic bond cleavage leading to lowering of the molecular weight which is manifested as reduction of the viscosity of aqueous solutions. It is interesting to note that degradation rate for HA appears to be higher than that of CMC.

Table 3.9 Effect of various antioxidants on Fe/EDTA induced oxidative degradation of 0.5% CMC solution after 4 hour exposure

antioxidant	concentration (%)	Viscosity (Cps) before Fe/EDTA	Viscosity (Cps) Fe/EDTA exposure (4 hours)
Control 0.5% CMC		36	11
mannitol	0.1	36	10
	0.5	38	17
glutathione (reduced)	0.1	37	18
	0.5	39	28
catalase	0.01	39	10
	0.1	38	13
histidine	0.1	38	12
	0.5	40	12
ascorbic acid (vitamin C)	0.1	38	11
	0.5	36	12
Aspirin	0.1	37	15
DMSO	0.5	38	35

Brookfield RVT-DVII, CP 40, 25°C, 375 (1/s)
Viscosities were measured at shear rate at which percent torque is greater than 10 %

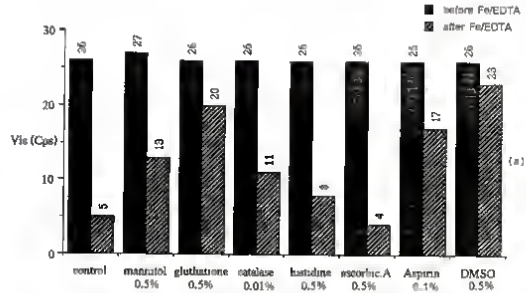

(a) 0.4% HA solution oxidized for 1 hour

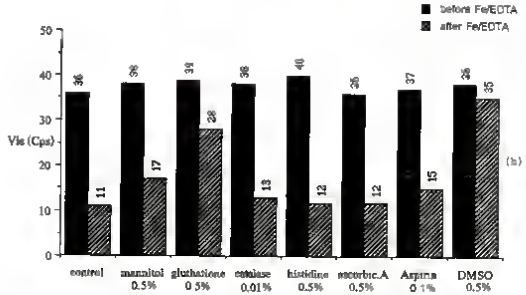

(b) 0.5% CMC solution oxidized for 4 hours

Figure 3.25 Effect of various antioxidants on Fe/EDTA induced oxidative degradation of HA and CMC solutions

This is probably due to a higher degree of substitution of carboxylate anions in CMC which allow a locally lower concentration of O_2 in the vicinity of the polymer chain due to electrostatic repulsions. This in turn lowers the collisional frequency of $OH^{\cdot}$, produced via O_2^{-}, with glycosidic bonds. Wedlock et al. have shown that CMC of a higher DS reacts with $OH^{\cdot}$ at much slower rate than CMC with lower degree of substitution of carboxylic groups (59).

It is possible that antioxidants capable of scavenging OH produced during inflammation, can enhance storage shelf life and minimize the in vivo degradation of HA and CMC solutions used as adhesion prevention devices. In addition, antioxidants may help reduce adhesion formation (158) and might be of therapeutic value when added to HA or CMC solutions. Moreover, the incorporation of antioxidants into viscous solutions or films might enhance topical local delivery at sites of injury and maximize rapid loss.

1.3.4 CMC Films and Membranes

Resorbable membranes have been investigated for use as surgical adhesion prevention devices. The prolonged mechanical separation of traumatized tissues afforded by such membranes may be useful in reducing the incidence and severity of surgical adhesions. Several membranes have been evaluated for use as surgical adhesion prevention devices. These membranes are generally designed to remain at surgical sites during the wound healing process, where adhesion formation occurs, then resorb under physiological conditions. In this context, CMC films and membranes were prepared and their properties evaluated. A variety of water insolubilization methods were investigated including ionic complexion and a novel thermal treatment method. A certain control over

the degradation of these membranes in physiological media can be gained by varying the degree of insolubilization

CMC films cast from aqueous solutions are flexible and optically clear However these films dissolve in water readily and may remain at injury sites for only relatively short periods of time CMC can be made partially water-insoluble by treatment with compounds capable of reacting with one or both functional groups (hydroxyl and carboxyl) Polyfunctional compounds such as dimethylol urea (DMU) urea formaldehyde melamine formaldehyde and polyamide epichlorohydrin can react with the OH groups and crosslink CMC (197) However these compounds are usually used at relatively high concentration which raises the question of potential toxicity In addition these reactions are generally performed in aqueous environments and the resulting product is a gel-like material which makes film casting difficult

3.3.4.1 Ionic complexation

Water solubility of CMC is mainly due to the presence of the carboxylic groups Exposing water soluble CMC films to cations such as Fe^{3+} Cu^{2+}, or Ca^{2+} which complex with the carboxylate anion provides some water resistance The properties of calcium modified CMC-F are shown in Table 3 18 A proprietary Genzyme corporation hyaluronic acid film (HAL-F) was included for comparison

Water soluble CMC films treated with aqueous solutions of $CaCl_2$ were weak and tacky The fact that calcium cations were introduced to CMC through an aqueous phase affects the integrity of CMC-F To minimize film swelling and breaking during crosslinking reactions mixtures of aqueous $CaCl_2$ and organic solvents (e g acetone) were used as described in section 3-3 2-2 2 The rationale for this method is to introduce calcium ions to CMC films via a liquid phase which does not

Table 3.10 Properties of $CaCl_2$ insolubilized CMC films

Films	Thickness (Mils)	Tensile[1] Strength (psi)	Weight Gain[2] (%)	Solubility in PBS[3] @25°C	Properties
HAL F[4]	1.5	--	--	>7 days	hazy flexible
CMC	1.8	5250-6250	--	10-15 mins	optically clear flexible
$CaCl_2$/water treated CMC	1.6	4500-8000	10	20 hrs	hazy, tacky
$CaCl_2$/acetone treated CMC	1.7	6100-10000	25	36 hrs	optically clear flexible

(1) According to ASTM method D-822
(2) After treatment
(3) Films were soaked in PBS at 25°C
(4) HAL-F, lot # C1255

dissolve CMC. Calcium chloride-treated CMC films remained optically clear and were easily dried at room temperature. The lower weight gain observed for CMC F treated with aqueous $CaCl_2$ compared to $CaCl_2$/acetone is probably due to partial dissolution of CMC films during the treatment. The mechanical properties of $CaCl_2$ treated CMC films appear to be slightly enhanced especially in the case of $CaCl_2$/acetone. Ionic complexation of this nature may not effect the mechanical properties significantly. However, insolubilized CMC films are much less hygroscopic than the untreated films which might enhance their mechanical properties.

One of the most important parameters for membranes used as adhesion prevention devices is their residence time in physiological media. The residence time of CMC F in PBS at room temperature is also shown in Table 3-10. The aqueous $CaCl_2$ treated CMC F have completely dissolved after 12 hours. Films treated with $CaCl_2$/acetone showed an enhanced residence time up to 36 hours which indicates that this method is more efficient for ionic complexation. However this residence time in PBS is still much lower than that of NAL F.

3.3.4.2 Thermal treatment of CMC films

In this part of the study, it was found that CMC F can be insolubilized to various degrees by thermal treatment at elevated temperatures for different periods of time. Thermally treated CMC F behave as "degradable hydrogels" which swell in water but dissolve if exposed to aqueous media for an extended period of time. Heat treatment was studied in air or in CO_2.

3.3.4.2.1 Swelling in PBS

Untreated CMC-F readily dissolves in water. Heat treated films retain their hydrophilicity but swell in water to varying degrees depending on time and temperature of the treatment. Figure 3.26 shows the water uptake of CMC films at room 25° C. HAL-F was included for comparison. The swelling of CMC-F in PBS decreases with increasing treatment time at a given temperature. Increasing the temperature has the same effect on the water uptake. The effect of treatment atmosphere can also be seen in Figure 3.26. CMC-F treated in CO_2 exhibited lower water uptake which is indicative of enhanced insolubilization. The horizontal line shows the water uptake of HAL-F, a developmental hyaluronic acid membrane from Genzyme Corporation. It appears then that CMC films having a wide range of water uptake and dissolution rates can be obtained by varying the time and temperature of heat treatment.

3.3.4.2.2 Residence time in PBS

A qualitative evaluation of the dissolution rate of CMC-F in PBS was conducted using an accelerated dissolution test. The results are summarized in Table 3.11. The residence time of heat treated CMC-F in PBS at 70°C varied from one hour up to more than 15 hours depending on the heat treatment conditions. The trend observed for water uptake correlated with dissolution rates in PBS. Films treated at higher temperatures showed slower dissolution rates. For a given temperature increasing the treatment time leads to an increase in water stability. Treatment in a CO_2 atmosphere resulted in further enhanced water stability.

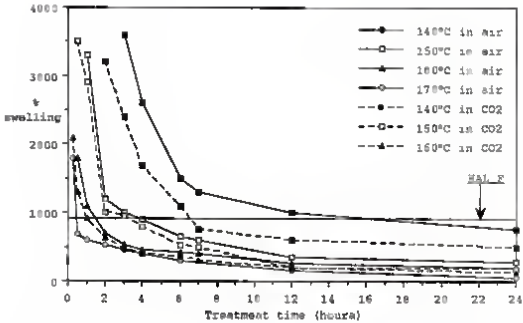

Figure 3 26 Percent water uptake of thermally treated CMC F at various temperatures in air and in CO_2 Swelling in PBS at 25°C

Table 3 11 Dissolution in PBS at 70°C for CMC films heat treated in air and in CO2

Treatment Temperature (°C)	Treatment time (hrs)								
	0 25	0 5	1	2	3	4	6	7	12	24
120 in air			1	1	1	1	1	1	1	2
120 in CO2		1	1	1	1	2	2	2	2	3
140 in air			1	2	3	3	6	6	6	6
140 in CO2		1	2	2	3	3	6	6	6	10
150 in air			4	6	6	10	10	10	10	10
150 in CO2	1	2	4	6	10	10	10	12	12	12
160 in air		10	11	11	>15	>15	>15	>15	>15	>15
160 in CO2	4	13	>15	>15	>15	>15	>15	>15	>15	>15
170	4	10	>15	>15	>15	>15	>15	>15	>15	>15
MAL F (1)					5					
INTERCEED TC 7					9					
	Residence time (hrs)									

Note This experiment was carried out for 15 hours All films have dissolved in PBS after 24 hours

(1) Lot # C1386C

The reactions responsible for CMC insolubilization are not entirely clear. In the light of the results obtained in this study a variety of crosslinking reactions or combinations of these reactions are possible. Crosslinking may occur by esterification according to reaction path shown in Figure 3-27. Enhancement of insolubilization observed in the presence of CO_2 may due to sodium hydroxide (a byproduct of the esterification reaction) reaction with CO_2 forming sodium bicarbonate thereby driving this crosslinking reaction to completion. CO_2 in combination with high moisture content of the CMC-F may provide a more acidic environment which could also enhance esterification.

This insolubilization can also be due to interresidue lactone formation. Lilely and coworkers reported the water insolubilization of a sodium salt of solemnic acid, a carboxylic group containing polysaccharide similar to CMC, by reaction with carbodiimide or by treatment with aqueous hydrofluoric acid. They attributed this phenomenon to the formation of interresidue cyclic lactones (205). An increase of the degree of esterification with decreasing pH was also observed which is consistent with our results in the presence of CO_2. Thermal treatment of cellulose or its derivatives may also involve a free radical mechanism. A number of investigators have studied the formation of free radicals in cellulosic materials heated at relatively low temperatures, using electron paramagnetic resonance spectroscopy. Arthur and Hinojosa reported the presence of a free radical signal in samples heated under vacuum for 30 minutes at temperatures as low as 160°C. The intensity of the signal increases sharply with increasing time and temperature, especially above 200°C (206). Milsch and coworkers detected free radicals in cellulose samples heated in nitrogen

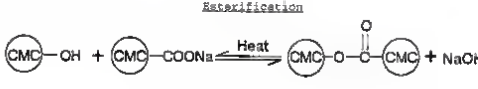

Figure 3 27 Possible reactions involved in CMC insolubilization by thermal treatment

at temperatures as low as 100°C (206) In the presence of oxygen free radicals could be expected to produce hydroperoxide groups Hydroperoxides have been shown to promote bond cleavage and subsequent depolymerization of cellulosic materials (206). However, CMC does not degrade significantly when heat treated as shown by increased residence time in PSC. This suggests that if radicals form, they recombine to form intermolecular crosslinks This is consistent with enhanced heat treatment insolubilization under anaerobic conditions where radicals are more likely to recombine than form hydroperoxides

FTIR spectrum of heat treated CMC films did not show any special features when compared to untreated films (Figure 3 28) The concentration of any newly formed functional groups (e g esters lactones) is probably too low to be detected by this technique Further investigation is needed to elucidate the mechanism involved in the insolubilization of CMC F.

Substantially water-insoluble CMC can be obtained by converting the carboxyl anion to the acid form. One method which has been proposed for preparing water insoluble CMC is to dissolve the sodium salt of CMC in a mixture of hydrochloride acid and a water miscible organic solvent, then heat treat the isolated material The acidification of CMC was further improved by directly treating solid water soluble CMC materials with hydrogen chloride gas and heating at temperatures as low as 100°C to produce a crosslinked, insoluble, partially acid form of CMC However, thermal insolubilization methods described in the present research allow better control over the extent of insolubilization by varying the time and temperature of the treatment.

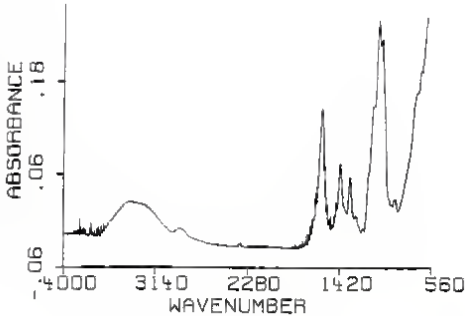

(a)

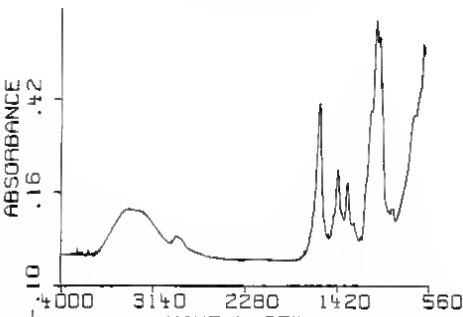

(b)

Figure 3.28 FTIR spectra of (a) uncreared CMC film
(b) CMC film heat treated in air at 160°C for 2 hours

It is important to note that surgical membranes used for adhesion prevention should stick to tissue and remain on surgical sites without the need for sutures. However, extensive CMC film insolubilization may interfere with this property and provide membranes with poor tissue "sticking" properties.

3.3.5 Biological Evaluations

3.3.5.1 In vitro rabbit endothelium wetting properties of various viscoelastics

In addition to maintaining the anterior chamber and enabling tissue manipulation, it is generally regarded that viscoelastics help avoid ocular tissue injury during cataract surgery. The ability of these high molecular weight polymer solutions to coat endothelial surfaces and thus provide a protective barrier against phacoemulsification trauma or damaging contact with an IOL or instrument is related to endothelium wetting properties. This study was conducted to evaluate endothelial surface wettability of various viscoelastics using goniometry. Contact angle measurements provide a generally useful quantitative method for investigating surface wettability. Low contact angles are indicative of good wettability and spreading of liquids on surfaces whereas high values suggest poorer surface wetting. This experiment was conducted according to the method described in section 3.3.2.2.1. The results for the contact wetting angle measurements are given in Table 3.12. For corneas free of superficial surface water Viscoat® and CMC V2 gave slightly lower initial contact wetting angle than Healon® or CMC V1. After three minutes, however, all solutions exhibited similar complete spreading on endothelial surfaces. When corneal surfaces were moistened with a drop of BSS prior to contact

Table 3.12. Contact angles of various viscoelastics on rabbit corneal endothelial surfaces in air

	Time (mns)	Healon®	Viscoat®	CMC-V1[1]	CMC V2[2]
water free endothelium	0	25	18	27	19
	1	17	11	20	12
	2	11	8	15	0
	3	0	0	0	0
moistened endothelium	0	0	0	0	0
	1	0	0	0	0

[1] 1.05% CMC-7HFPH in BSS filtered trough 10μ and autoclaved at 240°F for 20 mns

[2] 7HFPH/7L2P blend in BSS with 4.8% total concentration and 7HFPH 7L2P ratio of 3.5, filtered trough 10μ and autoclaved at 240°F for 20 mns

angle measurement, all samples gave no measurable contact wetting angle and immediate wetting. The immediate low contact wetting angles obtained for Viscoat® (HA/CS) (15°) and CMC V2 (13°) on water free rabbit endothelium surfaces as compared to 25° for HA and 27° for CMC V1 suggest that the HA/CS and CMC/V2 solutions exhibit slightly better endothelium wetting for dryer tissue surfaces. However, moist endothelial surfaces exhibited no differences in wettability among the various solutions tested. These results suggest that moist endothelium surfaces, which should represent the normal clinical situation during surgery, are wet immediately and equally well by all solutions tested. However, under conditions where endothelium surface drying could occur viscoelastic solutions containing high solids concentration and low MW polymeric chains exhibited somewhat better wetting qualities during the initial few minutes of contact. The similarity in endothelium wetting observed between Viscoat® (7% HA/CS) and CMC V2 (4.9% blended blend of 7HFPH and 7L2P) may be due to similar rheologies. Studies in our laboratories have shown Viscoat and CMC-V2 to exhibit somewhat higher low shear rate viscosity (40,000 Cps) than Healon and substantially less shear thinning (13%). This superior tissue affinity or "stickiness" is may be due to the presence of short chains (i.e., chondroitin sulfate in Viscoat and low molecular weight CMC (7L2P, 50,000) in CMC V2) which may better wet tissue surfaces due to higher mobility.

Reports dealing with differences in endothelial cell protection afforded by various viscoelastics are contradictory. These results suggest that, in real clinical conditions, all of the solutions tested are likely to provide similar level of endothelial protection based on their wettability. Superior endothelial cell protection reported by

some investigators could be primarily due to test procedures or factors other than tissue wetting properties of viscoelastics

2.3.5.2 In vivo evaluation of resorbable CMC membranes as adhesion prevention device in a rat cecal abrasion model.

Post operative adhesion formation is a major complication in a wide range of surgical procedures. The use of resorbable membranes to physically separate traumatized tissues and allow normal healing without adhesions is a promising approach to preventing post surgical adhesion formation. In vivo experiments were conducted to investigate the efficacy of insolubilized CMC membranes for prevention of peritoneal adhesion formation in a cecal rat model. Insolubilized CMC films having solubilities comparable to that of HAL-F (4-5 hours in PBS at 70°C) were selected for this experiment. These included CMC-F treated at 150°C in air for 1.0 hour and CMC-F treated at 150°C in air for 1.25 hours. From a practical point of view, it is important to note that insolubilized CMC membranes having lower solubility in PBS (≥ 5-7 hours in PBS at 70°C) have poor tissue "stickiness" and hence do not remain at surgical sites (i.e., slip off abraded tissue). A developmental HA membrane (HAL-F, Genzyme Corporation) was also included for comparison. This experiment was performed by Dr. Lynn Peck, Steven Farnworth and James Kirk.

Forty female Sprague-Dawley rats weighing 275 to 340 grams were randomly assigned to either treatment or control group with reoperation on day 7 postoperatively. Rats were housed at the University of Florida's Animal Resources facility, an AAALAC approved facility. The surgical protocol was approved by the University of Florida's Animal Care and Use Committee. Rats were anesthetized by intramuscular

injection of acepromazine (10 mg/ml), ketamine and xylazine (20 mg/ml) in a 1:3:3 ratio. Following surgical preparation and midventral abdominal incision, the ceca were exposed via a midventral laparotomy and two ml of PBS was placed intra abdominally. Each cecum was then exteriorized using PBS saturated cotton tipped applicators and each side was coated with an additional 1 ml of PBS prior to abrasion. A total of two circular areas (1.5 cm diameter each) were subjected to controlled, constant force rotary abrasion. Uniform abrasion was achieved using PBS coated gauze mounted on a rotating spline shaft designed to apply a fixed load of 70g. At 140 rpm, 60 revolutions per spot was used as a standard abrasion condition. For later identification the abraded area perimeter was marked in 4 places with a spot of India ink (Koh-i-noor Waterproof Black India ink, #3074 F), using a #4 (1.20 mm) technical pen (Koh-i-noor Rapidograph; Bloomsberg, N.J.). Control rats received no further treatment. Test rats received a 2 x 5 cm strip of tested membranes over abraded areas on each side of the cecum for all treatment groups. The abdomen was closed in two layers using continuous 2-0 polyglycolic acid sutures (Dexon; Davis-Geck). Rats were reoperated seven days after the abrasion procedure and adhesions scored on a 0-4 scale (Table 3-13). Adhesions with scores greater than 2 were considered clinically significant for area, strength of attachment or location. Adhesions were graded by Dr. Lynn Peck. The results are given in Table 3-14. PBS is usually used as surgical irrigation solution and served as control for this experiment. For PBS, the incidence of total adhesions was 90% (9 adhesions found in 10 rats). The percent of clinically significant adhesions (≥2) was 60%. The use of HAL-F showed a 50% reduction in clinically significant adhesions (from 60% to 30%). CMC-F1 and CMC-F2 were two CMC membranes prepared by thermal

Table 3-13: Description of scoring scale used in surgical adhesions in the rat cecal model.

Grade	Description
0	No adhesions
1	Filmy, fibrinous adhesions with easily identifiable plan
2	Mild adhesions with freely dissectible plane Fibrous with minimal area of attachment
3	Moderate adhesions with difficult dissection of plane. Fibrous with significant area and/or location of attachment.
4	Dense adhesions with undissectible plane. Moderate to major area of attachment

Table 3-14: Peritoneal adhesions in the rat cecal model using CMC F and HAL F as adhesion prevention membranes 70gms/60 revolutions/140 rpm/2 spots

	thickness (mils)	residence time in PBS @ 70°C	# rats	cecal adhesions found	%	≥2	%	%decrease vs PBS
PBS			10	8	80	6	60	
HAL F	2.0	5 hrs	10	6	60	3	30	50
CMC F1[1]	2.1	5 hrs	10	6	60	3	30	50
CMC F2[2]	1.9	6 hrs	10	4	40	2	20	67

[1] CMC F cast from 1% 7HFPH and thermally treated in air at 150°C for 1.0 hour

[2] CMC F cast from 1% 7HFPH and thermally treated in air at 150°C for 1.25 hour

insolubilization and have properties similar to those of HAL F (thickness and residence time in PBS). CMC-F1 (1.0hour at 150°C in air) also exhibited a 50% reduction in the number of significant adhesions CMC F2 (1.25 hours at 150°C in air) exhibited a slightly greater reduction in the number of significant adhesions (67%)

The rat cecal model suggests that CMC membranes can significantly inhibit postoperative adhesion formation when used as barrier film on traumatized tissue. These membranes were resorbed by the body over a relatively short period of time (1 week).

3.4 Conclusions for Viscoelastic Polymer Solution Studies

1. The rheological properties of aqueous solutions of carboxymethylcellulose (CMC) of molecular weights varying from 9.0×10^4 to 1.0×10^6 were investigated over a wide range of concentrations (0.5% to 5.0 %). Low shear rate viscosity (η_0) of CMC solutions was found to vary with concentration (c) according to a power law of the form $\eta_0 = Ac^n$ where A and n are two constants. Values of A and n were determined empirically for each molecular weight.
2. CMC solutions were found to exhibit pronounced pseudoplastic behavior which follows a power law of the form $\eta(s) = Bs^m$ where s is the shear rate, B and m are two constants. Values of B and n were also determined for various concentrations.
3. The addition of high salt concentrations (up to 40% NaCl) to CMC solutions had only a slight effect on the viscosity (5-15%). This suggests that rheological properties of CMC may not be solely due to its anionic polyelectrolyte behavior.

A model based on "junction zone" theory was proposed to explain network properties of CMC solutions

4 The rheology of filtered CMC solutions was investigated for various molecular weights and concentrations Solution viscosity was increased by 10% filtration Molecular weight measurements by laser light scattering GPC suggested that this may be due to removal of aggregated low molecular weight species and reorganization of solution structures The results are consistent with the "junction zone" model proposed The pseudoplastic behavior of CMC solutions was not affected by filtration

5 The effect of autoclaving for sterilization following filtration was also studied Lower viscosities for CMC solutions were observed after autoclaving below a critical concentration (c*) which in turn was found to be dependent on the molecular weight Solutions with concentrations greater than c* exhibited increased viscosity upon autoclaving Since no significant change in molecular weight was observed due to autoclaving, the change in viscosity was attributed to conformational changes Total hydrodynamic volume (c[η]) calculations at critical concentrations for various molecular weights revealed that the onset of increased viscosity upon autoclaving occurs at values of c[η] of 364 2 to 368 4 The change in viscosity was attributed to a generalized behavior related to a critical value of c[η] ((c[η])*) below which "junction zones" are disrupted by autoclaving (i e "melting" of junction zones)

6 CMC solutions prepared from blends of low molecular weight CMC (CMC 7LF) and high molecular weight CMC (CMC 7HFPM) showed negative synergistic behavior (i e shear viscosities observed were much lower

than those anticipated from additive blending law). Bimodal MWD CMC blends were also found to be less pseudoplastic.

7. Stability of CMC solutions was investigated by exposing solutions to normal storage conditions (25°C, normal light conditions) for a period of 6 months. Unprocessed (i.e. unfiltered and unautoclaved) CMC solutions exhibited a fast decrease in viscosity after 14 weeks which was attributed to bacterial degradation. However, sterile filtered and autoclaved solutions showed little change in viscosity for the time of the experiment (ca 4% decrease in viscosity during a 6 month period).

8. Oxidative degradation of CMC and HA was investigated in vitro via oxygen derived free radicals (ODFRs) produced by autoxidation of iron (Fe/EDTA system). Hydroxyl radical scavengers were the most efficient antioxidant in preventing ODFR-mediated degradation of HA and CMC. This suggests that hydroxyl radicals may be the major damaging species responsible for oxidative degradation of HA and CMC. Dimethylsulfoxide (DMSO) at 0.5% concentration afforded almost complete protection against degradation (95% inhibition of viscosity reduction) for both HA and CMC. Glutathione afforded 77% protection at 0.5% concentration. Such agents may be useful as antioxidants in HA and CMC to minimize degradation by free radicals produced at tissue injury sites in vivo by polymorphonuclear monocytes or as stabilizers to enhance solution stability during autoclaving and storage.

9. The preparation and evaluation of CMC films for adhesion prevention was studied. Films cast from aqueous CMC solutions were optically clear, flexible, and dissolved in water readily. In order to increase residence time in water of CMC films various

insolubilization methods were investigated. Ionic complexation of CMC films via calcium ions produced CMC membranes with enhanced residence time in PBS (36 hours). However, a novel insolubilization thermal technique (treating CMC films at temperatures varying from 120 to 170°C and times varying from minutes to 24 hours in air or in CO_2) produced CMC membranes which were insolubilized and remained optically clear and flexible.

In vivo evaluation of thermally insolubilized CMC membranes in a rat cecal model showed good adhesion prevention efficacy (50-67% reduction in clinically significant adhesions with CMC F treated in air at 150°C for 1.0 hour and CMC F treated in air at 150°C for 1.25 hours, respectively). Insolubilized CMC membranes may of interest as postsurgical adhesion prevention devices.

Endothelium wetting properties of two CMC viscoelastic solutions (a Healon like composition (1.85% CMC 7HFPH in BSS filtered and autoclaved) and a Viscoat like composition (4.8% 7HFPH/7L2P ratio 7HFPH:7L2P of 2.3 filtered and autoclaved)) were investigated by measuring the contact wetting angle on rabbit corneal endothelium. Although superficially dry tissue surfaces showed some wetting differences, BSS moistened endothelium was immediately wet by all samples. This suggests that in clinical situations there is probably little difference in endothelial wettability or tissue coating by various ophthalmic viscoelastic solutions (i.e., Healon®, Viscoat®, or CMC).

CHAPTER 6

FUTURE WORK

6.1 Hydrophilic Surface Modification of Ocular Implant Polymers

1 Investigate grafting of NVP/PVP mixtures with various NVP precook conditions

2 Investigate the morphology and thickness of PVP grafts prepared under various conditions using TEM structural analysis

3 Study the molecular weight and molecular weight distribution of grafting solutions using GPC and other methods

4 Investigate grafting of other anionic vinyl monomers (e g carboxylic acid group containing monomers)

5 Study the relationship between charge density of modified surfaces (neutral and anionic) and biological properties (cell adhesion, tissue protection)

6 Extend hydrophilic surface modifications to substrates other than PMMA and PDMS (e g polypropylene, polyurethane)

7 Investigate the incorporation of other bioactive molecules (e g protein growth factors) into hydrogel compositions

8 Conduct in vivo evaluation for all of the hydrophilic surface modified substrates

6.2 Tissue protective Hydrophilic Polymer Solutions and Membranes

1 Develop empirical equations for molecular weight rheology relationships similar to those developed for concentration rheology relationships

2 Study the viscoelastic properties of CMC solutions using dynamic measurements. Establish relationships between complex shear modulus and molecular weight.

3 Investigate further the effect of various mixing conditions (time and mixing speed), temperature, and pH on the rheology of CMC solutions

4 Investigate further the presence and nature of intermolecular associations in CMC solutions and their effect on the rheology using light scattering experiments.

5 Use the competitive inhibition approach to investigate the structure of junction zones in CMC solutions (i e study the rheology of CMC solutions after adding short CMC chains with well known length)

6 Investigate the effect of filter pore size and filtration pressure on the rheology of CMC solutions

7 Investigate other methods of filtration

8 Establish clear relationships between molecular weight of each component in CMC blends and solution rheology

9 Conduct accelerated stability tests on CMC solutions (i e storage at higher temperatures) and assess the effects of filtering and autoclaving.

10 Study the mechanical properties of CMC membranes before and after insolubilization.

11 Investigate further the effect of treatment atmosphere on thermal insolubilization of CMC (i e., HCl, HCl/CO_2)

12 Elucidate CMC thermal insolubilization reactions by high resolution FTIR or other analytical methods.

13 Investigate other methods for CMC insolubilization (i e esterification, lactonization)

14. Conduct in vivo evaluation test for various CMC viscoelastics especially with respect to postoperative intraocular pressure increase

REFERENCES

1. N S Jaffe, "The Outlook for Intraocular Lenses through 1990," J. Cataract Refract. Surg., 12, 267 (1986).

2. D J. Apple, N. Mamalis, K. Loftfield, J.M. Googe, L C. Nevyack, D.K. Van Norman, S.H. Brady, and S.J. Olsen, "Complications of IOLs. Historical and Histopathological Review," Surv. Ophthalmol. 29, 1 (1984).

3. V F. Deluise, "Complications of IOLs," Int. Ophthalmol. Clin. 27, 195 (1987).

4. H.E. Kaufman, J. Katz, J. Velenti, J.W. Sheets, and E.P. Goldberg, "Corneal Endothelium Damage with Intraocular Lenses: Contact Adhesion Between Surgical Materials and Tissue," Science, 198, 525 (1977).

5. J. Katz, H.S. Kaufman, E.P. Goldberg, and J.W. Sheets, "Prevention of Endothelial Damage from IOL Insertion," Trans. Am. Acad. Ophthalmol. Otolaryngol. 83, 204 (1977).

6. J.W. Sheets, Hydrophilic Polymer Coatings to Prevent Tissue Adhesion, Ph.D. Dissertation, University of Florida, 1983.

7. M.J. Lyndon, T.W. Minett, and B.J. Tighe, "Cellular Interactions with Synthetic Polymer Surfaces in Culture," Biomaterials, 6, 356 (1985).

8. A. Yehiaoui, Surface Modification of IOL Polymers by Hydrophilic Graft Polymerization for Improved Ocular Implants, Ph.D. Dissertation, University of Florida, 1990.

9. O. Larm, R. Larsson, P. Olsson, "A New Non-thrombogenic Surface Prepared By Selective Covalent Binding of Heparin via Reducing Terminal Residue," Biomat. Med. Devices Artif. Organs, 11, 161 (1983).

10. P.S. Larson, E.L. Lindstrom, and D.L. Skalnik, "Viscoelastic Agents," CLAO, 15, 151 (1989).

11. E.L. Graue, F.B. Polack, H.A. Balaza, "The Protective Effect of Na-hyaluronate to Corneal Endothelium," Exp. Eye. Res., 31, 119 (1980).

12. M S Passo, J T Ernest, and T K Goldstick, "Hyaluronate (Healon) Increases Intraocular Pressure When Used in Cataract Extraction", Br J Ophthalmol, 69, 572(1985)

13. T C M Trimbos-Kemper, J B Trimbos and E V Van Hall "Adhesion Formation After Tubal Surgery: Results of The Eighth Day Laparascopy in 188 Patients" Fertil Steril, 43, 385(1985)

14. B. Ellis, "The Cause and Prevention of Postoperative Intraperitoneal Adhesions", Surg. Gynecol. Obstet., 133 497(1971)

15. G. Holtz "Prevention and Management of Peritoneal Adhesions", Fertil Steril, 41, 497(1984)

16. J J Algar, and P U Fechner Fechner's Intraocular Lenses Thieme, Inc. New York. 1986.

17. R H S Langston, "Intraocular Lens Implantation: A Review," Artif Org, 2, 55(1978)

18. D J Apple N Mamalis, R J Olson, and M C Kincaid, Intraocular Lenses: Evolution, Designs, Complications, and Pathology, Williams and Wilkins, Baltimore. 1989

19. J E Pogla, J E Blaydes, K J Fritz, and S H Blaydes, "Clinicopathologic Observations of a Silicone Posterior Chamber Lens in a Primate Model" J Cataract Refract Surg, 12 281(1986)

20. C Skargic, R Menapace, H D Gnad, M Graal "Evaluation of 50 Silicone Posterior Chamber Lens Implantation", J Cataract Refract Surg, 13, 640(1987)

21. D J Apple, N Mamalis, K Loftfield, J M Googe, L C Novack B.K. Van Norman, S E. Brady, and R J Olson "Complications of IOLs: Historical and Histopathological Review" Surv Ophthalmol 28, 1(1984).

22. E P Goldberg,, F.M. Hofmeister, M. Yalen S Ids, J Stechely, P Martin A Yahimoui and J W. Sheets, "Hydrophilic surface Modification of IOL Implants to Reduce Surgical and Post operative Ocular Tissue Trauma" paper Presented at the Academy of Surgical Research Meeting. Boston, 1988.

23. H Hattori E P Goldberg, P. Martin, and D. Osborn, "Effect of Injected Cortex on Rabbit Implants with Surface Modified IOLs" paper Presented at the Symposium on Cataract, IOL and Refractive Surgery, ASCRS Boston April 1991

24. E. Battara, P. Martin, D. Osborn, and E.P. Goldberg, "A Cortex Induced Ocular Inflammation Model for Accelerated Evaluation of Surface Modified IOL Implants," paper presented at The Fourth World Biomaterials Congress. Berlin, April 1992

25. H. Ridley, "Intraocular Acrylic Lenses," Trans. Ophthalmol. Soc. UK., 71, 617(1951).

26. L. Allakherie, R. Knoll, and R.L. Lindstrom, "Soft Intraocular Lenses," J. Cataract Refract. Surg., 13, 607(1987)

27. N.T. Lee, B.R. Rajan, and H.F. Bushar, "Residual Ethylene Oxide Determination in PMMA Disks and IOLs by Gas Analysis and N.N.DMF Extraction," J. Pharm. Sci., 78, 40(1989)

28. A.C. Neumann, G.R. McCarty, and R.H. Osher, "Complications Associated with STAAR Silicone Implants," J. Cataract Refract. Surg., 13, 653(1987)

29. R. Champion, P.J. McDonnell, and W.R. Green, "Intraocular Lenses Histopathological Characteristics of a Large Series of Autopsy Eyes," Surv. Ophthalmol., 30, 1(1985)

30. T.T. Chen, "Clinical Experience with Soft Intraocular Lens Implantation", J. Cataract. Refract. Surg., 13, 50(1987)

31. M. Yelon, M. Blumenthal, and E.P. Goldberg, "Preliminary Study of Hydrophilic Hydrogel IOL Implants in Cats," Intra-Ocular Implant Soc. J., 10, 315(1984).

32. D. Williams, Concise Encyclopedia of Medical and Dental Materials, p. 289. The MIT Press. Cambridge, Massachusetts, 1990.

33. H.J. Mondino, G.M. Rejaeich, and H. Summer, "Comparison of Complement Activation by Silicone IOLs and PMMA IOLs with PP Loops," Arch. Ophthalmol., 105, 989(1987)

34. A.T. Milsuekae, "Posterior Capsule Opacification after Silicone Implantation and its Management," J. Cataract Refract. Surg. 13, 844(1987).

35. A.B. Jr. Ruedemann, "Silicone Intraocular Lens in Rabbits" Trans. Am. Ophthalmol. Soc., 75, 436(1977)

36. B.D. Ratner, and A.S. Hoffman, "Synthetic Hydrogels for Biomedical Applications," in Hydrogels for Medical and Related Applications, Vol. 31, p. 1. J.D. Andrade, Ed., American Chemical Society Symp. Ser., ACS. Washington, DC. 1976.

37. M. Yelon, M. Blumenthal, and E.P. Goldberg, "Preliminary Study of Hydrophilic Hydrogel IOL Implants in Cats," Intra-Ocular Implant Soc. J., 10, 315(1984)

38. P. Percival, "Prospective Study Comparing Hydrogel with PMMA Lens Implants," Ophthalm. Surg., 20, 255(1989).

39. A. Hernse, P.M. Corkhill, and B.J. Tighe, "Synthetic Hydrogels III. Hydroxyethylacrylate and Methacrylate Copolymers: Surface and Mechanical Properties," Polymer, 29, 1875(1988).

40. D.G. Pedley, P.J. Skelly, AND B.J. Tighe, "Hydrogels in Biomedical Applications," Br. Polym. J., 12, 99(1980).

41. B. Jansen, and G. Ellinghorst, "Modification of PEU for Medical Applications by Radiation Induced Grafting. 1. Grafting Procedure and Chemical Modification of Grafted Films," J. Biomed. Mater. Res., 13, 1085(1985).

42. D.M. Macrice, "Cellular Membrane Activity in The Corneal Endothelium of The Intact Eye," Experientia, 24, 1094(1968).

43. H. Cotlier, The Cornea, Mosos MA: St Louis, p. 35, 1970.

44. C.D. Binkhorst, "Inflammation and Intraocular Pressure after The Use of Healon in Intaocular Lens Surgery", Am. Intra-ocular Implant Soc. J., 6, 340(1980).

45. P. Percival, "Complications from use of Sodium Hyaluronate (Healonid) in Anterior Segment Surgery" Br. J. Ophthalmol., 66, 714(1982).

46. D.R. Absolom, W. Zing, and A.W. Newmann, "Protein Adsorption to Polymer Particles: Role of Surface Properties," J. Biomed. Mater. Res., 21, 161(1987).

47. J.D. AndrAde, "Principles of Protein Adsorption," in Surface and Interfacial Aspects of Biomedical Polymers, Vol. 2, p. 1, J.D. Andrade, Ed., Plenum Press, New York, 1985.

48. F. Grannell, "Cellular Adhesiveness and Extracellular Substrate" Int. Rev. Cyt., 53, (85)1978.

49. M.J. Lyndon, T.W. Minett, and B.J. Tighe, "Cellular Interactions with Synthetic Polymer Surfaces in Culture," Biomaterials, 6, 396(1985).

50. L. Aguadisch, "Cell Adhesion to Polymer Surfaces," Biomedical Engineering Center Publication, Materials Sciences and Engineering, University of Florida, Gainesville, FL, 1989.

51. M.E. Shrader and J.A. Lardamone, "Bioadhesion to Low Surface Energy Surfaces:Significance of the γ_c Window," J. Coll. Inter. Science, 104, 4(1985).

52 R E Baier, V A DePalma, D W Goupil, and E Cohen, " Human Platelet Spreading on Substrate of Known Surface Chemistry," J Biomed Mater Res , 19, 1157(1985)

53 N-G Marsudas "Sulphonated Polystyrene as an Optimal Substratum for the Adhesion and Spreading of Mesenchymal Cells in Monovalent and Divalent Saline Solutions-" J Cell Physiol , 90 511(1977)

54 A Kishida, N Iwata, Y Tamada, and Y Ikada, "Cell Behavior on Polymer Surfaces Grafted with Non-ionic and Ionic Monomers," Biomaterials, 12, 767(1661)

55 B M Cleymaa, M G Jaffe, M A Gelin, Intraocular Lens Implantation,Techniques and Complications C V Mosby, St Louis, 1983

56 D E Bifrig, 'Deposits on The Surface of Intraocular Lenses-A Pathologic Study " South Med J 73 6(1660)

57 J R Welter, "Cytopathology of Intraocular Lens Implantation, Ophthalmology 32, 135(1685)

58 A Chapiro, Radiation Chemistry of Polymeric Systems Wiley Interecience, New York 1662

56 A Charlesby Atomic Radiation of Polymers Pergamon Press Oxford, 1660

60 A R Shultz, P I Roth, and J M Berge, "Radiation Degradation of Polymethacrylates: Dose Rate and Medium Effects," J Polym Sci Part A, 1, 1651(1963)

61 A Todd, "The mechanisms of Radiation Induced Changes in Vinyl Polymer," J Polym Sci 152 223(1960)

62 A Planka, and K Pietruche, "Kinetics of Free Radical Decay in Gamma Irradiated PMMA." Radiat Phys Chem, 21 436(1983)

63 B Ranby and J F Rabek Photodegradation, Photo oxidation and Photostabilization of Polymers, Principles and Applications Wiley & Sons New York, 1675

64 B Menhoffer, and H Hensinger, "Radical Formation in Polydimethylsiloxanes and Polydimethyldiphenylsiloxanes Studied by the ESR Spintrap Technique " Radiat Phys Chem , 29 243(1987)

65 B J Parsons G O Phillips B Thomas D J Wadlock, and A J Clarke Struman "Depolymerization of Xanthan By Ire Catlyzed Free Radical Reactions," Int J Biol Macromol 7 187(1985)

66 N K Kochetkov, L I Kudryashov, and M A Chlenov, Radiation Chemistry of Carbohydrates p 141 Pergamon Press Oxford 1676

67 F A Bloute, and J C Arthur, Jr, "Degradation of Cotton in an Oxygen Atmosphere by Gamma Radiations" J Chem Eng Data 5, 470(1960)

68 J C Arthur,Jr, Energetics and Mechanisms in Radiation Biology p 153, Academic Press, London 1968

69 D J Wedlock, S J Parsons, G O Phillips, and E Thomas "Effect of Derivatisation on Free Radical Depolymerisation of Cellulose" Cellulose and its Derivatives Chemistry, Biochemistry, and Applications, p 503, Ellis Horwood Publishers, 1985

70 T P Nevell and S H Zaronian, Cellulose Chemistry and its Applications, p 308, Ellis Horwood Publishers 1985

71 N Grassie, "Polymer degradation" Macromolecular science V 8 p 276, Editios Butterworths London, 1985

72 N A Peppas Hydrogel in Medicine and Pharmacy V I p 15 CRC Press Boca Raton, 1986

73 F A Bovey, The Effect of Ionizing Radiation on Natural and Synthetic High Polymers, p 55, Interscience Publishers Inc., New York 1958

74 E Collinson and A J Swallow "The radiation Chemistry of Organic Substances" Chem Rev , 56, 471(1956)

75 I Sukurada, S Okamura, and S Kawasaki, "The Kinetics of Degradation of Macromolecular Linear Molecules I Theoretical Equations" J Soc Chem Ind Jpn Suppl 45, 415(1972)

76 I Sukurada, S Okamura and S Kawasaki "The Kinetics of Degradation of Macromolecular Linear Molecules III Oxidative Degradation," J Soc Chem Ind Jpn Suppl 45 416(1972)

77 F A Bovey The Effect of Ionizing Radiation on Natural and Synthetic High Polymers, p 56 Interscience Publishers Inc New York 1958

78 R J Ceresa, Graft and Block Copolymerization Vol 1, Wiley, New York, 1973

79 N Nishioka T Kuromatsu T Takakashi M Uno, and K Kosai "Permeability through Cellulose Membranes Grafted with Vinyl Monomers in a Homogeneous System III Methyl Methacrylate Grafted Cellulose Membranes" Polym J 18 131(1986)

80 N Nishioka Y Matsumoto, T Yunse, and K Kosai, 'Homogeneous Graft Copolymerization of Vinyl Monomers onto Cellulose in DMSO Paraformaldehyde Solvent Systems IV 2 Hydroxyethylmethacrylate,' Polym J 18 323(1986)

81 J C Arthur,Jr P J Baugh and O Hinojosa "ESR study of Reactions of Cellulose Initiated by the Ceric Ion Method," J Appl Polym Sci 12 1591(1968)

82 J C Arthur,Jr, O Hinojosa and M S Saina "ESR study of Reactions of Cellulose with OH Generated by Fe^{2+}/H_2O_2 " J Appl Polym Sci., 12 1411(1968)

83 D N Shultz "Water Soluble Polymer Synthesis Theory and Practice" Water Soluble Polymers, p 57, ACS, Washington, D C, 1991

84 S R Sandler W Karo, Polymer Synthesis Chap 8 Academic Press New York, 1977

85 D N Shultz, K Kitano, J A Banik and J J Kaladas, Polymers in Aqueous Media Performance through Association, Advances in Chemistry Series, p 165 ACS, Washington D C 1989

86 A Charlesby Atomic Radiation of Polymers Pergamon Press Oxford, p 300 1960

87 A Charlesby, "Gel Formation and Molecular weight Distribution in Long Chain polymers," Proc R Soc London, Ser A, 222 542(1954) 173, 679(1954)

88 K Katsura "On the Viscosity of Irradiated Polymers III Effect of Branching," J Phys. Soc Jpn., 15 2310(1960)

89 A Charlesby Atomic Radiation of Polymers Pergamon Press, Oxford, p 118 1960

90 F M Hofmeister Biosurface Properties of Ocular Implant Polymers, M S Thesis University of Florida 1989

91 S Reich, M Levy, A Mesherer M Slumenthal, M Yelan, J W Sheets and E P Goldberg, "Intraocular Lens Endothelial Interface Adhesive Force Measurements" J Biomed Mater Res 18 737(1984)

92 Thechnical brochure, Povidone, Polyvinylpyrrolidone USP GAF Chemicals Corporation, Wayne NJ, 1989

93 N A Peppas Hydrogel in Medicine and Pharmacy V I p 14 CRC Press, Boca Raton 1986

94 E Kiran and F Rodriguez, "Effects of Gamma Radiation on Aqueous Polymer Solutions A comparative Study " J Macromol Sci Phys 7, 209(1973)

95 N A Peppas Hydrogel in Medicine and Pharmacy V I p 1P CRC Press, Boca Raton 19P6

96 A Charlesby Atomic Radiation of Polymers, Perpamon Press, Oxford p 461, 1960

97 E D Callejo, A R Greus and J L G Ribelles "Study of Structural Relaxation by Dynamic Mechanical Methods in PMMA," Polymer 30 1433(1989)

9P N Inagaki, S Tasaka and N Miyazaki, "Sulfonic Acid Group Containing Thin Films Prepared by Plasma Polymerization " J Applied Polymer Science, 38 1829(1989)

99 P P Nveni and G D Rees, Proceedings of the ACS Division of Polymeric Materials: Science and Engineering, ACS Meeting, New Orleans, LA: p 477 American Chemical Society Washington DC 1997

100 T W Reihoffer, D J Lundberg and J E Glass "Influence of Polarity in Water-Soluble Polymer Synthesis" in Polymer in Aqueous Media, Advances in Chemistry Series p 149 American Chemical Society, Washington DC 1989

1P1 G Odian, Principles of Polymer Science, 2nd ed Wiley Interscience Publ , New York, 1991

1P2 C Nojiri, H Jacobs, and P W Kim, "Improved Blood Compatibility for Polymers Incorporated with Heparin " IEEE Engineering in Medicine and Biology Magazine, 8, 17(1989)

1D3 G Odian Principles of Polymer Science p 461 2nd ed Wiley Interscience Publ , New York, 1981

1D4 T Sato, M Abe, and T Otsu, "Application of Spin Trapping Technique to Radical Polymerization," Makromol Chem., 178 1081 (1977)

1P5 T C Laurent, "Biochemistry of Hyaluronan " Acta Otolaryngol , Suppl , 442, 7(1987)

1P9 E L Goldberg J D Seidman G Chi Bosso, and E P Toole "Endogenous Hyaluronate Cell Surface Interactions in 3T3 and Simian Virus transformed 3T3 cells," J Biol Chem , 259, 9440(1984)

197 R Larsson, "Biocompatible Surfaces Prepared by Immobilized Heparin or Hyaluronate " Acta Otolaryngol Suppl 442, 44(1987)

108 P Fagerholm, E Koul and S Trocme, "Corneal Endothelial Protection by Heparin and Sodium Hyaluronate Surface coating of PMMA Intraocular Lenses," Acta Ophthalmologica Suppl. 182, 110(1987).

109 K. Kawashima, "Immobilization of Enzymes and Microorganisms by Radiation Polymerization," Methods in Enzymology, V 135, p. 148, Academic Press, London 1987.

110 W D Comper and T C Laurent, "Physiological Function of Connective Tissue Polysaccharides," Physiol Rev. 58 255(1978).

111 M. Yalpani, Polysaccharides:Syntheses, Modifications and Structure/Property Relations, p 467 Elsevier New York 1988.

112 J C. Arthur Jr. "Graft Polymerization onto Polysaccharides," Advances Macromol. Chem. p. 255 Academic Press London, 1973.

113 J.C. Arthur Jr, "Intramolecular Energy Transfer in Cellulose and Related Model Compounds," Energy Transfer in Radiation Processes, p. 29. Elsevier, Amsterdam(1966).

114 P. Molyneux Water Soluble Polymers,Properties and Behavior. V I and II CRC Press, Boca Raton, Fl, 1982

115 W Sandlinker, K Watson, and T Sreea,"The use of Hydroxyethyl Starch for Regulation of Osmotic Pressure in Blood Substitutes". Europ. Pat. AP 261,802 (1988)

116 I. Paufique and J Charleux "Utilisation du Vitre Lyophilise Humain dans les Decollements Greve de la Retine." Bull. Soc Franc. Ophthalmol., 74 346(1961)

117 D M. Shaffer and J L Bussey "Further Experience with Vitreous Implants in Old Retinal Detachments." Arch Ophthalmol Chicago 60 225(1958)

118 H A. Eelens, "Importance of the vitreous body in Retina Surgery with Special Emphasis on Separations." Proceedings of the II Conference of the Retina Foundation, Igewich, 1958.

119 D. Miller and R. Stegmann, "Use of Sodium Hyaluronate in Human IOL Implantation," Ann. Ophthalmol., 13. 811(1981)

120 R Stegmann and D Miller, "Protective Function of Sodium Hyaluronate in Corneal Transplantation," Ocular Therapy & Surgery Nov/Dec, 28(1981)

121 E G Rosen Viscoelastic Materials:Basic Science and Clinical Applications, p 167, Pergamon Press, Oxford 1986

122 L G Pape,"Intracapsular and Extracapsular Technique of Lens Implantation with Healon " J Am Intraocul Implant Soc , 8 342(1980)

123 M J Roper-Hall, "Viscoelastic Materials in the Surgery of Ocular Trauma ' Trans Ophthalmol Soc UK 103, 274(1983)

124 J Scott, "The use of Viscoelastic Materials in the Posterior Chamber " Trans Ophthalmol Soc UK, 103 280(1983)

125 S Miyauchi and S Iwata,"Evaluation on the Usefulness of Viscous Agents in Anterior Segment Surgery I The Ability to Maintain The Deepness of the Anterior Chamber," J Ocular Pharm, 2, 267(1986)

126 S A Arshinoff, "Viscoelastic Substances Their Properties and Use when Placing an IOL in the Capsular Bag " Curr Can Ophthalmic Pract , 1 64(1986)

127 H Bothner and O Wik, "Rheology of Hyaluronate " Acta Otolaryngol , Suppl 442 29(1987)

128 A S Holmberg and B T Philipson, "Sodium Hyaluronate in Cataract Surgery I Report on the Use of Healon in two Different Types of Intracapsular Cataract Surgery " Ophthalmology 91 45(1984)

129 L G Pape, "Intracapsular and Extracapsular Technique of Lens Implantation with Healon," Am Intraocular Implant Soc J , 6 342(1980)

130 K J Hoffer, "Effects of Extracapsular Implant Techniques on Endothelial Density," Arch Ophthalmol 100 731(1982)

131 J M Groethar, G W Herrie, J A Davison, R H Watt, R R Widener and V Speaker "A Comparison of the Effects of Phacoemulsification and Nucleus Expression on Endothelial Cell Density," Am Intraocular Implant Soc J , 9, 420(1983)

132 D B Glasser, H B Katz, J E Boyd, J D Langdon, S L Shoke and R L Peiffer "Protective Effects of Viscous Solutions in Phacoemulsification and Traumatic Lens Implantation," Arch Ophthalmol 103, 1047(1985)

133 M T Crain, R J Olson, N Mamalis and R J Olson "Air Bubble Endothelial Damage During Phacoemulsification in Human Eye Bank Eyes: The Protective Effects of Healon and Viscoat " J Cataract Refract Surg , 16, 597(1990)

134 D B Glasser, D C Osborn, J F Nordsen and Y Min ' Endothelial Protection and Viscoelastic Retention During Phacoemulsification and Intraocular Lens Implantation," Arch Ophthalmol 109, 1438(1991)

135 S A Arshinoff "Comperative Physical Properties of Ophthalmic Viscoelastic Materials " Curr. Can. Ophthalmic Pract 7 1 (1989)

136 M E Hammer, T G Burch, "Viscous Corneal Protection by Sodium Hyaluronate Chondroitin Sulfate and Methylcellulose " Invest Ophthalmol Vis Sci 25, 1329(1984)

137 J J Algar A J Alper J Baco and D Chapman "Comparison of Healon and Viscoat in Cataract Extraction and Intraocular Lens Implantation," Ophthalmic Surgery, 100, 377(1985)

138 K Mentak, P Martin, E Rotter and E P Goldberg, "Rheology and Endothelium Wetting Properties of Viscoelastics," Submitted to the Journal of Cataract and Refractive Surgery 1992

139 S E Harrison, D E Sell, M Shayegan and T Clinch, "Chondroitin Sulfate A new and Effective Protective Agent for Intraocular Lens Insertion," Ophthalmology, 89, 1254(1982)

140 S A Baron M Busin and C Pege, "Comparison of the Effects of Viscoat and Healon on Postoperative Intraocular Pressure," Am J Ophthalmol 100 377(1985)

141 C D Kinkhorst "Inflammation and Intraocular Pressure after the Use of Healon in Intraocular Lens Surgery " J Am Intraocular Implant Soc., 6, 340(1980)

142 G M Cherfan W J Rich and G Wright "Raised Intraocular Pressure and Other Problems with Sodium Hyaluronate in Cataract Surgery." Trans Ophthalmol Soc UK 103 277(1983)

143 E A Balazs, "Sodium Hyaluronate and Viscosurgery," in Healon, A guide to Its Use in Ophthalmic Surgery p 5 28 Wiley Medical Publishers, New York 1983

144 S R Bean, R H Kestas and P A Weber 'Elimination of Sodium Hyaluronate induced Decrease in Outflow Facility with Hyaluronidase," Ophthalmic Surgery 17, 731(1985)

145 H Schubert, J L Bonlinger and E A Balazs, "Na Hyaluronate of Injected into The Anterior Chamber of Owl Monkey Effect on IOP and Rate of Disappearance (Abstract)," Invest Ophthalmol Vis Sci 20 Suppl 118(1981)

146 H Lang, H Mark and F A Miller " Shear Flow Characteristics of Sodium Hyaluronate Relationship to Performance in Anterior Segment Surgery " Arch Ophthalmol 102 1079(1984)

147 E A Balazs, "Viscosurgery Features of A True Viscoelastical Tool and Its Role in Ophthalmic Surgery," in Treatment of Anterior Segment Ocular Trauma p 167 Medicopes Montreal 1986

148 J L Denlinger H Schubert and E A Balazs 'Na Hyalcronate of Various Molecular Sizes Injected into The Anterior Chamber of Owl Monkey: Disappearance and Effect on IOP " Proc Int Soc Eye Res 1 88(1980)

149 S Iwata S Miyecchi and M Takahara " Biochemical Studies on The Use of Sodium Hyaluronate in The Anterior Eye Segment I Variation of Protein and Ascorbic Acid in Rabbit Aqueous Humor," Curr Eye Res 3 605(1984)

150 D Benedette and D Shaw, "Artificial Model of Trabecular Meshwork," Am Soc Intraocular Lenses and Ref Surg Annual Meeting 1987

151 S S Lane D W Neyler, L J Kolleratend K Knaeth and R L Lindstrom " Prospective Comparison of The Effects of Occucoat Viscoat and Healon on Intraocular Pressure and Endothelial Cell Loss " J Cataract Refractive Surg , 17, 21(1991)

152 E A Barron M Busim, and C Page, 'Comparison of The Effects of Viscoat and Healon on Postoperative Intraocular Pressure ' Am J Ophthalmol 100, 377(1985)

153 S Miyecchi and S Iwata, "Evaluations on The Usefulness of Viscous Agents in Anterior Segment Surgery 11 Effect on IOP and Clearance from the Anterior Chamber " J Ocular Pharmacology, 5 221(1989)

154 J J Strangel, J G Niebat and G Settles, "Formation and Prevention of Postoperative Abdominal Adhesions." J Reprod Med 29 143(1984)

155 N Ellis, "The Cause and Prevention of Postoperative Intraperitoneal Adhesions " Surg Gynecol Obstet 133, 497(1971)

156 G Haltz, "Prevention and Management of Peritoneal Adhesions," Fertil Steril , 41 497(1984)

157 A M Siegler, V Kontopoulos and C E Wang, 'Prevention of Postoperative Adhesions in Rabbits with Ibuprofen A Non-Steroidal Anti-Inflammatory Agent," Fertil Steril 34, 46(1980)

158 J M McCord, "Oxygen Derived Free Radicals in Postischemic Tissue Injury," N Engl J Med 312, 159(1985)

159 K J Doody R C Dunn, and V C Gottram Jr 'Recombinant Tissue Plasminogen Activator Reduces Adhesion Formation in a Rabbit Uterine Horn Model" Fertil Steril 51 509(1989)

150 G S Neuwirth and S M Khelef, "Effect of 32% Dextran 70 on Peritoneal Adhesion Formation," Am J Obstet Gynecol , 121, 420(1975)

161 B Ingeson, "Dextran - Later Clinical Studies" in Treatment of Post surgical Adhesions, p 165, Wiley Liss New York 1990

162 T Trimbos Kemper and G Veering "Anaphylactic Shock from Intracavitary 32% Dextran 70 during HysteraEscopy " Fertil Steril Col 51, 5(1989)

163 D Bergqvist and K G Arfors, "Effect of Dextran and Hyaluronic Acid on the Development of Postoperative Postsurgical Adhesion in Experimental Animals," Eur Surg Res 9, 321(1977)

164 D A Duncan, Y Yaeshi, E P Goldberg M Minns D O'Brian, F Congdon and M T Carmichael, "Prevention of Postoperative Pericardial Adhesions with Hyroghilic Polymer Solutions " J Surg Res 45, 44(1988)

165 M P Diamond A.H Decherney C.S. Lunsky T Cunningham and G Constantinou "Adhesion Reformation in The rabbit Uterine Horn Model I Reduction with Carboxymethylcellulose " Int J fertil 33, 372(1988)

166 T E Elkins, R T Bury, and J L Ritter, "Adhesion Prevention by Solution of Sodium Carboxymethylcellulose in The Rat," Fertil Steril , 41, 826(1984)

167 M P Diamond, C G Lunsky and T Cunningham, "Assessment of Carboxymethylcellulose and 32% Dextran 70 for prevention of Adhesions in Rabbit Uterine Horn Model " Int J Fertil 33, 278(1988)

168 C M Fredericks I Kotry, and G Holtz "Adhesion Prevention in the Rabbit with Sodium Carboxymethylcellulose " Am J Obstet Gynecol 155, 687(1986)

169 M P Diamond and A Hershley "Adhesion Formation/Reformation," in Treatment of Post Surgical Adhesions p 23 Wiley Liss New York 1990

170 M Greenberg and N H Lauersen "Postoperative Adhesions Etiology and Preventions " in Principals of Microsurgical Techniques in Infertility, p 215, Plenum Press New York, 1982

171 A G Decherney, "Preventing Postoperative Pelvic Adhesions with Intraperitoneal Treatment " J Reprod Med , 29 157(1984)

172 E P Goldberg, J W Sheets, and M B Habal "Peritoneal Adhesions Prevention with The Use of Hydrophilic Polymer Solution Centrige" Arch Surg , 115, 776(1980)

173 E B Goldberg, Y Yaacobi, J W Burns, M Staples et al "Water soluble Polymers for Tissue Protection during Surgery," Polymer Preprints, 30, American Chemical Society Meetings 1989

174 L S Peck, J M Quigg, S T Farnsworth, K Mentak, and E F Goldberg, "Effect of Solution Volume on Prevention of Surgical Adhesion Using Hyaluronic Acid And Carboxymethylcellulose Tissue Precoating Solutions," Seventh Annual Scientific Session of the Academy of Surgical Research, Scottsdale Arizona 1991

175 Y Yaacobi, J W. Burns, and E F. Goldberg, "Prevention of Postoperative Adhesions by Precoating Tissues with Dilute Sodium Hyaluronate Solutions," in Proceedings of second International Symposium on Postoperative Adhesions, J Wiley New York 1993 (in press)

176 Y Yaacobi, L M Ramed, K B Kaul, and M M Fanous "Reduction of Postoperative Adhesions Secondary to Strabismus Surgery in Rabbits," Ophthalmic Surgery, 23, 123(1992)

177 B P. Meyers and D. Jansen, "Gore-Tex Surgical Membrane," in Treatment of Post surgical Adhesions, p 93, Wiley-Liss New York 1990.

178 G B Ratta, A. Debarbieri, A. Sauco, G. Campa, D. Zacchero, and G Motta, "Use of Polytetrafluroethylene Surgical Membranes for Control of Intraabdominal Adhesions," Italian J Surg. Sci., 10, 165(1988)

179 M F. Diamond, T. Cunningham, C B. Linsky, L. Kamp, R F. McConnell and R W. Grecy, "Interceed (TC 7) As an Adjuvant for Adhesion Reductive Animal Studies," in Treatment of Post surgical Adhesions, p 131, Wiley Liss, New York, 1990.

180 C B. Linsky, M F. Diamond, T. Cunningham, A.H. Dacherney, and G diZerega, "Effect of Blood on the efficacy of Barrier Adhesion Reduction in the Rabbit Uterine Horn Model," Infertility, 11, 273(1988)

181 O. Smidsrod and A. Haug, "Estimation of The relative Stiffenses of the Molecular Chain in Polyelectrolytes from Measurements of Viscosity at Different Ionic Strength," Biopolymers, 10, 1213 (1971).

182 M Yalpani, Polysaccharides,Synthesis, Modificatsons and Structure/Property Relations, p 17, Elsevier New York 1988

183 G Barth, H. Anger, I. Pleshchina, G Brendo, and V B Tolstogimov, Carbohydrate Polymers, 2, 1(1982)

184 B R Morris, D A Rees, and E J Welsh "Conformation and Dynamic Interactions in Hyaluronate Solutions" J Mol Biol 138 383(1980)

185 W W Graessley in Physical Properties of Polymers p 97 American Chemical Society, Washington 1984

186 M Yalpani Polysaccharides,Syntheses, Modifications and Structure/Property Relations p 182 Elsevier New York 1988

187 D A Rees 'Conformations in Polysaccharide Molecules' in Carbohydrates MTP Int Rev Sci V 7 p 251 Butterworths, London 1975

188 D A Pathrick "Molecular Motion in Concentrated Polymer Systems High frequency Behavior" in Polymer Solutions, Theoretical Considerations and Newer Methods of Characterization p 239 Plenum Press, New York 1986

189 E R Morris, A H Cutler S B Ross Murphy, D A Rees and J Price, "Concentration and Shear Rate Dependence of Viscosity in Random Coil Polysaccharide Solutions." Carbohydrate Polymers 1 5(1981)

190 A H Clerck, and S B Ross Murphy "Shear Modulus Concentration Relationships for Biopolymers Gels Comparison of Independent and Comparative Crosslink Description" in Physical Networks, Polymers and Gels p 202, Elsevier London 1988

191 D Durand, C Bertrand, J F Busnel J B Emery M Axelos J F Thibaut, J Lefebvre and J L Doublier, "Physical Gelation Induced By Ionic Complexation Pectin Calcium System" in Physical Networks, Polymers and Gels p 283, Elsevier, London 1988

192 M Yalpani Polysaccharides,Syntheses, Modifications and Structure/Property Relations p 93 Elsevier New York 1988

193 M Glicksman and R E Sand, Industrial Gums p 197, Academic Press New York, 1973

194 E R Morris D A Rees, E J Welsh "Conformation and Dynamic Interactions in Hyaluronate Solutions," J Mol Biol 138 383(1980)

195 E J Welsh, D A Rees E R Morris, and J K Madden, "Competitive Inhibition Evidence for Specific Intermolecular Interactions in Hyaluronate Solutions" J Mol Biol 138 375(1980)

196 M Yalpani, Polysaccharides,Syntheses, Modifications and Structure/Property Relations p 114 Elsevier, New York 1988

187. Technical Brochure Aqualon Cellulose Gum, Sodium Carboxymethylcellulose:Physical and Chemical Properties Aqualon Wilmington, Delaware, 1980.

188 L.H. Sperling, Introduction to Physical Polymer Science, p. 56 Wiley Interscience, New York, 1986

196. T.E. Newlin, S.E. Lovell, P.R. Saunders, and J.D. Ferry "Long Range Intermolecular Coupling in Concentrated Poly n-Butyl Methacrylate Solutions and Its Dependence on Temperature and Concentration," J. Colloid Sci., 17, 408(1962)

200 Y. Boucher, F. Lafuma, C. Quiveron, J.C. Milec, and S. Sillion, "Evidence by Light Scattering of Hydroxyethylcellulose Aggregation Induced by Filtration," Polymer Bulletin, 12, 327(1984)

201 M. Doi and S.F. Edwards, The Theory of Polymer Dynamics Oxford University Press, Oxford, 1986

202 J.A. Kornfield, G.G. Fuller, and D.S. Pearson "Infrared Dichroism Measurements of Molecular Relaxation in Binary Blend Melt Rheology," Macromolecules, 22, 1334(1989)

203 M. Doi, W.W. Graessley, E. Helfand, and D.S. Pearson, "Dynamics of Polymers in Polydisperse Melts," Macromolecules, 20, 1900(1987)

204 M. Yalpani, Polysaccharides:Synthesis, Modifications and Structure/Property Relations, p. 387, Elsevier, New York, 1988

205 M.A. Lifely, A.J. Gilbert, and C. Moreno, "Sialic Acid Polysaccharide Antigens of Neisseria meningitidis and Escherichia coli: Esterification Between Adjacent Residues," Carbohydrate Research, 94, 193(1981)

206 T.P. Nevell, and S.H. Zeronian, Cellulose Chemistry and its Applications, p. 274, Ellis Horwood Publishers, New York, 1985

BIOGRAPHICAL SKETCH

Khalid Mantak was born on August 3, 1964 in Sefrou, in the Atlas mountains of Morocco. He attended high school at "Lycée Moulay Youssef" in Rabat and obtained his "Baccalaureat Sciences Mathématiques" in 1983. He entered undergraduate studies at the "Université Mohammed V" and graduated with a bachelor's degree in physics and chemistry in 1987.

In 1988, Khalid Mantak joined the doctoral program in the Department of Materials Sciences and Engineering at the University of Florida. He obtained his M.S. in materials sciences and engineering in 1992.

While pursuing M.S. and Ph.D. studies at the Materials Sciences and Engineering Department, where the author specialized in polymer science and biomedical engineering, he served as research assistant and was a member of the American Chemical Society and the Society of Plastics Engineers.

I certify that I have read this study and that in my opinion it conforms to acceptable standards of scholarly presentation and is fully adequate in scope and quality as a dissertation for the degree of Doctor of Philosophy

Eugene P Goldberg Chair
Professor of Materials Science and Engineering

I certify that I have read this study and that in my opinion it conforms to acceptable standards of scholarly presentation and is fully adequate in scope and quality as a dissertation for the degree of Doctor of Philosophy

Christopher D Batich
Professor of Materials Science and Engineering

I certify that I have read this study and that in my opinion it conforms to acceptable standards of scholarly presentation and is fully adequate in scope and quality as a dissertation for the degree of Doctor of Philosophy

Anthony B Brennan
Assistant Professor of Materials Science and Engineering

I certify that I have read this study and that in my opinion it conforms to acceptable standards of scholarly presentation and is fully adequate, in scope and quality as a dissertation for the degree of Doctor of Philosophy

Stan R Bates
Associate Engineer of Materials Science and Engineering

I certify that I have read this study and that in my opinion it conforms to acceptable standards of scholarly presentation and is fully adequate in scope and quality as a dissertation for the degree of Doctor of Philosophy

Dinesh O Shah
Professor of Chemical Engineering

This dissertation was submitted to the Graduate Faculty of the College of Engineering and to the Graduate School and was accepted as partial fulfillment of the requirements for the degree of Doctor of Philosophy

May 1993

Winfred M Phillips
Dean College of Engineering

Madelyn M Lockhart
Dean Graduate School